



HAL
open science

Design, structuration and rheological properties of Laponite based polymeric nanocomposites

Omar Abakar Adam

► **To cite this version:**

Omar Abakar Adam. Design, structuration and rheological properties of Laponite based polymeric nanocomposites. Other. Le Mans Université, 2012. English. NNT : 2012LEMA1014 . tel-00756711

HAL Id: tel-00756711

<https://theses.hal.science/tel-00756711>

Submitted on 23 Nov 2012

HAL is a multi-disciplinary open access archive for the deposit and dissemination of scientific research documents, whether they are published or not. The documents may come from teaching and research institutions in France or abroad, or from public or private research centers.

L'archive ouverte pluridisciplinaire **HAL**, est destinée au dépôt et à la diffusion de documents scientifiques de niveau recherche, publiés ou non, émanant des établissements d'enseignement et de recherche français ou étrangers, des laboratoires publics ou privés.



Elaboration, structuration et propriétés rhéologiques de nanocomposites polymères modèles à base de Laponite

THÈSE

Présentée à

L'Université du Maine

Pour obtenir le titre de

DOCTEUR de l'Université du Maine

Mention Chimie et Physico-chimie des Polymères

Par

Omar ABAKAR ADAM

Composition du jury :

M. E. VERRON	Ecole Centrale de Nantes	Rapporteur
M. F. PROCHAZKA	Université Jean Monnet, Saint Etienne	Rapporteur
M. C. CHASSENIEUX	Université du Maine, Le Mans	Examineur
M. A. KASSIBA	Université du Maine, Le Mans	Examineur
M. G. BROTONS	Université du Maine, Le Mans	Examineur
M. J. F. TASSIN	Université du Maine, Le Mans	Directeur de thèse

Soutenu le 24 Septembre 2012

Polymères, Colloïdes et Interfaces
IMMM-UMR CNRS 6283
Institut des Molécules et Matériaux du Mans

Ecole Doctorale
3MPL
Matière, Molécules, Matériaux
en Pays de la Loire

Acknowledgement

I would like to express my deep and sincere gratitude to my supervisor, Prof. Jean Francois Tassin, for his patience, motivation and enthusiasm. His guidance helped me in all the time of research and writing this thesis. I could not have imagined having a better advisor and mentor for my Ph.D. study.

I wish to express my warm and sincere thanks to Prof. Christophe Chassenieux for his kind help. I also would like to thank my thesis committee: Prof. Erwan Verron, Prof. Frederic Prochazka, Prof. Abdelhadi Kassiba, and Dr. Guillaume Brotons for their encouragement, insightful comments, and hard questions.

I owe my most sincere gratitude to nanocomposites group of Prof. Jean Francois Tassin: Dr. Jesmy Jose, Dr. Frédérick Niepceron, Julien Plattier, and Radouane Sellak for the stimulating discussions and an excellent collaboration.

I warmly thank Dr. Gireeshkumar Dr. Tuan Phan, Dr. Celine Charbonneau and Achutha Prabhu for the sleepless nights we were working together before deadlines, and for all the fun we have had in the last three years.

Last but not the least, I owe my loving thanks to my very dear mother and father, the most precious gift of heaven who made the earth a much better place and for supporting me spiritually throughout my life.

Chapter -1: Bibliography

	General Introduction	1
1	Introduction	3
2	Polymer matrix based nanocomposites	4
2.1	Chemical and structural characteristics of layered-silicate nanoparticles.	4
2.2	Nanoclays-polymer matrix based nanocomposites: structure and synthesis	5
2.2.1	Structure of polymer based nanocomposites	5
2.2.2	Influence of the molar mass of the matrix	6
2.2.3	Preparation methods of polymer nanocomposites	8
2.3	Structure-rheology relationships for polymer matrix based nanocomposites	9
2.3.1	Rheological properties of polymer based nanocomposites	9
2.3.2	Structural characterization of polymer based nanocomposites	12
2.4	Applications of polymer matrix based nanocomposites	12
2.4.1	Automotive applications	13
2.4.2	Biomedical applications	13
3	Polymer blends and polymer blends nanocomposites	13
3.1	Introduction	13
3.2	Classifications of polymer blends	14
3.3	Thermodynamics of polymer blends	16
3.4	Phase diagram of polymer blends	16
3.5	Polymer blends nanocomposites	17
3.5.1	Influence of nanoparticles on the miscibility of polymer blends	17
3.5.2	Influence of nanoparticles on the thermal, and dynamics properties of polymer blends.	21
3.5.3	Influence of nanoparticles on the mechanical properties of polymer blends	23
4	Conclusion:	26

Chapter -2: Polymer nano-composites based on Laponite and poly (ethylene oxide)

2.1 Overview	33
2.2 A New Insight into the Structure and Rheology of Model Poly (ethylene oxide)/ Laponite Clay Nanocomposites	35
2.2.1 Introduction	35
2.2.2 Experimental Section	37
2.2.3 Results	40
Rheology.	40
SAXS Results:	45
DSC Results:	49
2.2.4 Discussion.	53
2.2.5 Conclusion	56
2.2.6 References	57
2.3 Influence of Molecular Parameters on the Structure and Rheology of Model Poly (ethylene oxide)/ Laponite Clay Nanocomposites	61
2.3.1 Introduction	61
2.3.2 Experimental	62
Materials	62
Characterization.	64
2.3.3 Results	65
Identification of nanocomposite structures by SAXS	65
Rheology	68
Master curve analyses of the viscoelastic moduli	71
Role of adsorbed polymer chain dynamics	75
2.3.4 Discussion and concluding remarks	77
2.3.5 References	80

2.4 Influence of the route of protecting the particles	84
2.4.1 Introduction	84
2.4.2 Experimental Section	85
Materials:	85
Conversion of Hydroxyl-PEGs to Trymethylammonium-PEGs	85
Nanocomposites preparation:	86
Rheological characterization	86
2.4.3 Results	87
Results for samples prepared by melt dispersion	87
Results for samples prepared by solution mixing	89
2.4.4 Discussion	91
2.4.5 Conclusion	94
2.4.6 References	95
2.5 General conclusion	97
Chapter-3: Polymer blends nanocomposites based on PMMA-PEO blends/Laponite	
3.1 Introduction	103
3.2 Experimental part	105
Materials	105
Samples preparation	105
Measurements	105
3.3 Results and discussions	106
Miscibility of PMMA/PEO blends.	106
Rheological properties	116
Effect of Laponite concentration	119
3.4 Conclusions	124
Conclusion and perspectives	127

General Introduction

Polymers have brought major effects on the way we live. It is difficult to find an aspect of our life that is not affected by polymers. Although polymer research started over eighty years ago, when the notion of macromolecule was introduced by Staudinger, polymer science is still a very active field of research and rupture discoveries are still made, such as H-bonded elastomers with healing properties or malleable high temperature thermo-sets. The technology of reinforcing polymers, leading to so called composites, has been used for long, but it does not mean that the effect of fillers, either as nanoparticles or even frequently used carbon black, is fully understood. Since the beginning of the 90ths and the discovery of very stimulating properties of polyamide compounds containing organo-modified clays, a lot of research has been devoted to nanocomposites. More than 28000 papers have been published on polymer nanocomposites since 1990 and among them over 6500 are concerned with clay as particles. Without self-citations, each paper in this field is cited over 12 times in average; best cited reviews collecting over 2500 citations. However, although numerous studies have been reported and numerous patents filled, to our knowledge very few commercial polymer systems are making use of this technology. One can conclude that although much knowledge has been brought during 20 years, many obstacles are facing commercial development. One of them is probably linked to the difficulty in dispersing optimally the nanoparticles inside the polymer, so that they can reveal their very high specific surface on the order of several hundreds of square meters by grams, and develop strong interactions with the polymer chains, leading to efficient reinforcement. Substantial fundamental research is still necessary to provide a good understanding of these materials to enable full exploitation of their nano-engineering potential.

The scope of this thesis is to establish relationships between rheological behavior in the molten state and dispersion state of the particles, by using a model system. It consists in well-defined nanoparticles known as Laponite, which can be seen as nanometric disks of 25 nm diameters and 1 nm thickness. These synthetic clay particles are hydrophilic and disperse easily in water, down to the individual scale, contrarily to Montmorillonite that is frequently used in the literature. As matrix, polyethylene oxide (available in various molecular weights) was chosen, since it is also water soluble and develops strong interactions with Laponite, as known by previous studies carried out in our laboratory. However, polyethylene oxide is highly crystalline and possesses poor mechanical properties. In order to enter the field of solid state properties, Laponite particles were incorporated in polymethylmethacrylate using polyethylene oxide as compatibilizer since they form a pair of compatible polymers. This system has received much less attention since about 200 publications can be found. Many of them are related to rather highly filled systems for application in the field of solid state batteries, the filled polymer increasing the conductivity of ions.

The first chapter of this thesis presents a bibliographic situation concerning nanoclays, the preparation of nanocomposites, their characterization and their rheological properties as well as some applications of polymer nanocomposites. Since polymer blends will be considered, a part of this chapter is dedicated to blends and their nanocomposites.

The second chapter is presented in the form of 3 articles, preceded by an introduction and closed by a general conclusion where input of the 3 papers is considered. In this chapter we will focus on the influence of the preparation method on the structure and rheological properties, on the influence of the molecular weight of the matrix and finally on the influence of the type of protection of the particles.

The third chapter presents the methods used to introduce Laponite into polymethylmethacrylate and discusses the properties of the blends, in relation with their structure.

Chapter 1: Bibliography

1 Introduction

Polymer matrix based nanocomposites constitute a research and development field that has attracted interest far before the concept of nanotechnology has emerged. Actually, combining nanoscale fillers and a polymer matrix addresses a major question regarding the influence of the nanometric scale (so-called ‘nano-effect’) on the properties of materials since nanoscale materials may produce qualitatively new behavior when compared with their macroscopic counterpart¹⁻⁴. Furthermore, if the improvement of the mechanical properties of polymer matrices thanks to the inclusion of nanofillers was the main research goal for decades, it should be said that nowadays polymer matrix based nanocomposites have seen their functional properties widen thanks to the unique properties often reached through the combination of nanofillers with a polymer matrix.

Polymer matrix based nanocomposites may combine different kinds of fillers (organic –carbon black, carbon nanotube⁴, graphene-, inorganic -silica, ceramics, calcium carbonate-, polymeric, metallic...) and different kind of matrices. For most of the cases, reinforcement of polymer with nanofillers has resulted in polymer based nanocomposites exhibiting new functionality and better properties in terms of performance than the one exhibited by more traditionally filled polymeric materials. Historically, a real breakthrough has been achieved in the 1990’s by engineers from Toyota who have dispersed a few percents of montmorillonite (a natural nanoclay) into caprolactam in order to produce a polyamide-6 based nanocomposite. Since this pioneering work, much attention has been paid to the use of clays (natural or synthetic ones) as nanofillers in combination with different kinds of polymeric matrices; this work will only consider layered silicate nanoparticles for producing polymer-layered silicate nanocomposites. In the last decade, these materials have actually gained substantial interest due to their peculiar morphology, their “green” character, the natural abundance of the nanofillers, and the improved properties displayed by the nanocomposites such as (1) improved tensile strength and modulus without decreasing the impact strength; (2) increased thermal stability as well as self-extinguishing characteristics; and (3) reduced permeability to gases⁴⁻⁹. In this chapter, we will first discuss the chemical specificities of the nanofillers that are layered silicate nanoparticles. We will then present the different structures that may be encountered for polymer based nanocomposites and the different synthetic methods for obtaining them. We will then present different methods that have been used during this work for characterizing the structure and the properties of nanocomposites. Finally, we will discuss potential applications of polymer based nanocomposites.

Apart from the single reinforcement of polymer matrices expected when combining polymer chains with nanofillers, nanoclays have been shown to act as good compatibilizers for polymer blends which will be the subject of the second part of this chapter. We will describe polymer blends and will give examples from the literature where nanoclays have been used as fillers and compatibilizers.

2 Polymer matrix based nanocomposites

2.1 Chemical and structural characteristics of layered-silicate nanoparticles.

Nanoclays consist of platelets with an inner octahedral layer sandwiched between silicate tetrahedral layers as illustrated in figure 1.1. More generally, nanoclays belong to the family of layer silicates which are different kinds depending on their structural and chemical natures. Warshaw et al¹⁰ have classified layered silicates according to structural studies following three criteria :

- height of fundamental repeat unit or thickness of layer
- gross composition – number of dioctahedrons or trioctahedrons and ionic content of layer
- stacking sequence of layers and degree of order of the stacking.

Nomenclature committee from clay society¹¹ has classified layered silicates on the basis of structural and chemical characteristic into two categories : non-planner hydrous phyllosilicate and planner hydrous phyllosilicate, the latter one being diversified into seven groups according to the type of silica layer (1:1 or 2:1), the magnitude of the net layer charge per unit and the interlayer materials that compensates the layer charge. In this work we only consider phyllosilicate that belongs to the planner hydrous phyllosilicate series.

Phyllosilicate so-called lamellar silicates are alumino-silicated materials based on infinite bidimensional layers based on octahedrons interlocked between layers of tetrahedrons, the stoichiometry of the layers is either 1:1 or 2:1 (figure 1.1). The structural family of 2:1 phyllosilicate includes montmorillonite, saponite and hectorite. In this work, we will more specifically consider laponite particles a subdivision of hectorite.

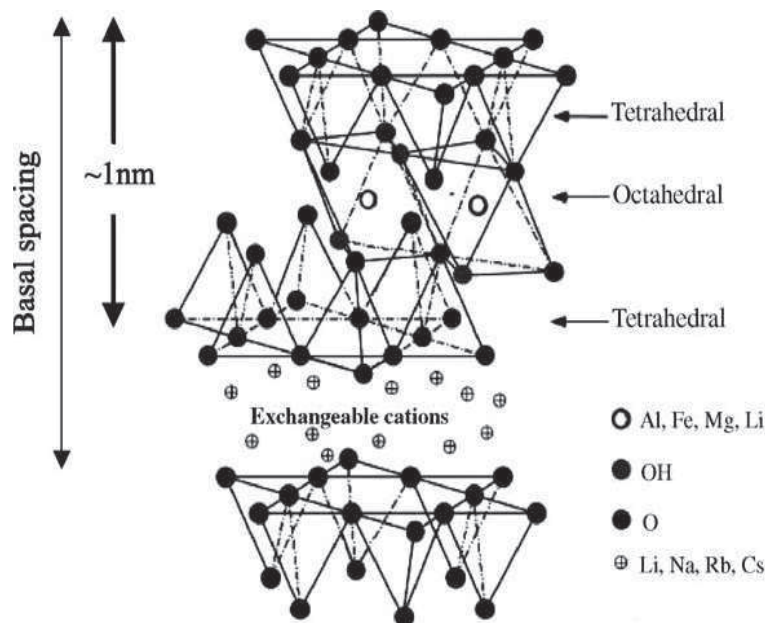


Fig. I.1 Structure of 2:1 phyllosilicates¹².

In its natural state, the nanoclays exist as stack of many platelets and the key point to achieve is a perfect control of their dispersion during the synthesis of the polymer based nanocomposites as discussed hereafter.

2.2 Nanoclays-polymer matrix based nanocomposites: structure and synthesis

The main purpose for dispersing nanofillers into a polymeric matrix is primary to improve the mechanical properties of the latter. In that sense, it appeared that the “nano-effect” previously discussed could lead to improved properties over that expected from continuum mechanics prediction. The “nano-effect” also deeply influences the crystallization rate and crystallinity when crystalline polymer matrices are considered but also the glass transition temperature. These properties are directly ruled by the structure of the nanocomposites which are described in the following paragraph.

2.2.1 Structure of polymer based nanocomposites

The properties of polymer based nanocomposites where the nanofillers is a clay, are clearly affected by their structure which can be classified into three main categories¹² depending on the way the nanoclays are dispersed within the polymer matrix and then depending on the interactions between these two components but also between the layers constituting the nanoclay itself, we can then consider the following cases :

- (1) Immiscible or phase separated nanocomposites which are obtained when the polymer matrix fails to intercalate between the layers of the nanoclays which stacked and which may be seen as microcomposites
- (2) Intercalated nanocomposites which are obtained when the polymer intercalates between the layers, and increases the space between them, but where attractive forces leave the layers remain regularly spaced.
- (3) Exfoliated nanocomposites which are obtained when the polymer intercalates between the layers and increases the space between them in such a way that there is no more interaction forces between the layers. The nanoclays are then perfectly dispersed with the polymer matrix.

The structure/properties relationship of these nanocomposites has been studied for instance by Koo et al¹³ who have analyzed three types of maleated polypropylene-layered silicate nanocomposites with different dispersion states of the layered silicate (immiscible, intercalated and exfoliated). Exfoliated nanocomposites show the largest improvement of the mechanical properties whereas intercalated ones display a moderated increase and deintercalated ones the smallest increase.

A key point to address is then the elaboration of exfoliated nanocomposites. In order to do so, the space between stacked layers of clay needs to be compatible with the radius of gyration of the polymer chains which constitute the polymer matrix that is bigger than in the sole nanoclay. Loiseau et al¹⁴ have controlled the specific interactions between the particles and the polymer matrix by surface treatment of the particles, either

by using adsorbed or grafted short polymeric chains on the surface of the particles for enhancing their dispersion degree. Their results showed that, the state of dispersion depended strongly on the treatment and on the amount of added chains, the grafted saturated particles being the best ones for reaching a fully exfoliated state as demonstrated by small angle X-ray scattering measurements (SAXS) (figure 1.2). Finally, the nanocomposites based on these particles show enhanced mechanical properties (increased storage modulus which became frequency independent) which agreed with the results of Koo et al¹³.

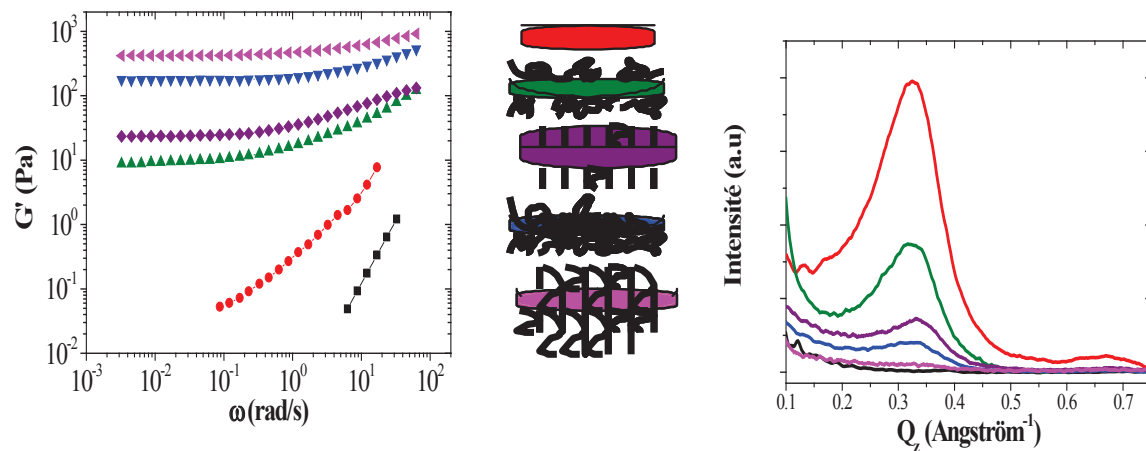


Figure I.2: Influence of the modification of nanoclay interfaces on the structure of the nanocomposite on their mechanical properties¹⁴

2.2.2 Influence of the molar mass of the matrix

Compatibility between the particles and the polymer matrix used for preparing polymer based nanocomposites is of prior importance for achieving a good dispersion state. However, once selecting suitable components, the dispersion state may also be affected by the molar mass of the polymer matrix as demonstrated by many authors^{9, 15-18}. Fornes et al¹⁶ with organoclay-nylon 6 based nanocomposites reported that higher molecular weight for polyamide yielded superior nanocomposites properties since a higher exfoliation for the nanoclay was achieved with respect to nanocomposites based on low molecular weight polyamide. This was attributed to the higher melt viscosities of the former which helped at transferring more stress/energy for achieving the separation of platelets. By opposition, low molecular weight polyamide imparted lower shear stress which could even skew the stack of platelets rather than separate them as depicted in figure 1.3.

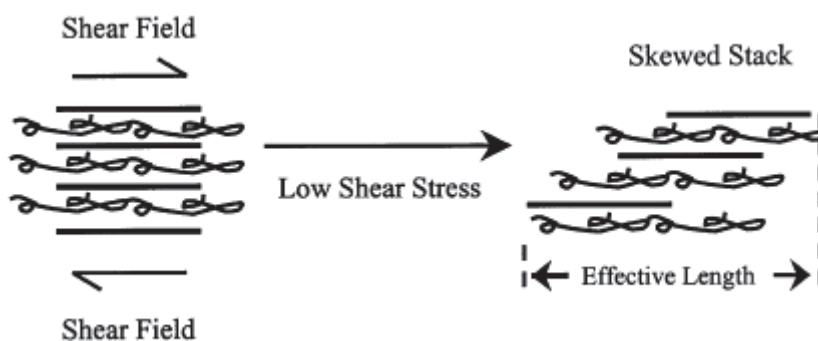


Figure I.3. A possible mechanism for causing larger effective particle size with low polymer molecular weight based nanocomposites¹⁶.

Results of Fornes et al^{16, 19} have been confirmed by Loiseau et al²⁰, with various molecular weight of poly(ethylene oxide) matrix used to prepare laponite-PEO based nanocomposites. It has been shown that both storage and loss moduli increase significantly with increasing the molar mass of PEO as shown in figure 1.4.

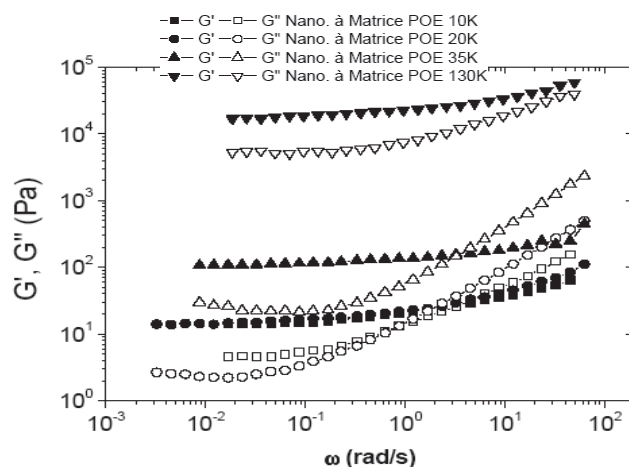


Figure I.4: Frequency dependence of G' and G'' for laponite-PEO based nanocomposites with various molar mass of PEO¹⁴.

This influence of the molecular weight of the matrix is even more pronounced when the chemical compatibility between the polymer matrix and the nanoparticles is high as observed by Loyens et al²¹ with cloisite-PEO based nanocomposites. The cloisite displayed different kinds of surface chemistry: native cloisite with sodium ions at the surface, cloisite modified with a polar additive and cloisite modified with an apolar additive, the latter being more compatible with PEO matrix. It has been shown that for cloisite containing an apolar modifier, both the structural organization and the resulting mechanical properties were found to be very dependent on the molecular weight of the matrix, whereas for the other kinds of cloisite-PEO based nanocomposites, intercalated

structures were achieved displaying only a moderated improvement of mechanical properties at high clay concentration regardless of the molecular weight of the matrix.

However, one should remind that the best mechanical properties are achieved with exfoliated nanocomposites which means that the polymer chains that constitute the matrix can efficiently achieve such a situation if they are not too big in order to rapidly disrupt the stacks of nanoclay as evidenced by several groups for montmorillonite-maleated polypropylene¹³, cloisite-nylon-6²² and cloisite-poly(ϵ -caprolactone)¹⁵ based nanocomposites. Optimizing the exfoliation rate of the nanoclays within the polymer matrix is possible thanks to the use of different preparation pathways for the nanocomposites and also by chemical modification of the surface of the nanoclays.

2.2.3 Preparation methods of polymer nanocomposites

In order to achieve the best exfoliation of the nanoclays within the polymer matrix, three synthetic paths have been mainly explored in the literature⁴ :

- Solution dispersion
- In-situ polymerization
- Melt intercalation

The use of each of these methods will depend on the type of polymer matrices involved and will in turn be sensitive to various parameters. For example, solution dispersion techniques need the use of a solvent which must be a good/theta solvent for the polymer and which must swell the nanoclays. Richard et al²³ have reported that, during polymer intercalation from a solution, a relatively large number of solvent molecules needs to be desorbed from the host to accommodate the incoming polymer chains, the desorbed solvent molecules gain one translational degree of freedom and the resulting entropic gain compensates the decrease in conformational entropy of the confined polymer. However, sometimes, an intercalation of the solvent can be favored instead of the intercalation of the polymer.

When nanocomposites are synthesized through melt intercalation technique, many factors can affect their the properties such as the mixing time, the temperature, the screw speed as reported in litterature¹⁴.

However the combination of these various techniques can lead to nanocomposites with better dispersion state of the nanoclays than if a single elaboration technique is processed as evidenced by Lepoittevin et al⁸ who have compared melt blending of PCL with montmorillonite and combination of in-situ polymerization and melt intercalation. There results showed that the combination method yielded intercalated/exfoliated nanocomposites which cannot be obtained by direct melt blending as proved by X-ray diffraction. Moreover, samples prepared by the combining method showed stiffness much higher than the corresponding microcomposites samples obtained by direct melt intercalation as showed in figure 1.5.

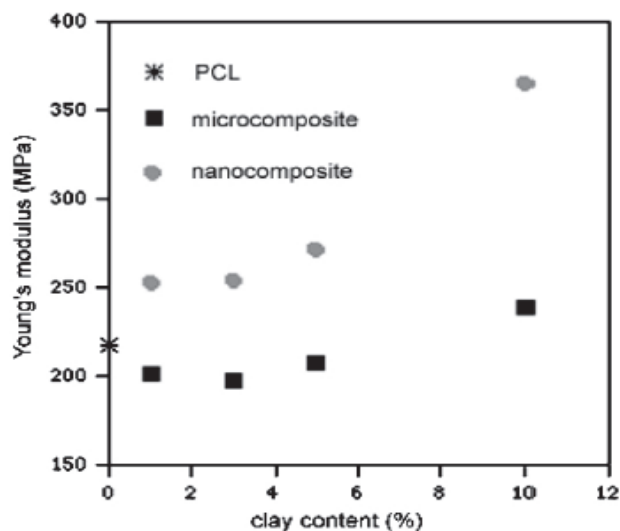


Fig I.5. Variation of the Young modulus with the content of clay for montmorillonite-PCL based microcomposites (obtained by direct melt blending) and nanocomposites (obtained by combination of melt and polymerization intercalation) ⁸.

2.3 Structure-rheology relationships for polymer matrix based nanocomposites

A great attention and significant interest has been paid for understanding structure-property relations for polymer nanocomposites, and how processing could affect both structure and properties as described in the following part.

2.3.1 Rheological properties of polymer based nanocomposites

Rheology is a powerful tool for gaining an integrated picture of the nanocomposite materials since it may provide information on the influence of the nanofillers on the local deformation rate of the polymer, the influence of the nanofillers orientation and/or exfoliation, and of their interactions.

It has been reported that percolation of the nanoclays within the polymer matrix occurs at relatively low nanoclay content and that their presence obviously affects the rheological properties of the polymer matrix. The rheological properties of the polymer based nanocomposites are then influenced by their mesoscopic structure and the strength of the interactions between the components. The dynamic response of polymer nanocomposites in the so-called nanoparticle limit (that is when the radius of gyration of the polymer chain is of the same order than the size of the nanofillers) can be classified into two domains: linear and non linear. However, both linear and non linear viscoelastic properties are correlated with the structure of the nanocomposites but in this study we will solely considered linear viscoelastic properties.

Measurement of rheological properties under the molten state reveals that nanofiller loading leads to increase in the shear viscosity η^* , the storage modulus G' , and

the loss modulus G'' of the nanocomposites^{18, 20, 24-25}. Moreover, the magnitude of these parameters is sensitive to the concentration of the nanofillers, their type, their interface chemistry, ... Loiseau et al^{14, 20} have investigated the rheological properties of laponite-PEO based nanocomposites, and how these properties were affected by the parameters listed above. Their results demonstrated that, mechanical properties showed a transition from viscoelastic liquids to solids above a critical concentration of laponite particles (0.5wt% or 0.2 volume fraction) as shown in figure 1.6. This critical concentration was shown to decrease when the particles were better dispersed (which depended on their surface chemistry as explained above). Usually, the rheological behavior at high frequency is used for estimating the influence of fillers on processing properties, whereas the low frequency domain is sensitive to the structure and to a possible percolation state of the nanofillers. Gopakumar et al²⁴ presented the same results as Loiseau et al^{14, 20}, with Montmorillonite-polyethylene based nanocomposites. Loyens et al¹⁸ have also worked on laponite-PEO based nanocomposites, where they analyzed the influence of clay modification and matrix molar mass on the rheological properties of the nanocomposites as a function of temperature and fillers content.

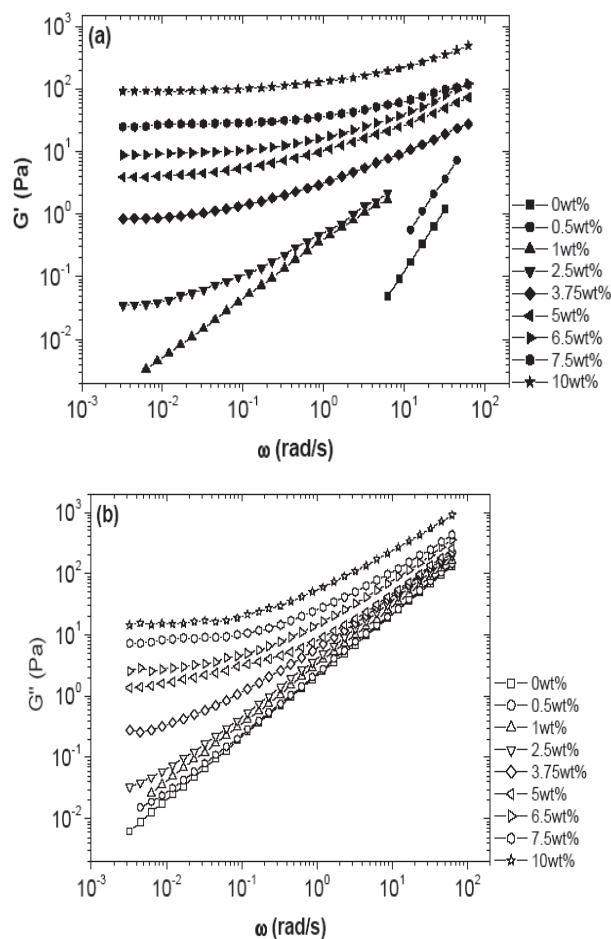


Figure I.6. Frequency dependence of G' (a) and G'' (b) for laponite-PEO based nanocomposites with various amount of laponite particles²⁰.

Koo et al¹³ have investigated the rheological properties of montmorillonite-maleated polypropylene based nanocomposites with different kinds of structure and different concentration of the nanofillers. However, their results demonstrated that, storage modulus G' , loss modulus G'' , and complex viscosity η^* were deeply affected by the filler concentration although no clear transition from liquid to solid has been clearly evidenced as shown in figure 1.7

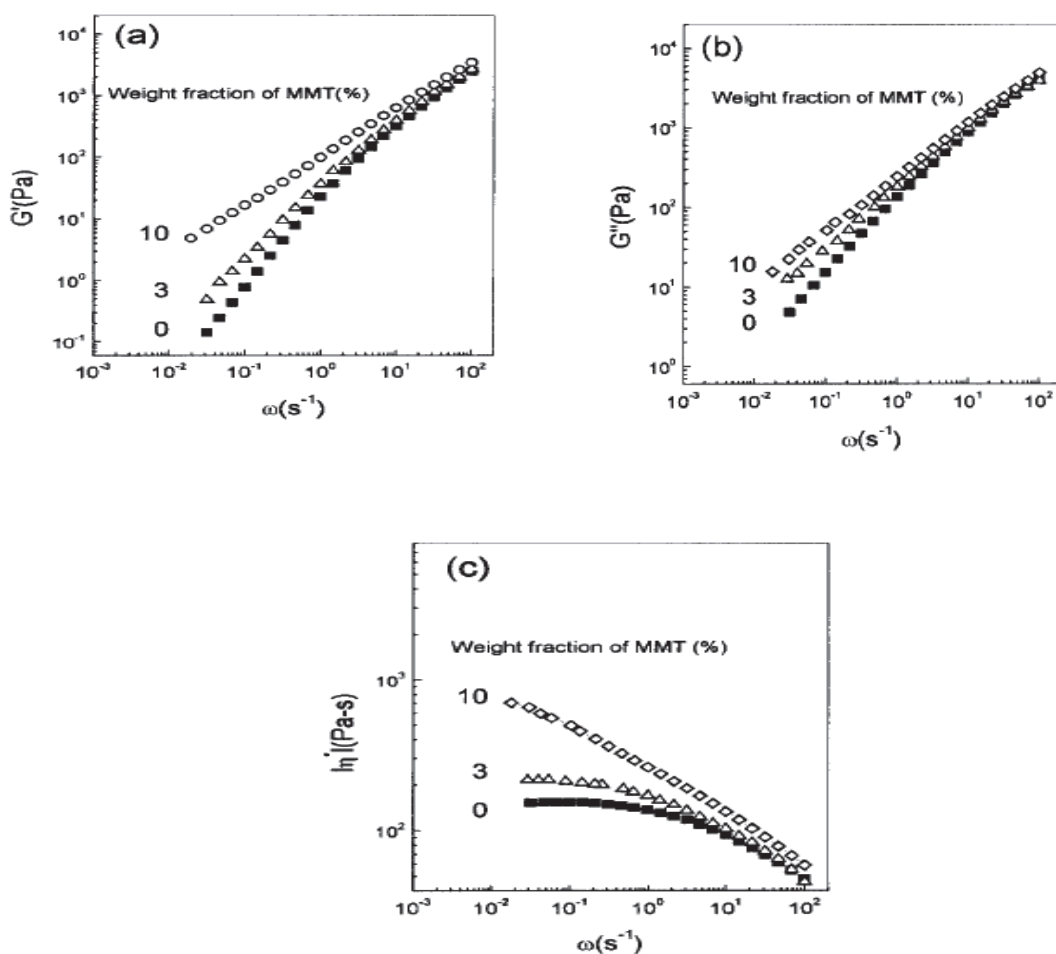


Figure I.7. Frequency dependence of G' (a), G'' (b) and viscosity (c) for montmorillonite-maleated polypropylene based nanocomposites with various amount of montmorillonite

Recently, Prachum et al²⁵ have reported on physical and mechanical properties of equivalent montmorillonite-polypropylene nanocomposites. They concluded that at low frequency, the storage modulus G' and the complex viscosity η^* increased significantly when the nanofillers were added and attributed to the existence of a percolated network. Many authors have proved the same²⁶⁻²⁸ but the sole rheology was not always enough to conclude and structural studies were needed to be performed on the same samples to firmly conclude

2.3.2 Structural characterization of polymer based nanocomposites

Structural characterizations of polymer nanocomposites can be achieved through a variety of techniques such as scattering techniques (wide and small angle X-rays scattering), microscopic techniques (SEM and TEM), and spectroscopic techniques (FTIR and NMR). These techniques are complementary to rheological investigation and thermal analysis. The goal of diversifying the methods of characterization is to provide a quantitative and accurate representation of the structure and of the properties of nanocomposites^{25, 29-31}.

Prachum et al²⁵ have characterized the morphology of montmorillonite-polypropylene nanocomposites, through variety of techniques such as X-rays scattering, TEM, and SEM, and linked these results to the rheological and thermal properties. The structure of the nanocomposites was shown to be either exfoliated or intercalated or both as demonstrated by TEM (Figure 1.8) and was nicely correlated with their mechanical properties.

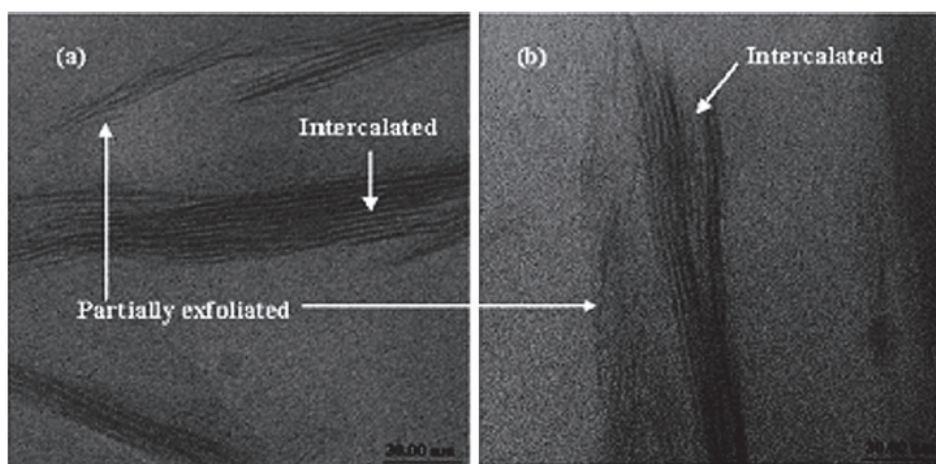


Figure I.8. TEM micrographs of the montmorillonite-polypropylène nanocomposites showing the intercalated and partially exfoliated layers for different concentration of the nanofillers²⁵.

In the same way, Scarfato et al²⁹ showed that, the structural characterization obtained through SEM, and X-ray diffraction was in agreement with what demonstrated the thermal and mechanical properties on equivalent samples. Liu et al³⁰ have reported on the structure and properties of a novel layered Zirconium phosphonate-chitosan nanocomposite, their results concerned thermal and mechanical properties which were supported by morphological characterization obtained through TEM, SEM, and X-ray diffraction.

2.4 Applications of polymer matrix based nanocomposites

Polymer based nanocomposites have mainly attracted interest due to the improvement of the mechanical properties but they also display properties of interest in terms of thermal

endurance, barriers properties, electrical and optical properties. In this paragraph, we will focus on the use of nanocomposites for various application fields.

2.4.1 Automotive applications

Polymers nanocomposites have been used as part of vehicle so far to improve manufacturing speed, enhance environmental and thermal stability, promote recycling, and reduce weight³²⁻³⁴. The first practical example of polymer nanocomposites in automotive application has been achieved by Toyota who have used clay-Nylon 6 based nanocomposites for making time-belt cover³⁵. Nanocomposites may be potentially manufactured at low cost, and may offer other advantages on density and processing with respect to metals and polymeric composites currently used in the fabrication of parts for automotive applications. Recently, it has been reported that widespread use of polymer nanocomposites by American manufacturers could save 1.5 billion liters of gasoline over the life of one year's production of vehicles and could reduce related carbon dioxide emission by more than 10 billion pounds³⁶⁻³⁷. More efforts have been going on, to give the potentials market opportunities for polymer nanocomposites in automotive application, since General Motors and supplier partners Basell, Southern Clay Products and Blackhawk Automotive Plastics have created a joint company to produce thermoplastic Olefin nanocomposites (TPO) for use in their vehicles³⁸.

2.4.2 Biomedical applications

Bio-nanocomposites combine properties of commercial polymer nanocomposites with low environmental impact of degradable materials, making them a topic of great current interest³⁹. There are different matrices (e.g. aliphatic polyesters, polypeptides and proteins, polysaccharides, and polynucleic acids) and fillers (e.g. nanotubes, nanofibers, clay nanoparticles, hydroxyapatite and metal nanoparticles) which can be selected as suitable materials, due to their chemistry and structure to suit the target field. Among all, elastomer based nanocomposites are gaining considerable attention as new materials for biomedical use; elastomers such as polyester, polyurethanes, and silicon rubber are excellent candidates as biomaterials in applications such as tissue engineering. Recently, laponite-PEO based nanocomposites have been used in tissue engineering as demonstrated by Gaharwar et al⁴⁰ who have shown that PEO can be physically cross-linked with Laponite to yield highly extensible, bio-nanocomposites which provide suitable substrates for fibroblast adhesion and guided cell growth.

3 Polymer blends and polymer blends nanocomposites

3.1 Introduction

Polymer blending is a convenient route for developing polymeric materials which combine the properties of each of their components⁴¹. Polymer blends are defined as materials of at least two polymeric species having constitutionally or configurationally differing features but not bounded to each other. Nowadays, the synthesis of new polymeric materials is achieved either by means of new polymerization methods, new

processing technology or by blending and reinforcing. However, the advantage of polymer blends versus developing new polymeric structures have been well-documented by Robeson et al⁴² in three points:

- ability to combine existing polymers into new composition offers the advantage of reducing research and development expenses.
- possibility to obtain combinations of properties more easily by polymer blending than with new polymeric structures
- faster answer for solving a problem with polymer blending.

3.2 Classifications of polymer blends

Polymer blends may be classified according to whether they consist of separated or single phases⁴³. More generally, they can be broadly divided into three categories:

(1) Immiscible polymer blends which is the most common group. The blend consists in two separated phases if it is made of two polymers. The morphology of the immiscible blend will be controlled by the relative amount of the two polymers as schematized on figure 1.9.

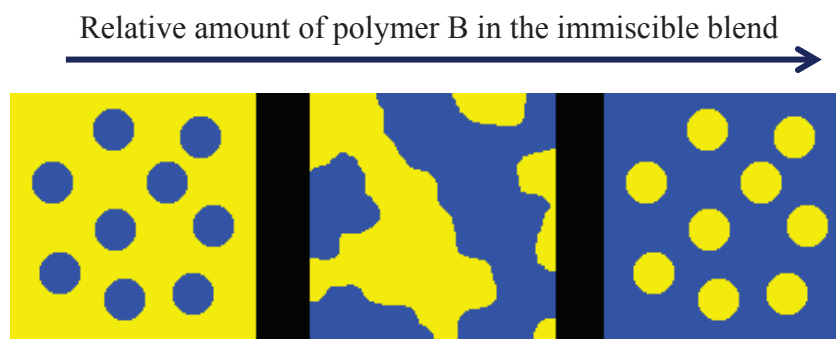


Figure 1.9 : Morphology of an immiscible blend depending on the volume fraction of each component.

When the domain of each of the component join together, the morphology is said co-continuous⁴⁴. Dell'Ebra et al⁴⁵ studied the morphology of mixtures of poly (L, L-Lactide) (PLLC) and poly (ϵ -caprolactone) (PCL) with 90/10, 80/20, and 70/30wt% composition. SEM investigation of these blends revealed the immiscibility between components, and how the morphology was affected by the amount of each component as presented in figure I.10, this result agreed with the theoretical scheme shown in figure 1.9.

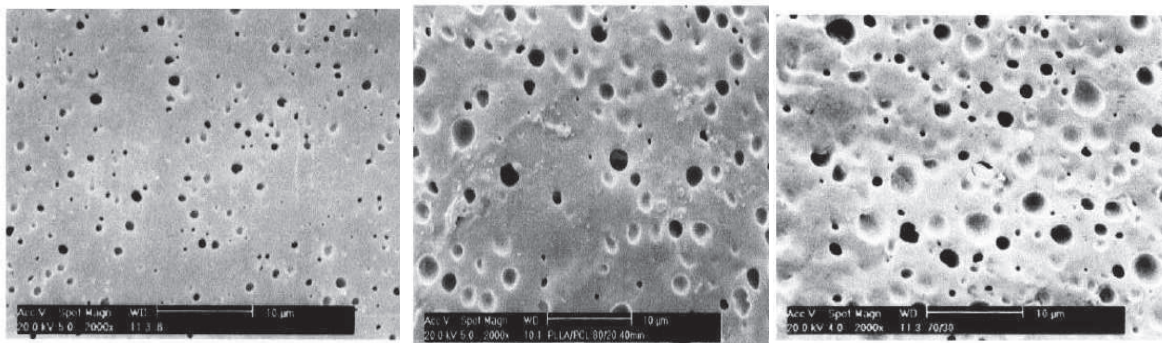


Figure I.10 SEM micrographs of smoothed and etched surface of binary blends of PLLC and PCL from left to right 90/10wt%, 80/20wt%, and 70/30wt%.

(2) Compatible polymer blends which exhibit macroscopically uniform physical properties caused by sufficiently strong interactions between the component polymers. Doleman et al⁴⁶ have prepared compatible blends of poly(vinyl acetate) and poly(methyl methacrylate) (PVA/PMMA) which have been used for producing a series of electrically conducting carbon black composites.

(3) Miscible polymer blends which are homogeneous consisting in a single-phase structure. Polymer miscibility is governed by thermodynamics parameters like Gibbs free energy and miscibility parameter. It was believed that a single glass transition temperature, which was intermediate between the glass transition temperature of the pure components was expected for miscible blends⁴⁷ but, it should be said that two glass transition temperatures do not necessarily indicate immiscibility, This observation has been pointed out by Lodge et al⁴⁸, who used DSC to investigate blends of PEO and poly(methylmethacrylate) (PMMA) over a complete composition range.

Only a few polymer pairs can be mixed but most of the polymer blends are immiscible. However some strategies have been reported for improving the miscibility between polymers that are basically immiscible⁴⁹⁻⁵¹. Recently Ren et al⁵¹ have investigated the miscibility in blends of PMMA and poly(styrene-acrylonitrile) (SAN) copolymers with different acrylonitrile contents. Their results indicated that when AN contents in SAN copolymers were 5, 35, and 50%, the PMMA/SAN blends formed two phases, and polymers were judged to be immiscible, while blends with copolymer containing 25wt% of AN was miscible, as proved by TEM and SEM.

Even though potential work has been done for improving the miscibility of polymers blends, this does not mean that immiscible polymer blends are not interesting for practical use. Ciardelli et al⁵² have shown that, some properties such as impact strength and barrier properties can only be reached through immiscibility. The properties of miscible polymers system are intermediate between those of individual components, whereas synergies may be obtained in immiscible polymer blends provided that the phase morphology and the interfacial tension are judiciously controlled as stated by Utracki et al⁵³.

3.3 Thermodynamics of polymer blends

Most of the theoretical considerations on the miscibility of polymeric system have been developed through the mean-field theory of Flory and Huggins due to its simplicity⁵⁴⁻⁵⁵. Starting with the classical Flory-Huggins equation for polymer solution, it follows that for polymer blends the configurational entropy is vanishingly small and the free energy of mixing can be expressed as⁵⁶⁻⁵⁷

$$\Delta G_m/RTV \cong \chi'_{12}\phi_1\phi_2$$

Where R, T, V, ϕ_i are respectively: the gas constant, the temperature, the (molar) volume of the system and the volume fraction component $i=1,2$. The polymer-polymer interaction parameter χ'_{12} contains both the enthalpic and the entropic parts.

Suvorova et al⁵⁸ have investigated Polymer-Polymer interaction parameter mentioned above, in blends of crystalline PEO and amorphous PMMA or poly(methyl acrylate) (PMA). Their results demonstrated that when the amorphous components (PMMA and PMA) was added to crystalline PEO, the melting point of PEO decreased from 66°C to 62°-52°C and the degree of crystallinity decreased from 74% to 45%-60%. The melting point values were used to calculate the polymer-polymer interaction parameter by using the Nishi-equation⁵⁹;

$$1/T_m - 1/T_m^0 = RV_2/\Delta H_2V_1 \chi_{12}\phi_1^2$$

Where T_m^0 and T_m denote the melting points of crystalline polymer and polymer blends respectively; ΔH_2 is enthalpy of fusion of PEO per mole of repeating unit; V_1 and V_2 are the molar volumes of the repeating unit of crystalline and amorphous polymer respectively, and ϕ_1 is the volume fraction of amorphous polymer.

The parameters χ'_{12} were shown to be -0.221 for PEO/PMA and -0.315 PEO/PMMA in the vicinity of the PEO melting point. These result confirmed that PEO/PMMA exhibit an excellent compatibility.

3.4 Phase diagram of polymer blends

The properties of polymer blends are intimately related to their morphology, which depends on the miscibility of the components, mechanism, and kinetics of phase separation. Phase diagram of polymer blends have been studied by many authors⁶⁰⁻⁶⁴. For example, Jo et al⁶¹ have reported the phase diagram of ternary polymer blends of poly(styrene-co-acrylic acid), PEO, and PMMA, the results are shown in figure I.11. The miscibility has been determined from the cloud point and the glass transition temperature. Blends with high PEO content are judged to be miscible when the cloud point was observed at temperature higher than the melting point of PEO or /when a single glass transition temperature was observed. Blends with low PEO content were judged to be miscible when the blend film was transparent at room temperature or / and when a single glass transition temperature was observed.

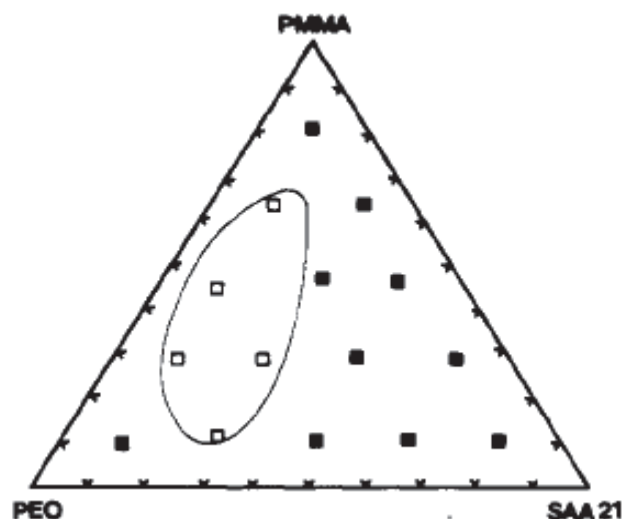


Figure I.11. Phase diagram of the blends PSAA/PMMA/PEO at room temperature. In the figure, ■ indicates that the blends film shows single T_g and clear melts, and □ indicates that the blends film shows cloudy and multiphases behavior⁶¹.

3.5 Polymer blends nanocomposites

Polymer blends nanocomposites started to attract attention in order to improve the miscibility between different polymers which are immiscible. In that sense, it was suggested that nanoclays could contribute to the compatibility of blends based on immiscible polymers and hence improve their properties⁶⁵⁻⁷⁰ as explained in the following section. Basically, for compatibilizing two polymeric phases, the surface tension between the phases needs to be lowered. Furthermore, during the blend processing, the coalescence of the particles needs to be prevented. In that sense, one expects nanoclays to play both roles with polymer blends.

3.5.1 Influence of nanoparticles on the miscibility of polymer blends

One of the traditional methods for improving the miscibility between two polymers is to use a third component so-called compatibilizer, which is compatible or miscible with both polymers. This compatibilizer may be a homopolymer or a block, graft or star-like copolymer. In the 2000s, inorganic nanoparticles have also been used as compatibilizers. They could improve the miscibility but novel properties can also originate from them. Nevertheless, it has been reported that, nanoparticles which play the role of compatibilizer, should be at least partially exfoliated and should have some interaction with both phases⁶⁶.

The first attempt for using organoclay as compatibilizer was demonstrated by Gelfer et al⁷¹ who have studied the effects of organoclay on the morphology, and on the thermal and rheological properties of PS/PMMA blends. However, even though they found out that PS/PMMA blends remained phase-separated after addition of organoclay, a drastic reduction in the average microdomain sizes (from 1-1.5 μm to ca. 300-500nm) was measured indicating that organoclay partially compatibilized the immiscible blend. Wang

et al⁶⁹ have investigated another clay (natural or modified montmorillonite) as a compatibilizer for immiscible PP/PS blends. Montmorillonite lead to significant improvement of the miscibility as displayed in figure I.12. The miscibility enhancement depended on the concentration of montmorillonite in the blends, whether the nanoparticles were organically modified or not. SEM images of pure PP/PS blends (figure I.12.a) revealed PS domains with a size of 3-4 μ m which decreased down to 2-3 μ m, 0.5-1.0 μ m and 0.3-0.5 μ m when 2wt%, 5-10wt%, and 30wt% of montmorillonite were respectively added. The miscibility enhancement between PP and PS was due to the intercalation of both PP and PS molecules into the same montmorillonite gallery. However, PP/PS blends with up to 30wt% of unmodified MMT showed almost the same size of PS domains as that of pure PP/PS blends, indicating that only the organically treated montmorillonite can be efficiently.

Sinha Ray et al⁶⁶ reported on the compatibilizing effect of organoclay in immiscible PS/PP blends or PS/polypropylene grafted with maleic anhydride (PP-g-MA). They studied the presence of the nanoparticles within the blends by various techniques including XRD, SEM, TEM and interfacial tension measurements, correlated to mechanical tests in the traction mode. Their results clearly indicated that organoclays acted at the same time as nanofillers and also as compatibilizers. In the case of PS/PP-g-MA, the decrease in domain size was more pronounced, and it was even not possible to distinguish the dispersed domains. This was attributed to fact that the compatibilization process was more efficient when PP was grafted with maleic anhydride which ensured interaction with the surface of nanoclays. The same results have been obtained by Sinha Ray et al⁶⁷ with an immiscible poly(carbonate) PC/PMMA blend where organoclays were added or with PP/poly[(butylene succinate)-co-adipate] (PBSA) and PP-g-MA/PBSA blends where montmorillonite was added as evidenced on figure 1.13.

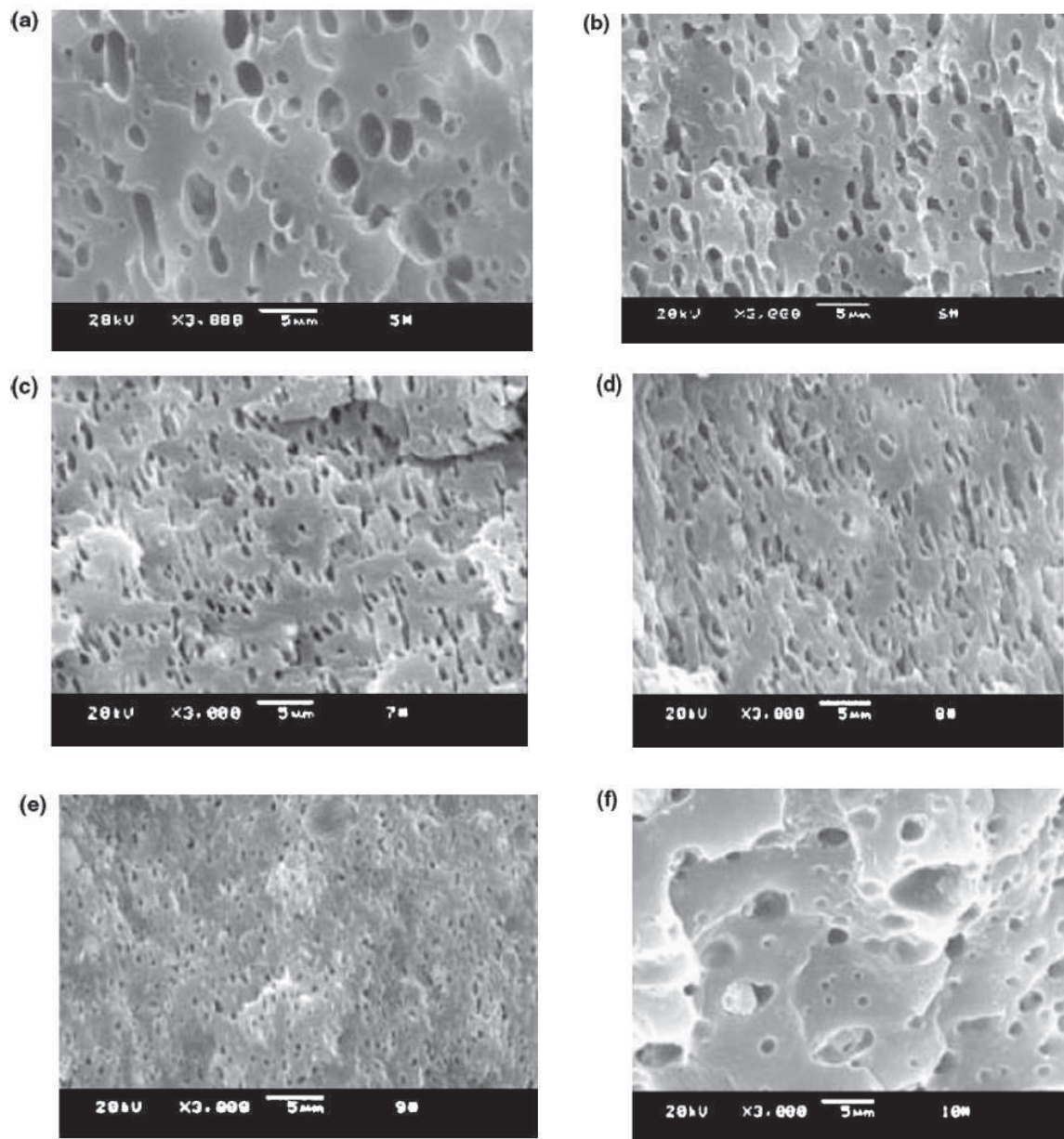


Figure I.12. SEM photographs of PP/PS blends with varying amount of modified montmorillonite: (a) 0% (b) 2% (c) 5% (d) 10% (e) 30%, and (f) PP/PS/MMT with 30% of unmodified MMT (PP/PS = 70:30)⁶⁹

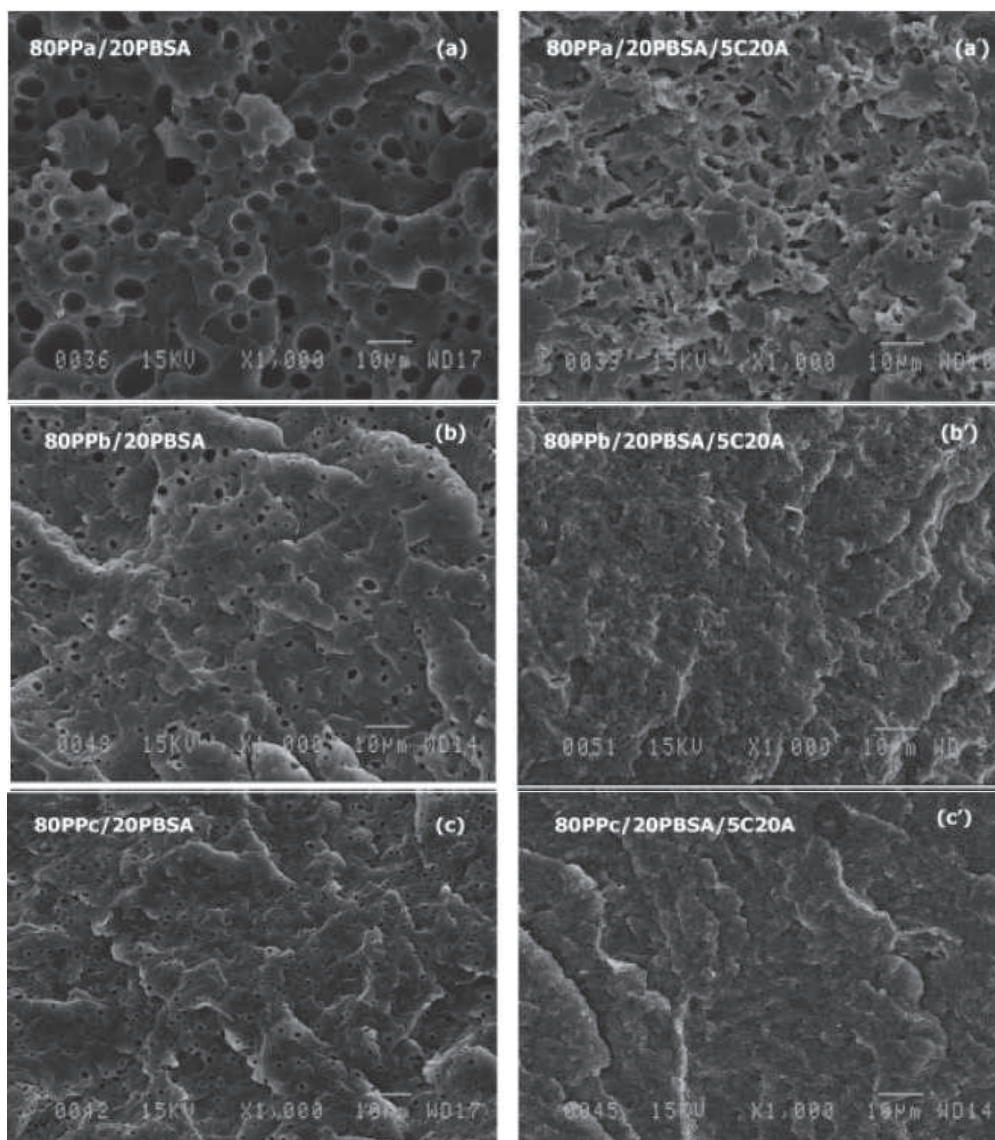


Figure I.13. Phase morphology of chemically etched freeze-fractured surface of annealed compression-molded samples of various virgin and organically modified nanoparticles PP/PBSA

Essay et al⁷⁰ have also supported the suggestion of using inorganic nanoparticles as compatibilizers for immiscible polymer blends, by studying the use of montmorillonite as reinforcing and compatibilizing filler for immiscible polymer blends of acrylonitrile-butadiene rubber (NBR) and styrene-butadiene rubber (SBR). SEM results showed that, the NBR domains were separated from the continuous SBR phase in the absence of filler. However, the incorporation of the fillers improves the compatibility between SBR and NBR resulting in almost a single phase. In this peculiar case, montmorillonite can act as compatibilizer regardless it was organically modified or not, whereas, for immiscible PP/PS blends, montmorillonite should be organically modified prior to be used as a compatibilizer⁶⁹.

Very recently, Chen et al⁶⁵ have verified the ability for clay to perform a compatibilizing role in immiscible blends of PS/poly(acrylonitrile-styrene) (ABS) .

However, the exact mechanism for the nanoparticles to act as compatibilizers and then increasing the miscibility of polymers blends has been investigated in a poor extend. Nesterov et al⁷²⁻⁷³ have proposed a theoretical background to account for such a phenomenon. Considering binary immiscible polymer blends (A and B) and filler S, the free energy of mixing (per unit volume) is given by :

$$\Delta G_{S+B+A} = RT (\chi_{SA}\varphi_S\varphi_{SB} + \chi_{SB}\varphi_S\varphi_B + \chi_{AB}\varphi_A\varphi_B) = \Delta G_{SA} + \Delta G_{SB} + \Delta G_{AB}$$

Where φ_S refers to the concentration of functional groups of the fillers interacting with corresponding functional group of the polymers.

If both polymeric components of the blends are strongly adsorbed onto the fillers surface, both interaction parameters of polymer A and B with the functional groups at the surface of the fillers (χ_{SA} and χ_{SB}), are then negative. These theoretical results were confirmed experimentally with PMMA/PVA blends reinforced with fumed silica since introducing the fillers into the blends leads to an increase of the phase separation temperature. Such an increase of the miscibility is due to a decrease of the interaction parameter until reaching a negative value. Other confirmations of this theory have been obtained by Wang et al and Sinha Ray et al⁶⁶⁻⁶⁹ who demonstrated that increasing the compatibility between fillers and polymer blends lead to an increase of the miscibility.

Lastly, to clear up the role of nanoparticles acting as compatibilizers, Ginzburg et al⁷⁴ have developed a thermodynamic multiscale approach for studying the behavior of model polymer-clay mixtures. They have combined Density Functional Theory (DFT)⁷⁵⁻⁷⁷ with Self-Consistent Field model (SCF)⁷⁸⁻⁷⁹ to calculate the phase behavior of the particles coated with surfactants and dispersed in a polymer. The long range interaction between the clay sheets was calculated using a SCF approach approximation. This approach allowed to explicitly taking into account the characteristics of the grafted fillers and the strength of their interactions with the polymer melt. The dependence of the phase behavior of the mixture on the volume fraction of clay and the Flory-Huggins parameter (polymer-polymer interaction) were studied by using DFT. Depending on the value of these critical parameters and on the clay volume fraction, the system can be isotropic or nematic. Furthermore, the model discriminated conditions that lead to the stabilization of the homogeneous exfoliated phase and to the narrowing of the immiscible two phase regions.

3.5.2 Influence of nanoparticles on the thermal, and dynamics properties of polymer blends.

As explained previously, nanoparticles can act as compatibilizers for polymer blends but they also play a great role for improving other properties such as thermal and dynamic properties of polymer blends as discussed in next section.

Understanding the dynamic of polymers in miscible and immiscible blends is considered to be an accurate way for understanding the blend properties⁸⁰⁻⁸⁴. Jeddi et al⁸⁵

have investigated the influence of nanolayered silicates on the segmental dynamics for PEO/PMMA. They concluded that, for the pure PEO/PMMA blend, the segmental dynamic of PEO chains was enhanced within the blend due to presence of the rigid PMMA matrix which confined PEO as shown in figure I.14 a. Moreover, with low contents of nanolayered silicate, the segmental dynamics was even more enhanced due to the ability for the nanoparticles to reduce the interaction between the components by creating more rigid structure around PEO chains as showed in figure I.14 b. However, high nanoclay content could destroy the packing and structural arrangement of rigid PMMA matrix around PEO chains and therefore reduced the confinement effect as well as segmental dynamics, as displayed in figure I.14. c.

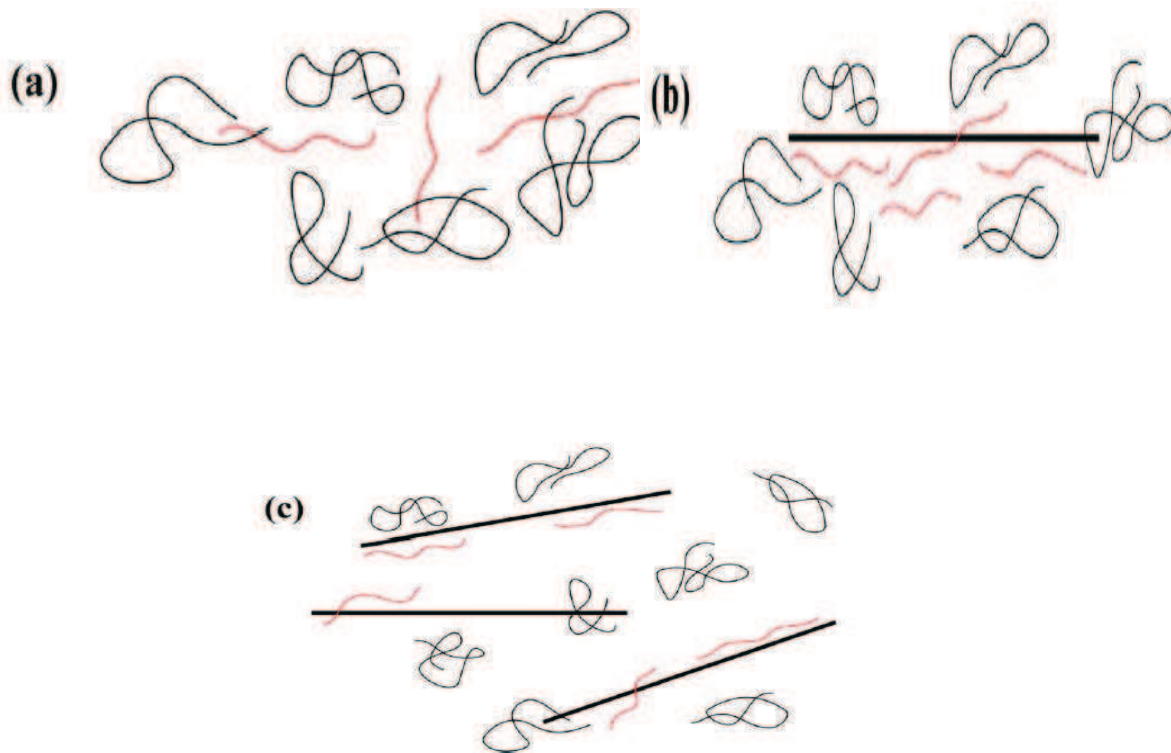


Figure I.14. A schematic representation of the influence of different amounts of nanolayered silicate on the confinement effect of PMMA matrix on PEO chain in a polymer blend: (a) pure PEO/PMMA blends (b) PEO/PMMA/2 wt% nanoclay, and (c) PEO/PMMA/5 wt% nanoclay

Jeddi et al have also investigated the thermal properties of PEO/PMMA miscible blends nanocomposites. They showed that the incorporation of nanoclay did not affect the glass transition temperature.

Ramirez-vargas et al⁸⁶ have investigated thermal stability of low-density polyethylene (LDPE) and polyethylene-co-vinyl acetate (PEVA) blends with different types of organo-modified montmorillonite. Aluminum hydroxide as a flame retardant system was also added. Their result showed that, the filled LDPE/PEVA blends presented

a huge decrease of the degradation rate when compared to the unfilled blends. Becso et al⁸⁷ have studied the thermal properties of polyamide 66 (PA66)/polyamide 12 (PA12)/clay based nanocomposites, by using modulated DSC and thermo-gravimetric analysis (TGA). Their results showed that, well-dispersed filler improved thermal oxidative stability, in particular dealing with PA66 rich blends. Gelfer et al⁷¹ reported that, the presence of organoclay affected the glass transition temperature for PS/PMMA blends. A single broad glass transition around 105°C was measured for the pure PS/PMMA blend whereas upon adding organoclays, two distinct T_g (at 78°C and at 115°C) were measured. However, the authors suggested that the lower T_g was related to the regions near the PS/PMMA interface, which was plasticized by free surfactant molecules originating from organoclay but had no explanations for the higher T_g . Essawy et al⁷⁰ have studied the influence of organoclay on the T_g of NBR/SBR blends. The DSC scan for the individual component of the blends, NBR, SBR, and for the NBR/SBR (50/50) blends with and without nanoparticles are displayed in the figure I.15. T_g for individual component were found to be -50°C and -30°C for SBR and NBR respectively. For unfilled blends, T_g of the SBR remained unchanged while that for NBR was shifted to -25°C. After loading with fillers, T_g of SBR shifted to -48°C while that of the NBR remained to -30°C which reflected new molecular interactions at the boundaries resulting from the presence of the filler at interface between NBR and SBR.

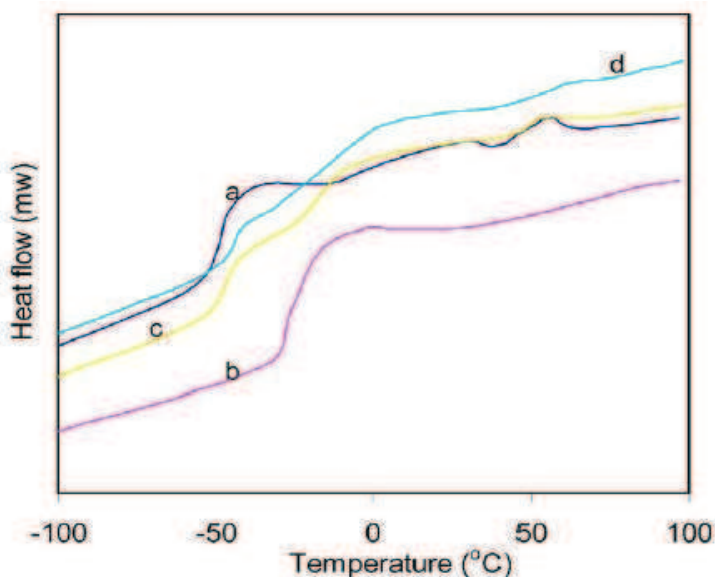


Figure I.15. DSC scans of (a) SBR, (b) NBR, (c) NBR/SBR (50/50), and NBR/SBR/Filler (50/50/20)

3.5.3 Influence of nanoparticles on the mechanical properties of polymer blends

Mechanical properties of three components (polymer/polymer/filler) nanocomposites have been less investigated compared to that for two components (polymer/filler) nanocomposites. However, in both cases it has been proven that, the mechanical properties of both formulations strongly depend on the morphology of the systems. For example, Esayev et al⁸⁸ have reported that for an immiscible polymer blend where

nanoparticles are added, the latter are localized in one of the domains. The modulus could then be evaluated on one hand by separately calculating the modulus of the phase containing particles and on the other hand by utilizing composite theories to determine the overall modulus of the entire system. Jeddi et al⁸⁵ have worked on miscible PEO/PMMA blends where montmorillonite has been added. XRD results proved the exfoliation of the nanoclays but only PEO chains were expected to interact with montmorillonite leading to an exfoliated structure.

Sinha Ray et al⁶⁶ have studied the mechanical properties of PS/PP and PS/PP-g-MA blends filled with nanoparticles. Their results demonstrated that addition of nanoparticles in the blends increased the modulus as well as the elongation at break, and decreased the tensile strength with respect to native blends. The influence of the nanoparticles on the mechanical properties of PS/PP-g-MA was more pronounced compared to that of PS/PP. This was due to the fact that nanoparticles acted as better compatibilizer with PS/PP-g-MA than with PS/PP as explained previously. These observations agreed with what has been reported in literature regarding the possible strong interactions between dispersed nanoclay and polymer matrix which could significantly impact the rheological behavior of the composites in the molten state. Actually, as for simple polymer matrix based nanocomposites, exfoliation of the nanoclays within the matrix lead to a liquid-solid transition. Gelfer et al⁷¹ have studied the influence of organoclays on the rheological properties of PS/PMMA blends by using oscillatory shear measurements. They found that the separate addition of organoclays in PS and PMMA did not change the frequency dependence of G' as shown in figure 1.16 and the systems exhibited a rheological behavior typical of melt regardless the important content of nanoclays. However, the apparent flow-activation energy decreased with increasing the clay content for both PMMA-clay and PS-clay nanocomposites (Figure 1.17) which indicated that clay particles in PMMA, PS, and PS/PMMA blends acted more like inert fillers rather than physical crosslinkers. Noteworthy, it should be mentioned that organoclays when added to PS/PMMA blends self-concentrated in the PMMA phase and at the interfacial region.

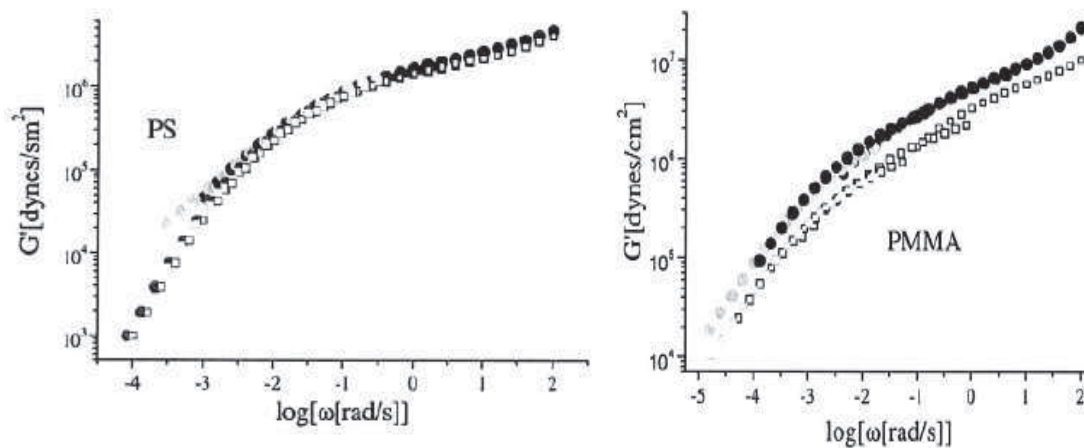


Figure I.16. Frequency dependence of G' when organoclays were added to PS and PMMA. Open symbols no organoclays added, black symbol 10wt% of nanoclays added⁷¹.

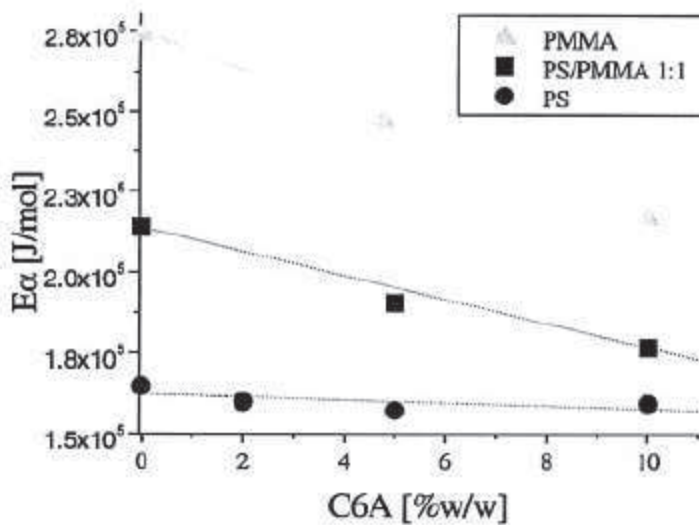


Figure I.17 Influence of organoclays on the flow-activation energy for PS, PMMA, and PS/PMMA blends⁷¹

4 Conclusion:

Nanoclays are useful particles for providing functional and improved mechanical properties to polymer matrix based nanocomposites. However, in order to optimize these properties, caution must be paid in order to fully exfoliate the sheets of nanoclay within the polymeric matrix. In order to do so, the chemistry of the nanoparticles must be well controlled and the mixing process of the nanoparticles with the polymeric matrix is of prior importance. Different characterization methods can be used in order to check at the local scale if the nanoclays are fully exfoliated or not. These structural investigations may be in a second step correlated with mechanical measurements.

Nanoclays can also be useful for compatibilizing polymer blends. They will then play two roles: first they will decrease the surface tension between the two polymeric phases and second they will prevent the coalescence of the microdomains.

After setting the state of the art regarding these two complementary topics, we will now focus on the experimental investigation of these both systems.

References

1. Koo, J. H., *Polymer nanocomposites: processing, characterization, and applications*. McGraw-Hill: 2006.
2. Gupta, R. K.; Kennel, E.; Kim, K. J., *Polymer nanocomposites handbook*. CRC Press.
3. Hatzigrigoriou, N. B.; Papaspyrides, C. D., Nanotechnology in Plastic Food-Contact Materials. *Journal of Applied Polymer Science* 122, (6), 3720-3739.
4. Bhattacharya, S. N.; Kamal, M. R.; Gupta, R. K., *Polymeric nanocomposites: theory and practice*. Carl Hanser Publishers: 2008.
5. Saad, G. R.; Abd Elhamid, E. E.; Elmenyawy, S. A., Dynamic cure kinetics and thermal degradation of brominated epoxy resin-organoclay based nanocomposites. *Thermochim. Acta* 524, (1-2), 186-193.
6. Dirote, E. V., *Focus on nanotechnology research*. Nova Science Publishers: 2004.
7. Mai, Y. W.; Yu, Z. Z.; Institute of Materials, M.; Mining, *Polymer nanocomposites*. CRC Press: 2006.
8. Lepoittevin, B.; Pantoustier, N.; Devalckenaere, M.; Alexander, M.; Kubbies, D.; Calberg, C.; R. Jérôme; Dubois, P., Polymer/layered silicate nanocomposites by combined intercalative polymerization and melt intercalation: a masterbatch process. *Polymer* **2003**, 44, 2033-2040.
9. Wang, M.; Pramoda, K. P.; Goh, S. H., Enhancement of interfacial adhesion and dynamic mechanical properties of poly(methyl methacrylate)/multiwalled carbon nanotube composites with amine-terminated poly(ethylene oxide). *Carbon* **2006**, 44, (4), 613-617.
10. Warsaw, C. M.; Roy, R., classification and a scheme for the identification of layer silicates. *Geol. Soc. Am. Bull.* **1961**, 72, (10), 1455-1492.
11. www.calys.org, Revised classification of clays materials. *clay and clay minerals* **1991**, 39, (3), 333-335.
12. Alexandre, M.; Dubois, P., *Materials Science and Engineering* **2000**, (28), 1-63.
13. Koo, C. M.; Kim, M. J.; Choi, M. H.; Kim, S. O.; Chung, I. J., Mechanical and rheological properties of the maleated polypropylene-layered silicate nanocomposites with different morphology. *Journal of Applied Polymer Science* **2003**, 88, (6), 1526-1535.
14. Loiseau, A. Elaboration et caractérisation de Nanocomposites modèles Laponite/Polyoxyde d'ethylene. Ph.D, du maine, Le mans, 2006.
15. Ko, M. B.; Jho, J. Y.; Jo, W. H.; Lee, M. S., Effect of matrix viscosity on clay dispersion in preparation of polymer/organoclay nanocomposites. *Fiber. Polym.* **2002**, 3, (3), 103-108.
16. Fornes, T. D.; Yoon, P. J.; Keskkula, H.; Paul, D. R., Nylon 6 nanocomposites: the effect of matrix molecular weight (vol 42, pg 9929, 2001). *polymer* **2002**, 43, (7), 2121-2122.
17. Tanoue, S.; Utracki, L. A.; Garcia-Rejon, A.; Sammut, P.; Ton-That, M. T.; Pesneau, I.; Kamal, M. R.; Lyngaae-Jorgensen, J., Melt compounding of different grades of polystyrene with organoclay. Part 2: Rheological properties. *Polym. Eng. Sci.* **2004**, 44, (6), 1061-1076.
18. Ioyens, W.; Jannasch, P.; Maurer, F. H. J., Poly(ethylene oxide)/Laponite nanocomposites via melt-compounding: effect of clay modification and matrix molar mass. *Polymer* **2004**, 46, 915-928.
19. Fornes, T. D.; Yoon, P. J.; Keskkula, H.; Paul, D. R., Nylon 6 nanocomposites: the effect of matrix molecular weight. *Polymer* **2001**, 42, (25), 09929-09940.

20. Loiseau, A.; Tassin, J. F., Model Nanocomposites Based on Laponite and Poly(ethylene oxide): Preparation and Rheology *Macromolecules* **2006**, 39, 9185-9191.
21. Loyens, W.; Jannasch, P.; Maurer, F. H. J., Effect of clay modifier and matrix molar mass on the structure and properties of poly(ethylene oxide)/Cloisite nanocomposites via melt-compounding. *Polymer* **2004**, 46, 903-914.
22. Kim, S. W.; Jo, W. H.; Lee, M. S.; Ko, M. B.; Jho, J. Y., Effects of Shear on Melt Exfoliation of Clay in Preparation of Nylon 6/Organoclay Nanocomposites. *Polymer Journal* **2002**, 34, (3), 103.
23. Vaia, R. A.; Ishii, H.; Giannelis, E. P., Synthesis and Properties of Two-Dimensional Nanostructures by Direct Intercalation of Polymer Melts in Layered Silicates. *Chem.mater* **1993**, (5), 1694-1696.
24. T.G. Gopakumar, J. A. L., M. Kontopoulou, J.S. Parent, Influence of clay exfoliation on the physical properties of montmorillonite/polyethylene composites. *polymer* **2002**, 43 5483-5491.
25. Prachum, Y.; Strauss, R. H. A.; Kiatkamjornwong, S., The Physical and Mechanical Properties of Beta-Nucleated Polypropylene/Montmorillonite Nanocomposites. *Journal of Applied Polymer Science* **2011**, 122, (2), 1066-1076.
26. Wang, K.; Liang, S.; Zhao, P.; Qu, C.; Tan, H.; Du, R.; Zhang, Q.; Fu, Q., Correlation of rheology-orientation-tensile property in isotactic polypropylene/organoclay nanocomposites. *Acta Materialia* **2007**, 55, (9), 3143-3154.
27. Solomon, M. J.; Almusallam, A. S.; Seefeldt, K. F.; Somwangthanaroj, A.; Varadan, P., Rheology of Polypropylene/Clay Hybrid Materials. *Macromolecules* **2001**, 34, (6), 1864-1872.
28. Kim, D. H.; Fasulo, P. D.; Rodgers, W. R.; Paul, D. R., Structure and properties of polypropylene-based nanocomposites: Effect of PP-g-MA to organoclay ratio. *polymer* **2007**, 48, (18), 5308-5323.
29. Scarfato, P.; Russo, P.; Acierno, D., Preparation, Characterization, and Release Behavior of Nanocomposite Microparticles Based on Polystyrene and Different Layered Silicates. *Journal of Applied Polymer Science* **2011**, 122, (6), 3694-3700.
30. Liu, C.; Wu, H.; Yang, Y.; Zhu, L.; Teng, Y., The structure and properties of a novel nanocomposite films from chitosan and layered zirconium phosphonate. *Journal of Applied Polymer Science* **2011**, 120, (2), 1106-1113.
31. Pistek, D.; Merinska, D.; Dujkova, Z.; Tupy, M., The mechanical and optical properties of the PVB nanocomposites. In *Proceedings of the 3rd WSEAS international conference on Advances in sensors, signals and materials*, World Scientific and Engineering Academy and Society (WSEAS): Faro, Portugal, 2010; pp 26-29.
32. Alam, M. A.; Azarian, M. H.; Osterman, M.; Pecht, M., Prognostics of Failures in Embedded Planar Capacitors using Model-Based and Data-Driven Approaches. *J. Intell. Mater. Syst. Struct.* **2011**, 22, (12), 1293-1304.
33. Paul, D. R.; Robeson, L. M., Polymer nanotechnology: Nanocomposites. *polymer* **2008**, 49, (15), 3187-3204.
34. Lloyd, S. M.; Lave, L. B., Life Cycle Economic and Environmental Implications of Using Nanocomposites in Automobiles. *Environmental Science & Technology* **2003**, 37, (15), 3458-3466.
35. Sevastyanova, O.; Qin, W.; Kadla, J. F., Effect of nanofillers as reinforcement agents for lignin composite fibers. *Journal of Applied Polymer Science* 117, (5), 2877-2881.

36. 97-02-0047, A. P. B.-. Nanocomposites New Low-Cost, High-Strength Materials for Automotive Parts. www.patapsco.nist.gov **1997**.
37. Krishnamoorti, R.; Giannelis, E. P., Rheology of End-Tethered Polymer Layered Silicate Nanocomposites. *Macromolecules* **1997**, 30, (14), 4097-4102.
38. www.azonano.com
39. Xie, F., Halley, Peter J, Bio-nanocomposites based on starch In *Nanocomposites with biodegradable polymers: Synthesis, properties and future perspectives* Mittal, V., Ed. Oxford University Press: 2011; pp 21-40.
40. Gaharwar, A. K.; Schexnailder, P. J.; Dundigalla, A.; White, J. D.; Matos-Perez, C. R.; Cloud, J. L.; Seifert, S.; Wilker, J. J.; Schmidt, G., Highly Extensible Bio-Nanocomposite Fibers. *Macromol. Rapid Commun.* **2011**, 32, (1), 50-57.
41. Koning, C.; Van Duin, M.; Pagnouille, C.; Jerome, R., Strategies for compatibilization of polymer blends. *Prog. Polym. Sci.* **1998**, 23, (4), 707-757.
42. Robeson, L. M., *Polymer blends: a comprehensive review*. Hanser: 2007.
43. *Review of Science and Technology in ESCWA Member Countries*. UN: 2001.
44. www.pslc.ws.
45. Dell'Erba, R.; Groeninckx, G.; Maglio, G.; Malinconico, M.; Migliozi, A., Immiscible polymer blends of semicrystalline biocompatible components: thermal properties and phase morphology analysis of PLLA/PCL blends. *polymer* **2001**, 42, (18), 7831-7840.
46. Doleman, B. J.; Sanner, R. D.; Severin, E. J.; Grubbs, R. H.; Lewis, N. S., Use of compatible polymer blends to fabricate arrays of carbon black-polymer composite vapor detectors. *Anal. Chem.* **1998**, 70, (13), 2560-2564.
47. Chen, C. Segmental dynamics in poly(ethylene oxide)/poly(methyl methacrylate) blends. PhD, The Pennsylvania State University, Pennsylvania, 2006.
48. Lodge, T. P.; Wood, E. R.; Haley, J. C., Two calorimetric glass transitions do not necessarily indicate immiscibility: The case of PEO/PMMA. *Journal of Polymer Science Part B: Polymer Physics* **2006**, 44, (4), 756-763.
49. Zhuang, H.; Pearce, E. M.; Kwei, T. K., Self-association in poly(styrene-co-4-vinylbenzenephosphonic acid) and miscibility of its blends. *polymer* **1995**, 36, (11), 2237-2241.
50. Zhu, K. J.; Chen, S. F.; Ho, T.; Pearce, E. M.; Kwei, T. K., Miscibility of copolymer blends. *Macromolecules* **1990**, 23, (1), 150-154.
51. Ren, L.; Zhang, M. Y.; Wang, Y. R.; Na, H.; Zhang, H. X., Investigation on the Miscibility of the Blends of Poly(methyl methacrylate) and Poly(styrene-co-acrylonitrile). *Journal of Applied Polymer Science* **2012**, 123, (1), 292-298.
52. Ciardelli, F.; Penczek, S.; Division, N. A. T. O. S. A., *Modification and blending of synthetic and natural macromolecules*. Kluwer Academic Publishers: 2004.
53. Utracki, L. A., *Polymer blends handbook*. Kluwer Academic Publishers: 2002.
54. Pascault, J. P.; Polymères, G. F. d. E. e. d. a. d.; Lyonnais, F. d. P., *Polymer blends*. Wiley-VCH: 2003.
55. Titievsky, K.; Rutledge, G. C., Mixtures of interacting particles with well-defined composition field coupling chi parameters. *The Journal of Chemical Physics* **2008**, 128, (12), 124902-10.
56. Utracki, L. A., *Polymer alloys and Blends*. Hanser: new york, 1989.
57. Barlow, J. W.; Paul, D. R., Polymer blends and alloys—a review of selected considerations. *Polymer Engineering & Science* **1981**, 21, (15), 985-996.
58. Suvorova, A. I.; Tyukova, I. S.; Khasanova, A. K.; Nadol'skii, A. L., Structure and phase diagrams of poly(ethylene oxide) blends with amorphous polymers. *Vysokomol. Soedin.* **2000**, 42, (1), 35-42.

59. Nishi, T.; Wang, T. T., Melting Point Depression and Kinetic Effects of Cooling on Crystallization in Poly(vinylidene fluoride)-Poly(methyl methacrylate) Mixtures. *Macromolecules* **1975**, *8*, (6), 909-915.
60. Suvorova, A. I.; Hassanova, A. H.; Tujkova, I. S., Phase equilibrium in blends of crystalline poly(ethylene oxide) – amorphous poly(methyl acrylate) or poly(methyl methacrylate). *Polymer International* **2000**, *49*, (9), 1014-1016.
61. Jo, W. H.; Kwon, Y. K.; Kwon, I. H., Phase behavior of ternary polymer blends of poly(styrene-co-acrylic acid), poly(ethylene oxide), and poly(methyl methacrylate). *Macromolecules* **1991**, *24*, (16), 4708-4712.
62. DuPrez, F. E.; Tan, P. W.; Goethals, E. J., Poly(ethylene oxide)/poly(methyl methacrylate) (semi-)interpenetrating polymer networks: Synthesis and phase diagrams. *Polym. Adv. Technol.* **1996**, *7*, (4), 257-264.
63. Müller, M.; Binder, K.; Albano, E. V., Phase diagram of polymer blends in confined geometry. *Journal of Molecular Liquids* **2001**, *92*, (1-2), 41-52.
64. Avella, M.; Martuscelli, E., Poly-d(-)(3-hydroxybutyrate)/poly(ethylene oxide) blends: phase diagram, thermal and crystallization behaviour. *polymer* **1988**, *29*, (10), 1731-1737.
65. Chen, B.; Evans, J. R. G., Mechanical properties of polymer-blend nanocomposites with organoclays: Polystyrene/ABS and high impact polystyrene/ABS. *Journal of Polymer Science Part B: Polymer Physics* **2011**, *49*, (6), 443-454.
66. Sinha Ray, S.; Pouliot, S.; Bousmina, M.; Utracki, L. A., Role of organically modified layered silicate as an active interfacial modifier in immiscible polystyrene/polypropylene blends. *polymer* **2004**, *45*, (25), 8403-8413.
67. Sinha Ray, S.; Bousmina, M., Compatibilization Efficiency of Organoclay in an Immiscible Polycarbonate/Poly(methyl methacrylate) Blend. *Macromol. Rapid Commun.* **2005**, *26*, (6), 450-455.
68. Sinha Ray, S.; Bandyopadhyay, J.; Bousmina, M., Effect of Organoclay on the Morphology and Properties of Poly(propylene)/Poly[(butylene succinate)-co-adipate] Blends. *Macromolecular Materials and Engineering* **2007**, *292*, (6), 729-747.
69. Wang, Y.; Zhang, Q.; Fu, Q., Compatibilization of Immiscible Poly(propylene)/Polystyrene Blends Using Clay. *Macromol. Rapid Commun.* **2003**, *24*, (3), 231-235.
70. Essawy, H.; El-Nashar, D., The use of montmorillonite as a reinforcing and compatibilizing filler for NBR/SBR rubber blend. *Polymer Testing* **2004**, *23*, (7), 803-807.
71. Gelfer, M. Y.; Song, H. H.; Liu, L.; Hsiao, B. S.; Chu, B.; Rafailovich, M.; Si, M.; Zaitsev, V., Effects of organoclays on morphology and thermal and rheological properties of polystyrene and poly(methyl methacrylate) blends. *Journal of Polymer Science Part B: Polymer Physics* **2003**, *41*, (1), 44-54.
72. Nesterov, A. E.; Lipatov, Y. S.; Ignatova, T. D., Effect of an interface with solid on the component distribution in separated phases of binary polymer mixtures. *Eur. Polym. J.* **2001**, *37*, (2), 281-285.
73. Nesterov, A. E.; Lipatov, Y. S., Compatibilizing effect of a filler in binary polymer mixtures. *polymer* **1999**, *40*, (5), 1347-1349.
74. Ginzburg, V. V.; Singh, C.; Balazs, A. C., Theoretical Phase Diagrams of Polymer/Clay Composites: The Role of Grafted Organic Modifiers. *Macromolecules* **2000**, *33*, (3), 1089-1099.
75. Sholl, D.; Steckel, J. A., *Density Functional Theory: A Practical Introduction*. John Wiley & Sons: 2011.

76. Seminario, J. M.; Politzer, P., *Modern density functional theory: a tool for chemistry*. Elsevier: 1995.
77. Xuan, X. P.; Wang, Y. L.; Wang, N., Density functional theory calculations of structure, FT-IR and Raman spectra of S-phenyl thioacetate. *Spectroc. Acta Pt. A-Molec. Biomolec. Spectr.* **2011**, 81, (1), 236-241.
78. Fliflet, A. W.; Lee, R. C.; Read, M. E.; DC., N. R. L. W., *Self-Consistent Field Model for the Complex Cavity Gyrotron*. Defense Technical Information Center: 1987.
79. Lee, W. B.; University of California, S. B. C. E., *Self-consistent field theory for inhomogeneous polymers with reversible bonding*. University of California, Santa Barbara: 2007.
80. Lutz, T. R.; He, Y.; Ediger, M. D.; Cao, H.; Lin, G.; Jones, A. A., Rapid Poly(ethylene oxide) Segmental Dynamics in Blends with Poly(methyl methacrylate). *Macromolecules* **2003**, 36, (5), 1724-1730.
81. Chen, C. X.; Maranas, J. K., A Molecular View of Dynamic Responses When Mixing Poly(ethylene oxide) and Poly(methyl methacrylate). *Macromolecules* **2009**, 42, (7), 2795-2805.
82. Kumar, S. K.; Shenogin, S.; Colby, R. H., Dynamics of miscible polymer blends: Role of concentration fluctuations on characteristic segmental relaxation times. *Macromolecules* **2007**, 40, (16), 5759-5766.
83. Shenogin, S.; Kant, R.; Colby, R. H.; Kumar, S. K., Dynamics of miscible polymer blends: Predicting the dielectric response. *Macromolecules* **2007**, 40, (16), 5767-5775.
84. Zawada, J. A.; Ylitalo, C. M.; Fuller, G. G.; Colby, R. H.; Long, T. E., Component relaxation dynamics in a miscible polymer blend: poly(ethylene oxide)/poly(methyl methacrylate). *Macromolecules* **1992**, 25, (11), 2896-2902.
85. Jeddi, K.; Qazvini, N. T.; Jafari, S. H.; Khonakdar, H. A.; Seyfi, J.; Reuter, U., Investigating the Effect of Nanolayered Silicates on Blend Segmental Dynamics and Minor Component Relaxation Behavior in Poly(ethylene oxide)/Poly(methyl methacrylate) Miscible Blends. *J. Polym. Sci. Pt. B-Polym. Phys.* **2011**, 49, (4), 318-326.
86. Ramirez-Vargas, E.; Sanchez-Valdes, S.; Parra-Tabla, O.; Castaneda-Gutierrez, S.; Mendez-Nonell, J.; Ramos-deValle, L. F.; Lopez-Leon, A.; Lujan-Acosta, R., Structural Characterization of LDPE/EVA Blends Containing Nanoclay-Flame Retardant Combinations. *Journal of Applied Polymer Science* **2012**, 123, (2), 1125-1136.
87. Besco, S.; Lorenzetti, A.; Roso, M.; Modesti, M., PA66/PA12/clay based nanocomposites: structure and thermal properties. *Polym. Adv. Technol.* **2011**, 22, (11), 1518-1528.
88. Isayev, A. I., *Encyclopedia of Polymer Blends: Volume 1: Fundamentals*. John Wiley & Sons: 2010.

Chapter 2: Polymer nano-composites based on Laponite and poly (ethylene oxide)

2.1 Overview

The aim of our work in this chapter is to establish the relationships between rheological properties in the molten state and dispersion state of the particles. As shown in the bibliographic part, in recent years, an impressive number of studies indicated that, when clay particles are largely exfoliated, the melt rheology of nanocomposites can change from melt-like or liquid-like behaviors to gel-like or solid-like behavior, which essentially suggests that the dispersed clay platelets behave as physical crosslinkers. As we mentioned in first chapter, the rheological properties and dispersion state of the clay nanoparticles have been driven by many parameters. In this chapter we are focusing on three very important parameters (preparation methods, molecular weight of polymer matrix, and the type of protection of the particles) that have a great effect on rheological properties of model nanocomposites based on geometrically well-defined nano-particles (Laponite) and poly (ethylene oxide) (PEO).

So far, here we fixed two parameters and study the effect of third parameter. For example; we studied the effect of the type of protection of the particles by using same molecular weight of polymer matrix, (PEO of molecular weight 10 000 g/mol) and compared data using the same method of preparation. In case of studying the effect of preparation methods, the matrix molecular weight and type of protection of the particles should be fixed whereas preparation methods are varied.

The influence of preparation methods on the rheological properties of PEO/Laponite nanocomposites is first considered in this work. We present the results in the form of a draft paper that focused on the influence of preparation methods, by investigating the linear viscoelastic response of various controlled dispersions using dynamic linear rheology and by describing the fine characterization of the filler dispersion inside the polymer matrix on a local and large scale using SAXS and DSC. We finally link the linear viscoelastic response of the materials at low deformation with the nanocomposites structure. Furthermore, here all the results presented in this draft deal, with samples that contain Laponite particles protected by PEO adsorbed chains of 10,000 g/mol and PEO of the same molecular weight as the matrix.

The second parameter investigated in this work is the influence of matrix molecular weight. The linear viscoelastic properties as well as state of dispersion for PEO/Laponite nanocomposites are strongly changed with change of matrix molecular weight. So far, we present a draft paper that analyzes the results of linear viscoelastic properties and dispersion state of Laponite particles. We propose the construction of master curves to bring some kind of universality in this system. We link the structures with the properties as mentioned in the first paper. It is noteworthy to mention that we will compare the samples issued from different kinds of preparation methods.

Influence of the type of protection of Laponite particles on properties and structure of PEO/Laponite nanocomposites is presented in a third draft paper. Critical point of this study is to establish the relationships between type of protection of the particles and linear viscoelastic properties of nanocomposites. Especially, what is the main difference between protecting the particles by using adsorbed-PEO10k and grafted-*trimethylammonium-poly(ethylene glycol)* on properties of PEO/Laponite nanocomposites? In case of grafted short chains, how does the size of these chains affect the properties of PEO/Laponite nanocomposites? Third draft paper aims to answer these aforementioned questions.

Finally a general conclusion is added to this chapter. It includes some results not given previously which show the coherence of our data.

2.2 A New Insight into the Structure and Rheology of Model Poly (ethylene oxide)/ Laponite Clay Nanocomposites

2.2.1 Introduction

Polymer layered-silicates hybrids encompasses the high level polymer processability with unique and superior material properties at “fairy dust” filler levels - typically not shared by their more conventional microscopic counter parts. Some of these properties, for example include (1) improved tensile strength and modulus without sacrificing the impact strength; (2) a remarkable increase in thermal stability as well as self-extinguishing characteristics for flammability; and (3) a several-fold reduction in the permeability of gases. This is attributed to an increased clay-polymer interaction by the extraordinarily high specific surface together with nanometric features of the anisotropic clay suspended in the polymer medium¹⁻⁵. In a broad sense, dispersion of layered clay is favored by clay-polymer phase miscibility as well as an effective clay exfoliation during processing. Understanding the state of filler dispersion during processing is therefore crucial for the control and optimization of nanocomposite properties. Although the concept is well established, fundamental studies have lagged towards the control and optimization of particle spatial distribution for tailoring various properties, owing to the lack of well-defined polymer-clay model systems and adequate characterization methodologies.

Rheology of clay filled polymer nanocomposites has been widely investigated due to its bifold benefits: the sensitivity towards nanocomposite structure, and its own right for predicting processability. The existence of a transition between a viscoelastic liquid and a viscoelastic solid upon increasing the particle's concentration seems to be well established although in many cases the low frequency plateau of the storage modulus G' is not as flat as expected for a solid. Of particular interest is the origin of the linear viscoelastic response corresponding to the solid-like behavior of terminal plateau modulus at clay concentrations much above the critical percolation⁶. Although numerous experimental and simulation studies have suggested possible explanations, a consensus is yet to be reached concerning the physical explanation for the plateau behavior. An earlier accepted view was the existence of a sample spanning clay particle network structure⁷⁻⁹, which has also been experimentally observed by Vermant et al.¹⁰ in PP/ montmorillonite nanocomposites at a 5 wt% clay loading. Other observations (and simulations) have also suggested that polymer-particle interactions can also lead to such effects¹¹⁻¹³. It has been

proposed that in such instances the polymer segments can be “immobilized” near the particles, leading to the formation of particle-mediated transient polymer networks which can result in significant enhancements in elasticity and accounts for the solid-like behavior at pretty low values of nanoparticles concentration¹⁴. A third view suggests a strain amplification effect where the addition of microscopic filler particles to polymer matrices results in a distortion in the applied strain fields, leading to an enhancement in the macroscopic viscoelastic properties of the composite¹⁵⁻¹⁷. A very recent view is to consider these anisotropic dispersions as “nano suspensions” with a clustered clay structure suspended in the polymer melt^{15, 18, 19}. Consequently, scaling concepts by considering fractal clay aggregates (or/and polymers) have been used to understand rheological characteristics of polymer clay reinforced systems. In this approach, the fractal nature of the aggregates is influenced by several factors like processing, molecular parameters, etc. The nature of the network structure responsible for the rheological properties in nanocomposites depends largely on the systems investigated and often remains controversial. However, none of these studies could establish precisely the nature of the network overall length scales involved, neither any fractal dimension has been directly measured in nanocomposites using scattering techniques. On the contrary, mechanical measurements, and more precisely the power law exponent of the evolution of the modulus with the clay concentration has been used to evaluate a fractal dimension. It relies however on a model.

In the present study, we used nanocomposites based on Poly(ethylene oxide) and Laponites model systems to obtain controlled dispersions of Laponite discoid nanoparticles in polymer melts to further investigate the structure-rheology correlation in such nanocomposites. The model character of PEO-Laponite systems stems from several considerations among which the well defined nanometric dimensions of Laponite particles, that appear as disc like particles with a diameter of 25 nm and a thickness of 1 nm, the fact that these particles can be dispersed down to the individual scale in water under well defined conditions. PEO offers the advantage to be available with various molecular weights.²⁰ Dispersion control was achieved by using two strategies. An optimized and probably highest state of dispersion experimentally achievable was obtained using a specially designed solution preparation. A more realistic one for practical applications was obtained by dilution of a master batch in the molten state.

It has been shown that Laponite particles can be dispersed in water and that PEO chains adsorb from solution onto Laponite particles giving stable dispersions in water, thanks to the additional particles steric stabilization via the adsorbed chains^{21,22}. Furthermore, PEO readily intercalates the galleries of Laponite clay owing to the enthalpy gain due to crown ether formation and also by an entropic gain by releasing confined water molecules previously bound to the metal counter ion²³. Taking advantage of this factor, nanocomposite samples of varying particle loadings were prepared by a freeze drying procedure in order to limit the effect of the attractive van der Waals interactions and thus reach a particularly good dispersion of Laponite particles in the PEO matrix. Various states of filler dispersions were further achieved by using dilution of a master batch that offers a combined view of the processing effects on structure and morphology of polymer-clay systems. Mixing in flow fields (especially shear) is thought to show layer by layer exfoliation to give stable dispersion and was therefore used for preparing nanocomposites from concentrated master batches. The small angle X-ray scattering technique (SAXS) has proven to be a unique tool for quantitative analysis of the nanocomposite dispersion in polymer clay nanocomposites²⁴⁻²⁶.

This paper follows a previous study, where it was shown that the low frequency modulus was related to the fraction of well dispersed particles, which was varied by changing the type of steric protection of the Laponite particles. Here, we present a new approach to describe the frequency and filler volume fraction dependences of the viscoelastic moduli of a model nanocomposite system obtained by adding very small to large amounts of Laponite clay into a PEO matrix. First we will investigate the linear viscoelastic response of the various controlled dispersions using dynamic linear rheology. Secondly we will describe the fine characterization of the filler dispersion inside the polymer matrix on a local and large scale using SAXS and DSC, and, finally we link the linear viscoelastic response of the material at low deformation with the nanocomposite structure.

2.2.2 Experimental Section

Materials: Poly(ethylene oxide) of molecular weight $M_w = 10000$ g/mol was purchased from Sigma Aldrich and was used as received. The melting temperature as measured by DSC is 67.5 °C, while size exclusion chromatography (SEC) in THF gave $M_w = 9850$ g/mol and $M_w/M_n = 1.08$. Laponite RD, obtained from Rockwood additives Ltd.

(U.K.), with density 2570 kg/m^3 was used. The cation exchange capacity is 0.95 mequiv/g , and the specific surface is $750 \text{ m}^2/\text{g}$.

Preparation: Samples were prepared via two routes, by solution-exfoliation⁵ and by melt compounding. To begin with, the Laponite particles were at first protected by adsorption with PEO (of the same molecular weight) in water to improve the compatibility of the particles with the polymer matrix.

Protection of Laponite particles. Laponite powder and PEO were dispersed separately under gentle stirring in deionized water (milli Q) for 24 hours at a concentration of 1 % (w/w). The two solutions were mixed in equal proportions and were kept under agitation for 36 hours to allow for the adsorption of free PEO chains. From our earlier adsorption isotherm studies for PEO 10000 onto Laponite, the surface coverage at saturation was found to be 1.14 g/g with PEO 10000. Thus in the above solution, each individual Laponite particle was expected to be covered at least partly by PEO chains and are hereafter termed as adsorbed particles.

Preparation by solution route. In this preparation method, a calculated volume (0.1 -9 wt% for final Laponite concentration) of the above prepared PEO 10000 adsorbed Laponite solution was mixed with a 5% solution of PEO 10000, and kept under stirring for 4-5 hours. In order to preserve as much as possible the homogeneous state of dispersion, this sterically stabilized suspension, in which the majority of particles are still non-aggregated, was frozen rapidly with liquid nitrogen and was freeze dried for 12 to 18 hours at $-46 \text{ }^\circ\text{C}$ to remove the water. The freeze drying yields a fluffy powder that was finally compressed at $110 \text{ }^\circ\text{C}$ (in the molten state of PEO) for 2 hours, to form 1 mm thick discs.

Preparation by Melt Compounding. Here, the final freeze dried powder with a given Laponite concentration (3.4, 6.1 and 9.1 wt%) obtained via solution route was considered as a concentrated master batch for melt intercalation. Nanocomposites (0.1 -5.75 wt % final Laponite concentration) were prepared by diluting the concentrated master batch by adding the matrix polymer PEO 10000, in the molten state, using a Haake Minilab Microcompounder under corotating twin-screws operating at $110 \text{ }^\circ\text{C}$, and 50 rpm for 10 min. The processing conditions have been optimized for maximum rheological properties. The extrudates were finally compressed in the same way to give 1 mm thick discs.

Hereafter, the particle concentrations in the materials are defined by the amount of bare Laponite. Eventually adsorbed PEO chains are thus not included in the particle's concentration but are counted in the PEO matrix weight and volume fractions.

Characterization.DSC Measurements. Calorimetric measurements were performed on a 2920 modulated DSC from TA Instruments using sealed aluminum pans. Instrument was calibrated for the melting endotherm using Indium standard. About 8-10 mg of the sample was used. The thermal history of the samples was erased by heating to 110 °C at 10 °C/min followed by an isothermal annealing in the molten state at 110 °C for 5 min. Samples were subsequently cooled at 10 °C/min until -20 °C and finally the melting behavior was analyzed at varying heating rates.

Rheology Measurements. Viscoelastic properties of PEO/Laponite nanocomposites were studied using a stress controlled TA ARG2 rheometer equipped with 25 mm diameter stainless steel parallel plates at 1 mm separation. Measurements were performed under oscillatory shear in the linear domain at a fixed temperature of 110 °C, which is well above the melting temperature of PEO. The viscoelastic properties of nanocomposites have been found to depend strongly on the flow history and they undergo a structural ripening with time^{10, 27, 28}. Therefore, in order to allow for complete micro structural equilibration, the samples were first subjected to thermal annealing in the rheometer at a frequency of 0.1 rad/s(*Supporting information*). The time sweep data collected at the end of equilibration indeed showed a relatively faster attainment of constant moduli in solution prepared nanocomposites. Frequency dependency of storage and loss modulus of the equilibrated nanocomposite samples were measured by imposing very small deformation in the frequency range from 100 to 5×10^{-3} rad/s.

Small Angle X-ray Scattering Studies (SAXS).X-ray scattering was performed at room temperature for a wide range of wave vectors ranging from 0.02 Å to 5 Å⁻¹ obtained by combining a low noise 2D gas detector and a “flat image plate” for large angles using a RigakuTM copper rotating anode ($\lambda \sim 1.54$ Å) with high flux and resolution. A pair of OsmicTM confocal mirrors delivered a cylindrical beam of 2×10^7 photons/s over 350µm in diameter with angular divergence below 0.5mrad. All the X-ray beam path and the 1 mm thick nanocomposite pellets were under vacuum (10^{-3} bar) during measurement. For reasons of clarity, the intensities are presented up to 1 Å⁻¹(large angle peaks of crystallization of PEO chains are omitted), with absolute intensity scale units (cm^{-1} *i.e.* cm^2 per cm^3 of sample).

2.2.3 Results

Rheology.

Figure 1 shows the frequency dependence of viscoelastic moduli measured at 110 °C for samples prepared by solution route with various Laponite loadings ranging from 0 to 9.1 weight percent. The pure PEO is predominantly viscous, with the loss modulus always higher than the storage modulus. The viscoelastic moduli show the expected power law behavior over the measured frequency range, i. e., $G' \approx \omega^{-1}$ and $G'' \approx \omega^2$, (G' of pure PEO can only be detected at intermediate frequencies due to rheometer inertia at higher frequencies).

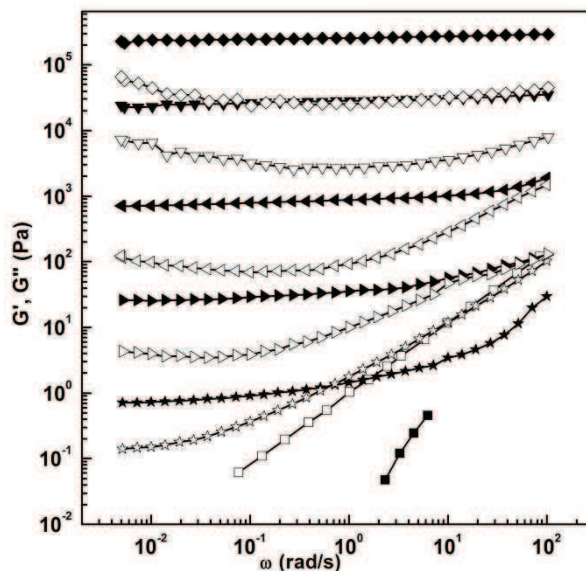


Figure 1. Storage modulus G' (closed symbols) and loss modulus G'' (open symbols) vs. frequency ω at 110 °C for samples prepared by solution route having several different Laponite loadings (weight percent). PEO 10000 neat (\blacksquare \square), 0.1 % (\star \star), 0.5 % (\blacktriangleright \triangleright), 2.0 % (\blacktriangleleft \triangleleft), 5.75 % (\blacktriangledown \triangledown) and 9 % (\blacklozenge \lozenge).

Upon addition of Laponite, even with an amount as low as 0.1 weight percent, the predominant viscous behavior of the pure polymer was suppressed by the drastically increased storage modulus at low frequencies. The elastic modulus, G' becomes higher than G'' , and weakly dependent on oscillating frequency. Consequently, an additional intersection between the elastic and viscous moduli was observed at around $\omega = 0.5$ rad/s, above which the nanocomposite behavior was predominantly that of pure PEO 10000. The existence of a low frequency terminal plateau with an elastic modulus around 1 Pa is a clear evidence of a fragile elastic solid having some structural connectivity. As seen from figure 1, for nanocomposites having up to 2 wt% of Laponite the G' , G'' crossover

frequency as well as the moduli values at the crossover, both increased with increasing clay content suggesting a predominant elastic contribution. For samples with clay content beyond 2 wt% the viscoelastic behavior, especially the elastic modulus G' , was found independent over whole the measured frequency range and the previously observed G' and G'' crossover failed to occur. This would indicate an elastic clay network structure with no polymer relaxation processes over the time scales ranging between 1×10^{-1} - 2×10^2 seconds. However, some extent of dissipation does happen at longer times, which presumably is due to slow structural rearrangements remaining after annealing for 8 hours. The higher the filler content, the greater is the time extent of such network rearrangements. This behavior has been observed in several systems like pastes.

For a further understanding of the solid-like network elastic structure, the aforementioned findings were compared with the viscoelastic response of samples with same Laponite content but prepared by a differing processing procedure, i.e., via melt route. Figure 2 gives the evolution of viscoelastic moduli of the melt prepared samples obtained by diluting a 9.1 wt% of master batch concentration. The overall viscoelastic behavior, including the apparition of plateau at low frequencies was similar to the solution prepared nanocomposite samples. However, the value of storage modulus was systematically lower for melt prepared samples. Moreover for a given Laponite loading the observed additional G' , G'' crossover occurred at lower frequencies as compared to solution prepared samples.

The behavior of the loss tangent provides deeper insight into the apparent solid behavior. Figure 3 compares the evolution of $\tan \delta$ as a function of frequency between solution and melt prepared samples having identical Laponite contents.

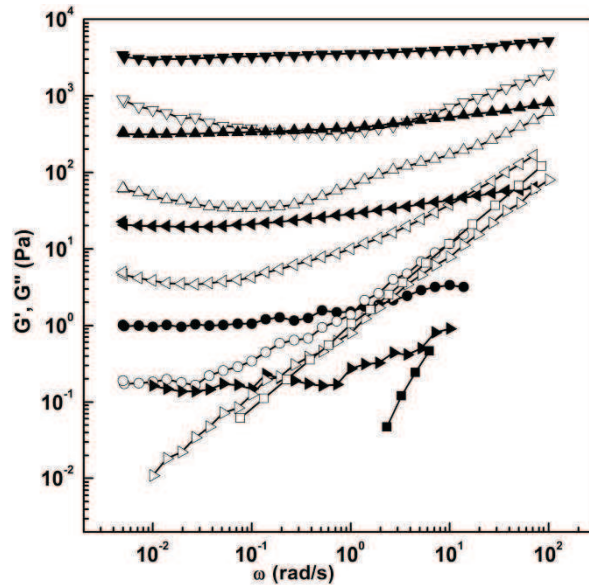


Figure 2. Storage modulus G' (closed symbols) and loss modulus G'' (open symbols) vs. frequency ω at 110 °C for samples prepared via melt route from an initial master batch concentration of 9.1 % to yield several different final Laponite particle loadings (weight percent). PEO 10000 neat (■□), 0.5 % (▶▷), 1.0 % (●○), 2.0 % (◄◄), 3.3 % (▲△) and 5.75 % (▼▽).

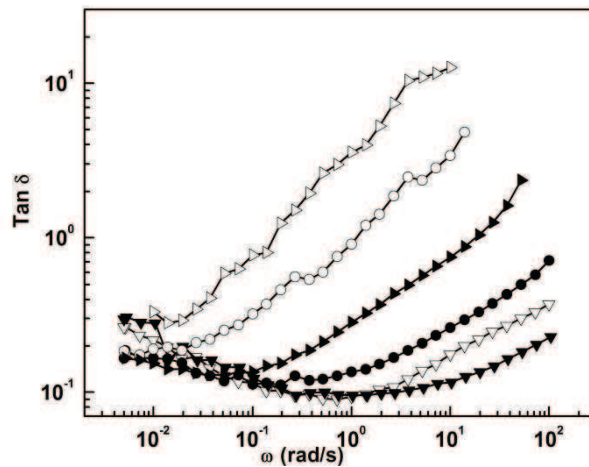


Figure 3. Comparison of $\tan \delta$ vs. frequency ω curves for solution (closed symbols) and melt prepared samples (open symbols) measured at 110 °C samples having Laponite concentrations: 0.5 % (▶▷), 1.0 % (●○) and 5.75 % (▼▽).

In all cases, the $\tan \delta$ decreased with lowering frequencies, goes through a minimum before increasing slightly at low frequencies. The negative slopes in the low frequency side suggest slow rearrangements without any disruption of the elastic polymer / clay network structure. Moreover, as seen from figure 3, for a fixed Laponite loading the relaxation time corresponding to the onset of predominant elastic behavior due to the clay

network structure varied for the dispersions obtained via different processing routes. The apparition of the network effects on viscoelasticity was delayed by an order of magnitude in samples prepared via melt procedure.

The variation in viscoelastic response between the various dispersions is obtained from the scaling plots given in figure 4.

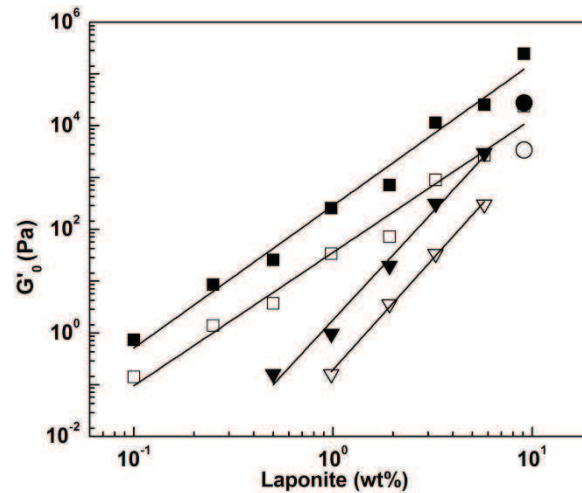


Figure 4: Scaling laws of G'_0 (closed symbols) and G''_0 (open symbols) vs. the Laponite weight fraction for nanocomposites prepared by solution route (■□) and via melt method (▼▽). Also shown are the plateau modulus values of 9.1 wt% Laponite prepared via solution route and further directly extruded by melt procedure G'_0 (●) and G''_0 (○). (G'_0 values corresponds to the storage modulus values at a frequency of 0.01 rad/s, whereas the plateau loss modulus corresponds to the minimum of G'' versus frequency curves).

The moduli varied as a power law of Laponite concentration, i.e., $G \approx \phi^\alpha$, and the values of the power law exponent are given by Table 1. The existence of a scaling behavior for plateau moduli would indicate a composition range far above the percolation threshold in both dispersion types. The percolation concentration is expected to be lower than 0.1 wt % of Laponite, and is, to the best of our knowledge, the lowest value for percolation concentration reported so far for clay modified nanocomposites. Noticeably, the expected percolation threshold is much lower than those observed in aqueous Laponite gels, which is at 0.3 wt% of Laponite²².

Moduli (Pa)	Power law exponent (α)	
	Solution route (S)	Melt route (M)
G'_0	2.7 ± 0.2	4.1 ± 0.1
G''_0	2.6 ± 0.2	4.3 ± 0.2

Table 1: Values of power law exponents for solution and melt prepared Laponite /PEO dispersions

Plateau moduli were consistently lower for melt prepared samples. An identical behavior was also observed with the viscous modulus. Noticeably, the behavior of a mixture of 0.5% prepared in solution is very close to a 2% mixture prepared by the melt route, and obtaining the modulus G' of the mixture prepared by solution method at 0.1% requires ten times more Laponite through melt route. Comparing the loss tangents of the nanocomposites with similar plateau moduli (G'_0) revealed close but not fully similar relaxation behavior as shown in figure 5.

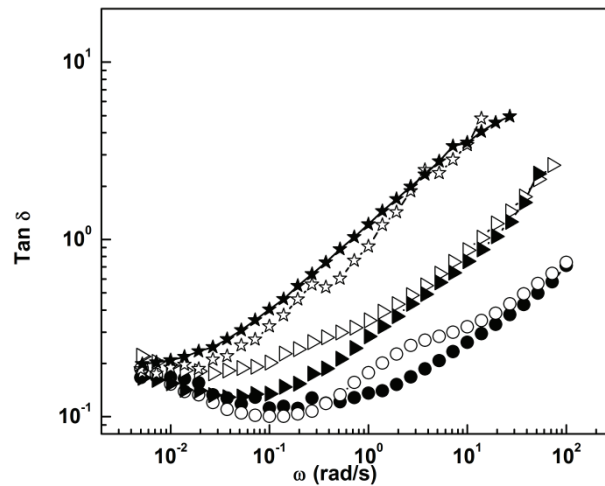


Figure 5. Comparison of $\text{Tan } \delta$ vs. frequency ω curves between solution (closed symbols) and melt prepared (open symbols) nanocomposites with identical G'_0 plateau modulus values measured at 110 °C: 1.0% (●) & 3.4%(○), 0.5 % (▲) & 2 % (▷), 0.1 % (★) & 1.0 % (☆).

Indeed, at identical "macroscopic" modulus at low frequencies, the melt prepared samples show an additional relaxation process at intermediate frequencies. The characteristic frequency increases upon increasing the concentration of particles.

In order to study the effect of initial master batch concentration on the terminal plateau modulus, 1 wt% melt prepared samples were produced from solution prepared

master batches at various concentrations (9.1, 6.1 and 3.4 %). Figure 6 shows that, at a given final concentration of particles, the modulus is greatly reduced when the amount of added pure PEO 10000 polymer increases. Quantitatively, the variation of G' is greater than 10-fold when diluted from 9.1 wt% or 3.4 wt%. If it is admitted that a high level of modulus reflects a high level of connectivity between the particles, it can be deduced that concentrated master batches are more difficult to disperse in molten PEO than less concentrated ones.

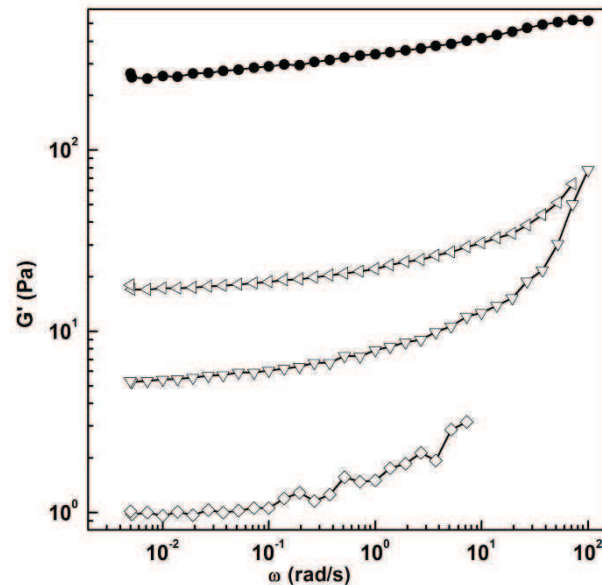


Figure 6. Storage modulus as a function of frequency for 1 % (in weight percent) Laponite in PEO 10000 nanocomposite prepared by solution route (●) compared with melt prepared samples (open symbols) with a same final 1 % Laponite obtained from different initial master batch concentrations; 3.4% (Δ), 6.1 % (∇) and from 9.1 % (◇).

SAXS Results:

To link rheological observations with structure, scattering measurements were performed on a wide range of scattering vectors. Unlike rheological measurements carried out in melt, structural characterization was carried out at room temperature, i.e., with crystallized PEO chains. At large scattering angles, the Bragg peaks due to the crystalline structure of PEO appear (not shown in the figures). The crystallinity decreases slightly when the concentration of particles in the mixtures is increased. Figure 7 shows the $I(Q)$ vs. momentum transfer (Q) curve for the mixtures prepared by solution route.

The crude Laponite powder SAXS curve shows a correlation peak located at 0.5 \AA^{-1} that reflects the parallel stacking of bare Laponite particles and indicates the presence of a relatively soft smectic order (aligned stacked clays). The highly crystalline pure PEO

presents markedly diffuse "wiggles" at small angle, as already reported in the literature²⁹⁻³¹. These oscillations reflect a degree of periodicity between amorphous regions and crystalline lamellae. Thanks to the relatively low molecular weight of the polymer chains, one PEO chain embedded in lamellae can form several folds at the surfaces. For instance, the peak at 20.3 nm corresponds to 2 folds of PEO chains. At small angles, the addition of Laponite generates a strong increase in the SAXS intensity, thereby reflecting an increase in the amount of Laponite-PEO interface per sample unit volume since particles come with a high contrast prior to amorphous or crystalline PEO (~ 0.39 electrons. \AA^{-3} for PEO and ~ 0.85 electrons. \AA^{-3} for Laponite). The intensity falls along a characteristic slope in log-log scales corresponding to a Q^{-2} scattering law, the same slope obtained by the diffraction of the PEO crystalline smectic sheets. Correspondingly, the oscillations existing in the pure polymer progressively disappear and become virtually invisible above 2% particles, masked by the strong scattering of the Laponite discs/PEO interface and the possible increase in PEO disorder. It may be noted that although the system is in the form of a viscoelastic solid (in the molten state), there remains a fraction of Laponite smectic aggregates, each made of a few particles, giving a structure correlation peak corresponding to a stacking distance of 1.9 nm. For composite samples, this peak is shifted towards lower Q values from that of pure Laponite, showing evidence of intercalation of polymer chains in such clay stacks³². The intensity of this peak increases with the concentration of Laponite, and, follows an overall linear increase with the fraction of introduced particles as verified by the inset graph in figure 7 with intensity versus amount of Laponite at a value of $Q = 0.93 \text{ \AA}^{-1}$. This shows, within a first approximation, that the fraction of stacks, with respect to the total number of particles remains constant.

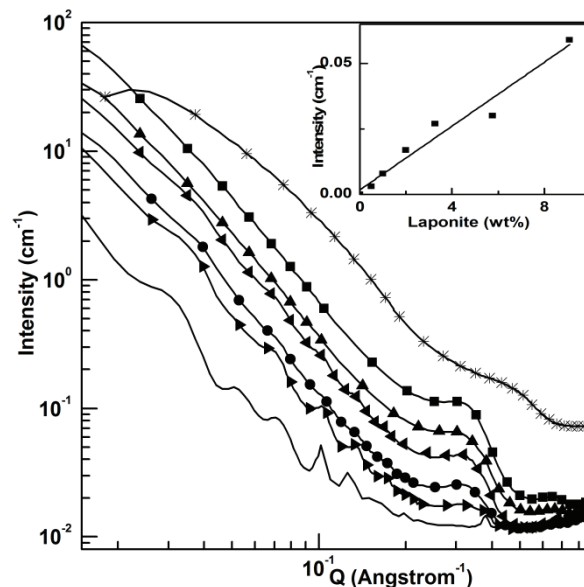


Figure 7. Small angle X-ray scattering profiles of nanocomposites prepared via solution route having different Laponite concentrations (weight percent). PEO 10000 neat (—), 0.5 % (▶), 1 % (●), 2.0 % (◀), 3.3% (▲), 9.1 % (◆) and crude Laponite (*). The crude Laponite curve comes with an arbitrary shifting factor and is thus not plotted on absolute scale of the intensity, contrarily to all other curves, since the sample thickness cannot be established unambiguously for a dry clay powder. The inset graph gives the intensity values at $Q = 0.93 \text{ \AA}^{-1}$ versus Laponite concentration.

While rheological measurements show clear differences, SAXS curves for samples prepared by solution and melt route, as shown in Figure 8 are quite similar. In particular, the peak reflecting the presence of aggregates with few stacked particles is unchanged both in position and intensity. The main differences lie in the changes in the wiggles due to the crystalline lamellae. Wiggles tend to be less pronounced in samples prepared by the melt route.

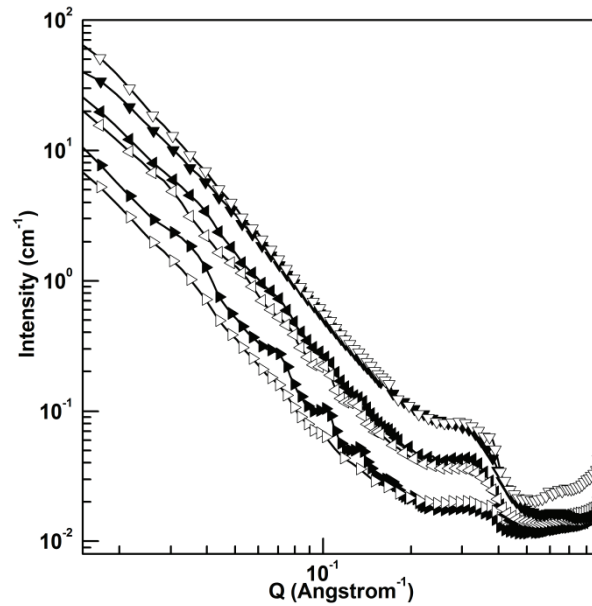


Figure 8. Small angle X-ray scattering curves of Laponite / PEO 10000 (in weight percent) nanocomposites compared between those prepared by solution (closed symbols) and via melt route (open symbols) having different Laponite concentrations (weight percent). 0.5 % ($\blacktriangleright\triangleright$), 3.3% ($\blacktriangle\triangle$), 5.75 % ($\blacktriangledown\triangledown$).

We also studied the SAXS response of 1% dispersions prepared by the dilution of master batches with initially different concentrations. As revealed from figure 9, the mesoscopic structure probed with X-rays over length scales extending from the particles diameter to the particles thickness (0.02 to 1\AA^{-1} Q-range), is globally unaffected. We can conclude that these samples possess almost equal fractions of dispersed Laponite particles (responsible for the strong scattering that follows a Q^{-2} law as expected for plate like particles observed from 0.02 to 0.2\AA^{-1}) and comparable fraction of small Laponite aggregates made of few stacked particles (peak at $Q = 0.35\text{\AA}^{-1}$).

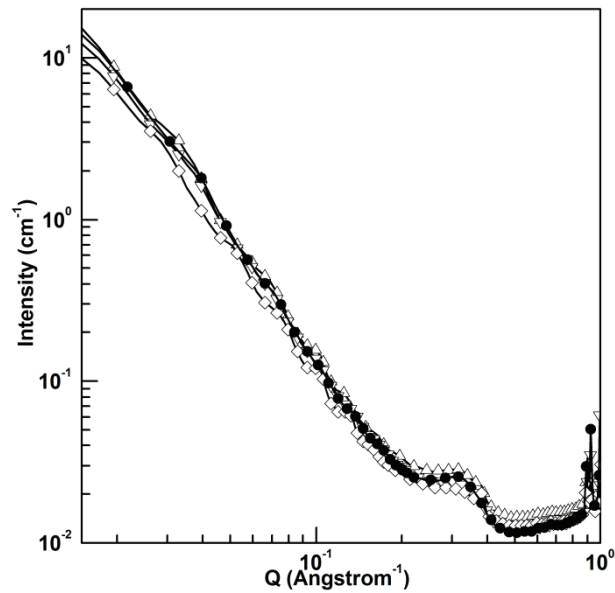


Figure 9. Small angle X-ray scattering curve of 1 % (in weight percent) Laponite concentration in PEO 10000 prepared by solution route (●) compared with melt prepared samples (open symbols) having a final 1 % concentration obtained from different initial master batch concentrations; 3.4% (△), 6.1 % (▽) and from 9.1 % (◇).

DSC Results:

The dispersion effect on the melting behavior of PEO has been studied using DSC measurements and the results are given in figures 10-11 and table 2. Pure PEO 10000 exists in a single crystalline form as revealed from the single melting endotherm at 67.5°C (solid lines in figure 10 & 11). The percentage crystallinity was calculated from the integrated DSC peak areas corrected for the weight fraction of crystallizable component, i.e., the PEO polymer. The enthalpy of fusion of pure PEO was taken as 197.8 J/g³³. As given by table 2, the crystallinity decreased slightly by the addition of Laponite as generally observed for PEO clay nanocomposites³⁴⁻³⁶. In nanocomposites prepared by solution route the fraction of crystallizable PEO however was relatively lower than the melt prepared dispersions.

	Laponite (wt %)	T _{m1} (°C)	T _{m2} (°C)	χ (%)
PEO 10000		67.5	-	94.2
Solution route	1.9	64.3	75.2	87.0
	3.3	63.9	73.3	88.4
	5.75	63.3	69.3	88.3
	9.1	62.0	68.2	86.7
Melt route	1.9	67.2	-	92.4
	3.3	66.7	-	90
	5.75	66.0	-	87.5

Table 2: Values of melting point and crystallinity for nanocomposite samples

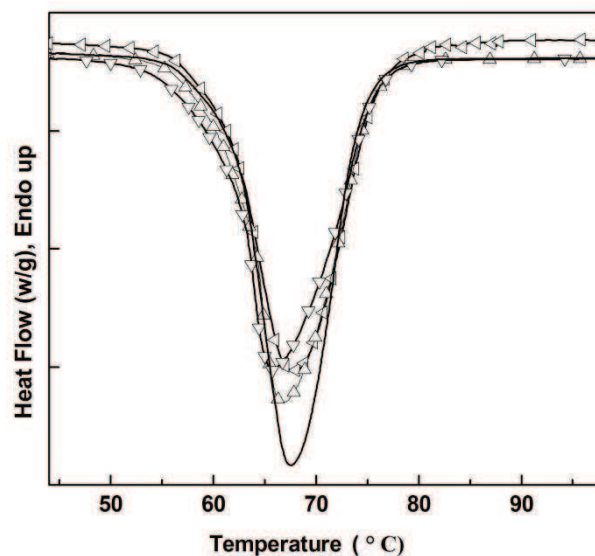


Figure 10. Melting endotherms for the nanocomposite samples with varying Laponite content prepared by melt procedure .Pure PEO 10000 (solid line), 2 % (◁), 3.3 % (△), 5.75 % (▽) and 9.1 % (◇).

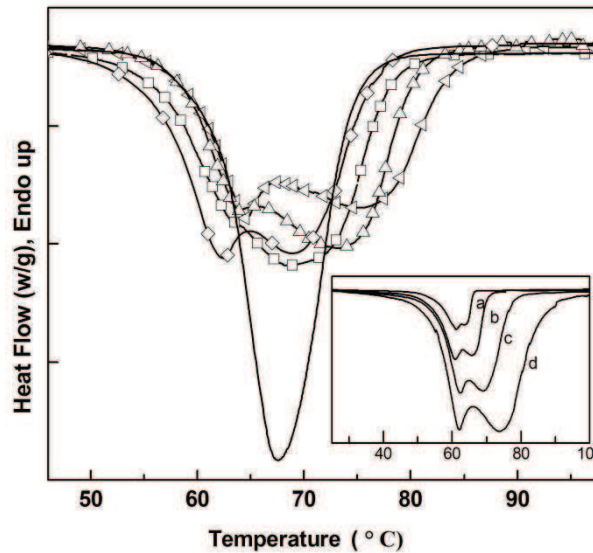


Figure 11. Melting endotherms for the solution prepared nanocomposite samples with varying Laponite content. Pure PEO 10000 (solid line), 2 % (\triangleleft), 3.3 % (\triangle), 5.75 % (∇) and 9.1 % (\diamond). Inset graph: Melting endotherm for 9.1 wt % sample prepared via solution route at varying heating rates. (a) 2 °C/min (b) 5 °C/min (c) 10 °C/min and (d) 20 °C/min.

Figure 10 shows the melting endotherm for the samples prepared by melt procedure. The PEO melting point at 67.5 °C (T_{m1}) decreased slightly with Laponite addition due to the smaller crystalline domains formed in the presence of nanoclay (Table 2). The overall shape of the melting curves of nanocomposites were however comparable with pure PEO 10000. In contrast, in nanocomposites prepared by solution route (figure 11), the PEO melting peak T_{m1} was strongly broadened and a second peak (T_{m2}) was observed at higher temperatures. Notice also that the temperatures at which melting proceeds with maximum rate decreases for both endotherms. PEO crystal reorganization and/or re-crystallization is a possible cause for the high temperature T_{m2} peak and were checked by studying the melting behavior at varying heating rates³⁷. Inset graph in figure 11 shows the melting behavior of 9.1 wt % solution prepared at different heating rates. As shown in the inset picture, the start of the melting is least affected by heating rate. The PEO melting point T_{m1} remained unchanged. If the higher melting endotherm T_{m2} is associated with the melting of reorganized material, one would expect the magnitude of this endotherm to decrease with increasing heating rate. In contrast the magnitude of the high temperature peak (T_{m2}) increased with increasing heating rate, and therefore rules

out PEO crystal re-organization as well as re-crystallization as origins for the observed multiple peaks. The large angle crystallization peaks from SAXS data (not discussed here) revealed no new peaks and thus further confirm the absence of any altered PEO crystalline characteristics. In the absence of any polymer, the pure Laponite seemingly failed to produce any endotherm in the studied temperature range. Considering the variable heating rate behavior in the 9.1% sample the additional high temperature peak (T_{m2}) is supposedly caused by a super heating phenomena³⁸. At higher heating rates the heat is supplied to the sample faster than the melting of the crystals can take place whereby the interior of the crystal heats above the equilibrium melting point giving additional peaks at higher temperatures. Similar findings have been reported recently for few PE based nanocomposites³⁹. As a further approach, we performed a deconvolution of the multiple DSC peaks using PeakFit- V4 software to determine the ratio between the T_{m1} and T_{m2} peak areas. The procedure uses a Gaussian response function with a Fourier deconvolution/filtering algorithm that ensures the conservation of total area. The filtering was set between 75-80% for better noise reduction. The curves were fitted using three variable parameters, namely the peak width at half maxima positions, peak center and the corresponding amplitudes. The results are tabulated in Table 3. According to table 3, the high temperature peak area decreased with increased Laponite amount, i.e., the peak behavior is dependent on the amount of Laponite.

Laponite (wt %)	T_{m1} (°C)	peak area (%)	T_{m2} (°C)	peak area (%)
1.9	64.1	32	75.2	68
3.3	63.4	32.6	73.1	67.4
5.75	63	39.7	71.2	60.3
9.1	61.6	42.5	69.4	57.5

Table 3: Results from the deconvolution analysis on the DSC curves of solution prepared nanocomposites.

2.2.4 Discussion.

The connectivity of solid particles (which may involve polymer chains) responsible for the behavior at low frequencies is highly dependent on the particle concentration and on the procedure used to prepare the sample. Even with melt prepared samples at a given particle concentration, but issued from master batches at different concentrations, huge differences are observed in the rheological behavior, although the structural variations seen in the small angle X-ray scattering data are at least very weak, if not negligible.

One can speculate about the existence of assemblies of connected particles, via particles contacts especially since we are dealing with concentrated solutions or via polymer chains linking two particles. From SAXS data we can deduce that the structure that generates such high levels of moduli is produced either on a larger scale than the one probed here with X- rays (greater than 60nm) or not pictured from the particle distribution in the scales probed. Note that the subtle PEO connections between separated particles would be non addressable from such static scattering techniques where most of the X-ray contrast comes from the particles/PEO interface. In melt route, the dilution by free PEO chains (involving moderate shear) and further annealing at 110 ° C for up to 6-8 hours before the rheological measurement cannot separate particles (from solution prepared master batch) consisting of Laponite stacks (responsible for Bragg peak) on a scale large enough to allow their dispersion. This can be explained fairly well by the analogy with the rheology of immiscible polymer blends. The initial nanocomposite with a high particle concentration can be associated with a high modulus phase (containing Laponite) to be dispersed in a matrix of lower viscosity (pure PEO). Greater the difference in viscosity, lower will be the dispersion, or at least the rupture of the disperse phase.

The concept is further elaborated in the schematic representation of molten nanocomposites given by figure 12, where the possible state of 1 wt% sample obtained by melt processing from concentrated master batches of widely varying initial Laponite concentrations, say 9.1 and 3.4 wt % is sketched.

High Laponiteloadings (S-9.1 wt%)



Dilution with
PEO 10000 g/mol via
Melt Route

PEO/ Laponite (M-1.0 wt %) sample

Low Laponiteloadings (S-3.4 wt%)



 - Laponite

 - PEO 10000 chains in the solution prepared master batch (S)

 - PEO 10000 chains added during dilution by melt method (M)

Figure 12. Schematic representation of the analogous polymer blend behavior explained for melt prepared sample (M) obtained from varying concentration of solution prepared (S) master batches made of dispersed particles. Clusters made of interconnected clay particles (via polymer chains or particles contacts), are surrounded by a dotted line on the figures. They can be considered as a piece of the original solution prepared master batch surrounded by added pure polymer. We did not picture the intercalated Laponite (stacks of few aligned particles) from X-rays.

The structure of high modulus concentrated master batch made of dispersed clays, S-9.1 wt% could be considered as finely dispersed nanoclay network surrounded by an interfacial polymer layer with long relaxation times. It is known from the rheological characterization that it behaves as an elastic solid in the linear range. Upon processing via melt route (i.e., by the extrusion of solution prepared samples with addition of pure PEO 10000 in molten state) the flow field of the low viscous PEO 10000 matrix chains offers only a lubricant effect, and is ineffective in transferring the applied shear stresses to the highly viscous dispersed clusters of master batch having the original Laponite concentration (S-9.1 wt%) and thereby preventing its break up with steady shear in the extruder. Since the suspending fluid in the master batch and the diluent are chemically the same, the role of interfacial tension becomes negligible and dispersion of the master batch occurs by swelling of the PEO chains. Compared to the S-9.1 wt%, the relatively low viscosity of S-3.4 wt% facilitates the dispersion and dilution of clusters by PEO to a much higher extent to give the melt processed 1 wt % sample a 10 times higher modulus value. As observed earlier in figure 4, the linear scaling law of G' and G'' for the two preparation methods never intersect at a concentration of 9.1 wt%, the highest master batch concentration used for the melt route. This is further confirmed by subjecting the 9.1% sample prepared by solution to a passage in the extruder which also gave a drop in modulus (refer to figure 4). Interestingly, the terminal plateau behavior observed in our nanocomposites has also been reported for polymer blends with ultra high viscosity ratios

39-41

In view of the proposed nanocomposite morphology, the observed melting behavior of these model systems seen from DSC could be explained as follows. It has been now generally accepted that during the polymer crystallization, the clay particles are rejected from the developing crystal front to the amorphous regions and they likely reside at the inter-lamellar and/or inter-spherulitic regions. From our DSC studies, the crystallizable PEO in the solution prepared samples exhibited super heating (not seen for melt prepared samples)- i.e. a partial slow melting of the crystals giving multiple melting peaks. Super heating in macromolecular systems generally involves a transition mechanism which allows fast melting only at higher temperatures³⁸. If the amorphous phase involved in the transition is highly viscous so that the molecular motion is slow, or, if the molecular rearrangement to the new phase is slowed down or arrested, superheating is observed. Pertaining to the aforementioned view regarding highly viscous amorphous phase, we suggest that in solution prepared nanocomposites, the presence of well

dispersed highly viscous clay containing amorphous phase of PEO is possibly constrained, thereby restricting the PEO chains molecular motion causing super heating. In solution prepared nanocomposites the lowered PEO melting peak (T_{m1}) values indicate a highly homogeneous dispersion of smaller spherulites. The rheological studies provide further evidence for the finely dispersed clay structure in solution prepared nanocomposites, even at a very low particle concentration. Thus in solution prepared samples the fine clay dispersion facilitates increased extent of clay-polymer interactions. This explains the two separate peaks in the melting endotherms of solution prepared nanocomposites.

Again as evident from SAXS studies, the SAXS intensity “wiggles” due to the PEO lamellar crystallization were slightly more visible for solution prepared nanocomposites than for samples from melt route at same clay content at low loadings (Figure 8). From DCS studies, in melt prepared nanocomposites the pure PEO phase responsible for the T_{m1} peak is less affected by the presence of clay. To our interpretation, in solution prepared samples the clay dispersion is more homogeneous on both the nano and meso scales. In melt route the poor dispersion of the clusters that kept the structure of the solution master batch after poor mixing with pure polymer reduced the extend of pure PEO crystallized sheets and reduced the quantity of clay that goes in the amorphous domains, thus also reducing the X-ray contrast between pure PEO crystalline lamellae and clay containing amorphous regions. This further supports our view on the observed superheating phenomena in our nanocomposite samples.

2.2.5 Conclusion

In this paper we have attempted to explain the structure –property relationships responsible for the rheological behavior of polymer nanocomposites using a well defined PEO/Laponite model system. The effect of filler dispersion on the linear viscoelastic properties of the nanocomposites in the molten state is investigated. The solid like behavior of the filler network were compared for controlled dispersions obtained from two different processes; from solution and via melt processing. Comparison of the linear viscoelastic response for the various dispersions states suggests a reduction in the network structure modulus during melt processing, which, however fails to alter the clay spatial distribution in the nanoscale. This behavior was qualitatively explained using the analogy with the polymer blends.

2.2.6 References

1. Pavlidou, S.; Papaspyrides, C. D., A review on polymer-layered silicate nanocomposites. *Progress in Polymer Science* **2008**, 33, (12), 1119-1198.
2. Kumar, S. K.; Krishnamoorti, R., Nanocomposites: Structure, Phase Behavior, and Properties. *Annual Review of Chemical and Biomolecular Engineering* **2010**, 1, (1), 37-58.
3. DR, P.; LM, R., Polymer nanotechnology: nanocomposites. *Polymer* **2008**, 49, 3187.
4. Schmidt, D. F.; Giannelis, E. P., Silicate Dispersion and Mechanical Reinforcement in Polysiloxane/Layered Silicate Nanocomposites. *Chemistry of Materials* **2010**, 22, (1), 167-174.
5. Alexandre, M.; Dubois, P., Polymer-layered silicate nanocomposites: preparation, properties and uses of a new class of materials. *Materials Science & Engineering R-Reports* **2000**, 28, (1-2), 1-63.
6. Trappe, V.; Weitz, D. A., Scaling of the viscoelasticity of weakly attractive particles. *Physical Review Letters* **2000**, 85, (2), 449-452.
7. Galgali, G.; Ramesh, C.; Lele, A., A Rheological Study on the Kinetics of Hybrid Formation in Polypropylene Nanocomposites. *Macromolecules* **2001**, 34, (4), 852-858.
8. Wang, K.; Liang, S.; Deng, J. N.; Yang, H.; Zhang, Q.; Fu, Q.; Dong, X.; Wang, D. J.; Han, C. C., The role of clay network on macromolecular chain mobility and relaxation in isotactic polypropylene/organoclay nanocomposites. *Polymer* **2006**, 47, (20), 7131-7144.
9. Su, F. H.; Yan, J. H.; Huang, H. X., Structure and Melt Rheology of Long-Chain Branching Polypropylene/Clay Nanocomposites. *Journal of Applied Polymer Science* **2011**, 119, (2), 1230-1238.
10. Vermant, J.; Ceccia, S.; Dolgovskij, M. K.; Maffettone, P. L.; Macosko, C. W., Quantifying dispersion of layered nanocomposites via melt rheology. *Journal of Rheology* **2007**, 51, (3), 429-450.
11. Zhang, Q.; Archer, L. A., Poly(ethylene oxide)/silica nanocomposites: Structure and rheology. *Langmuir* **2002**, 18, (26), 10435-10442.
12. Krishnamoorti, R.; Giannelis, E. P., Rheology of end-tethered polymer layered silicate nanocomposites. *Macromolecules* **1997**, 30, (14), 4097-4102.
13. Sternstein, S. S.; Zhu, A.-J., Reinforcement Mechanism of Nanofilled Polymer Melts As Elucidated by Nonlinear Viscoelastic Behavior. *Macromolecules* **2002**, 35, (19), 7262-7273.
14. Manitiu, M.; Horsch, S.; Gulari, E.; Kannan, R. M., Role of polymer-clay interactions and nano-clay dispersion on the viscoelastic response of supercritical CO₂ dispersed polyvinylmethylether (PVME)-Clay nanocomposites. *Polymer* **2009**, 50, (15), 3786-3796.
15. Song, Y. H.; Zheng, Q. A., Linear viscoelasticity of polymer melts filled with nano-sized fillers. *Polymer* **2010**, 51, (14), 3262-3268.
16. Sereda, L.; Visconte, L. L. Y.; Nunes, R. C. R.; Furtado, C. R. G.; Riande, E., Effect of silica and rice husk ash fillers on the modulus of polysiloxane networks. *Journal of Applied Polymer Science* **2003**, 90, (2), 421-429.
17. Fornes, T. D.; Paul, D. R., Modeling properties of nylon 6/clay nanocomposites using composite theories. *Polymer* **2003**, 44, (17), 4993-5013.
18. Eslami, H.; Grmela, M.; Bousmina, M., Linear and nonlinear rheology of polymer/layered silicate nanocomposites. *Journal of Rheology* **2010**, 54, (3), 539-562.

19. Khalkhal, F.; Carreau, P. J.; Ausias, G., Effect of flow history on linear viscoelastic properties and the evolution of the structure of multiwalled carbon nanotube suspensions in an epoxy. *Journal of Rheology* **2011**, 55, (1), 153-175.
20. Loiseau, A.; Tassin, J. F., Model nanocomposites based on laponite and poly(ethylene oxide): Preparation and rheology. *Macromolecules* **2006**, 39, (26), 9185-9191.
21. Nelson, A.; Cosgrove, T., Dynamic light scattering studies of poly(ethylene oxide) adsorbed on laponite: Layer conformation and its effect on particle stability. *Langmuir* **2004**, 20, (24), 10382-10388.
22. Mongondry, P.; Nicolai, T.; Tassin, J. F., Influence of pyrophosphate or polyethylene oxide on the aggregation and gelation of aqueous laponite dispersions. *Journal of Colloid and Interface Science* **2004**, 275, (1), 191-196.
23. Vaia, R. A.; Ishii, H.; Giannelis, E. P., Synthesis and Properties of 2-Dimensional Nanostructures by Direct Intercalation of Polymer Melts in Layered Silicates. *Chemistry of Materials* **1993**, 5, (12), 1694-1696.
24. Broza, G., Thermoplastic elastomers with multi-walled carbon nanotubes: Influence of dispersion methods on morphology. *Composites Science and Technology* **2010**, 70, (6), 1006-1010.
25. Bandyopadhyay, J.; Ray, S. S., The quantitative analysis of nano-clay dispersion in polymer nanocomposites by small angle X-ray scattering combined with electron microscopy. *Polymer* **2010**, 51, (6), 1437-1449.
26. Drummy, L. F.; Wang, Y. C.; Schoenmakers, R.; May, K.; Jackson, M.; Koerner, H.; Farmer, B. L.; Mauryama, B.; Vaia, R. A., Morphology of layered silicate- (NanoClay-) polymer nanocomposites by electron tomography and small-angle x-ray scattering. *Macromolecules* **2008**, 41, (6), 2135-2143.
27. Mobuchon, C.; Carreau, P. J.; Heuzey, M. C., Structural analysis of non-aqueous layered silicate suspensions subjected to shear flow. *Journal of Rheology* **2009**, 53, (5), 1025-1048.
28. Wang, X. L.; Sun, P. C.; Xue, G.; Winter, H. H., Late-State Ripening Dynamics of a Polymer/Clay Nanocomposite. *Macromolecules* **2010**, 43, (4), 1901-1906.
29. Cheng, S. Z. D.; Chen, J.; Zhang, A.; Barley, J. S.; Habenschuss, A.; Zschack, P. R., Isothermal thickening and thinning processes in low molecular weight poly(ethylene oxide) fractions crystallized from the melt: 2. Crystals involving more than one fold. *Polymer* **1992**, 33, (6), 1140-1149.
30. Cheng, S. Z. D.; Chen, J. H.; Zhang, A. Q.; Heberer, D. P., Nonintegral and Integral Folding Crystal-Growth in Low-Molecular Mass Poly(Ethylene Oxide) Fractions .2. End-Group Effect - Alpha,Omega-Methoxy-Poly(Ethylene Oxide). *Journal of Polymer Science Part B-Polymer Physics* **1991**, 29, (3), 299-310.
31. Cheng, S. Z. D.; Zhang, A. Q.; Barley, J. S.; Chen, J. H.; Habenschuss, A.; Zschack, P. R., Isothermal Thickening and Thinning Processes in Low-Molecular-Weight Poly(Ethylene Oxide) Fractions .1. From Nonintegral-Folding to Integral-Folding Chain Crystal Transitions. *Macromolecules* **1991**, 24, (13), 3937-3944.
32. Stefanescu, E. A.; Stefanescu, C.; Donose, B. C.; Garno, J. C.; Daly, W. H.; Schmidt, G.; Negulescu, I. I., Polymer/clay nanocomposites: Influence of ionic strength on the structure and adhesion characteristics in multilayered films. *Macromolecular Materials and Engineering* **2008**, 293, (9), 771-780.
33. Mark, J. E., Ed, *Physical Properties of Polymer handbook*. AIP press: Woodbury, NY.
34. Loyens, W.; Jannasch, P.; Maurer, F. H. J., Poly(ethylene oxide)/Laponite nanocomposites via melt-compounding: effect of clay modification and matrix molar mass. *Polymer* **2005**, 46, (3), 915-928.

35. Loyens, W.; Jannasch, P.; Maurer, F. H. J., Effect of clay modifier and matrix molar mass on the structure and properties of poly(ethylene oxide)/Cloisite nanocomposites via melt-compounding. *Polymer* **2005**, 46, (3), 903-914.
36. Strawhecker, K. E.; Manias, E., Crystallization Behavior of Poly(ethylene oxide) in the Presence of Na⁺ Montmorillonite Fillers. *Chemistry of Materials* **2003**, 15, (4), 844-849.
37. Menczel, J. D.; Judovits, L.; Prime, R. B.; Bair, H. E.; Reading, M.; Swier, S., *Differential Scanning Calorimetry (DSC)*. John Wiley & Sons, Inc.: 2008; p 7-239.
38. Wunderlich, B., One hundred years research on supercooling and superheating. *Thermochimica Acta* **2007**, 461, (1-2), 4-13.
39. Liu, T. X.; Liu, Z. H.; Ma, K. X.; Shen, L.; Zeng, K. Y.; He, C. B., Morphology, thermal and mechanical behavior of polyamide 6/layered-silicate nanocomposites. *Composites Science and Technology* 63, (3-4), 331-337.
40. Everaert, V.; Aerts, L.; Groeninckx, G., Phase morphology development in immiscible PP/(PS/PPE) blends influence of the melt-viscosity ratio and blend composition. *Polymer* **1999**, 40, (24), 6627-6644.
41. Rameshwaram, J. K.; Yang, Y. S.; Jeon, H. S., Structure-property relationships of nanocomposite-like polymer blends with ultrahigh viscosity ratios. *Polymer* **2005**, 46, (15), 5569-5579.

Supporting Information

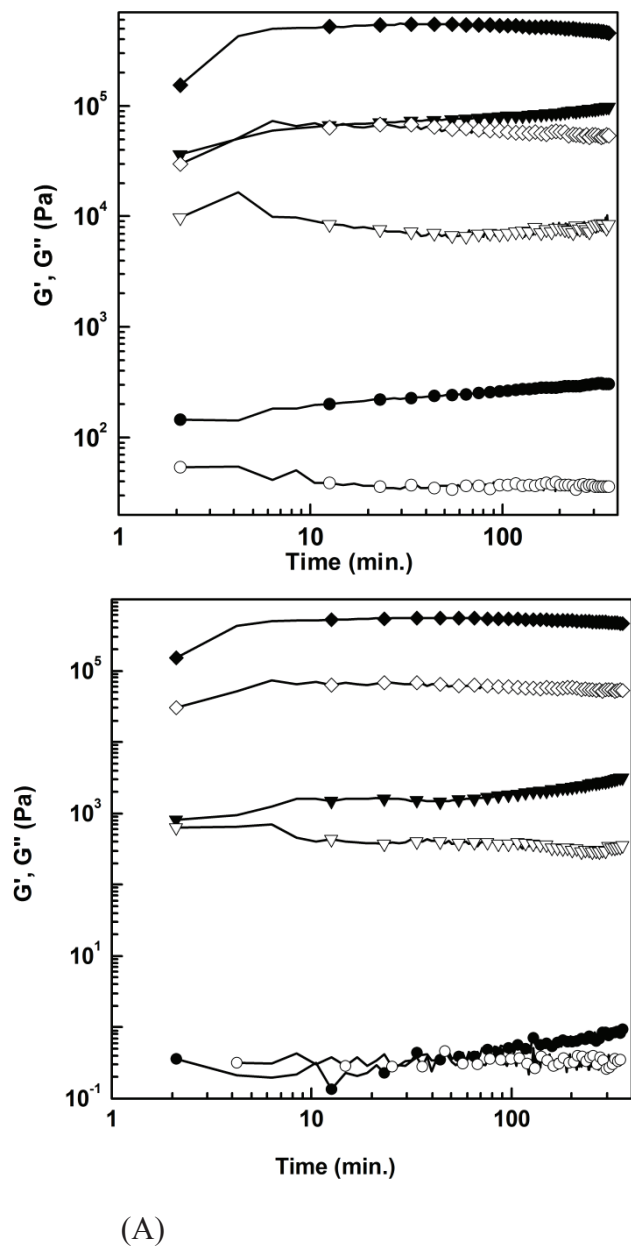


Figure: Storage modulus G' (closed symbols) and loss modulus G'' (open symbols) versus time (min) during annealing at 110 °C for samples prepared by (A) Solution route and (B) Melt route containing different Laponite contents (weight percent): 1.0 % (●○), 5.75 % (▼▽) and 9 % (◆◇).

2.3 Influence of Molecular Parameters on the Structure and Rheology of Model Poly (ethylene oxide)/ Laponite Clay Nanocomposites¹

2.3.1 Introduction

Dynamic response of polymer nanocomposites has been an area of active investigations where unique and intriguing observations have been gathered. A good example is the solid like behavior with a terminal plateau in the low frequency linear viscoelastic moduli signaling a lengthening of the terminal relaxation time [1-15]. Many hypotheses have been advanced, simulations performed and experimental evidence attributes the solid like behavior to (a) inter-particle interactions due to particle clustering via percolation caused by Van der Waals forces[16-18], H-bonding[19] etc., often coupled with (b) particle induced changes in polymer dynamics via polymer adsorption[3], confinement[20], chain bridging[21, 22], entanglement [18, 23-25] etc. Among all the evidences of elastic behavior, the role of polymer molecular weight in tuning the dynamic response is poorly understood. In the nanoparticle limit, for polymers above Me, the network solid viscoelastic response is supposed to be influenced by topological constraints due to entanglements that are manifested via relaxation through reptation and non reptation motions[23]. Some authors suggest that a high polymer molecular weight favors particle structure build up and elasticity [18, 26-28]. In contrast, others have suggested higher relative reinforcement with low polymer mass [29-31]. A third view also exists with a negligible effect of polymer matrix on viscoelasticity. Adding further complexity, the state of dispersion is not always documented in the vast majority of studies, further limiting the ability to explain the observed phenomena, and therefore adversely affecting the nanocomposite design and processing.

The present paper addresses the controversial role of the polymer entanglements in the structure and rheology using model systems based on Laponite and poly (ethylene oxide) capable of good dispersion control[32]. We have chosen to work with three molecular weights PEO having widely varying entanglement densities. It also provided a

¹ Paper in preparation for submission :

Coauthors : Jesmy Jose, Abakar Adam Omar, Guillaume Brotons, Jean-François Tassin

length scale R/R_g ranging between colloidal to nanoparticle limit. This further enabled us to understand the dynamics, as a first approximation in a continuum fluid-mechanics framework[33]. In section II we describe the sample preparation procedure and the measurements carried out. Section III describes the scattering and rheology results and the implications of polymer dynamics on the structure and viscoelasticity are discussed. A summary of results and conclusions are presented in section IV.

2.3.2 Experimental

Materials

Laponite RD, obtained from Rockwood additives Ltd. (U.K.), with density 2570 kg/m³ was used. The cation exchange capacity is 0.95 mequiv/g, and the specific surface is 750 m²/g. Particles were dispersed in PEO matrices ranging in molecular weight from 10000, 350000 and 130000 g/mol purchased from Aldrich. Polymer properties are listed in Table 1. The entanglement molecular weight, M_e in PEO is around 1800 g/mol making 10000, 35000 and 130000 moderate to highly entangled polymers. The zero shear viscosities were taken from the dynamic oscillatory measurements given by figure 1 where the PEO 130k shows a Non-Newtonian behavior. For better compatibility with the polymer, the clay particles were protected by adsorption with low molecular weight either PEO 10k or PEO 130k. A stock solution was prepared at a concentration of 1 % (w/w) by mixing (1/1 v/v) of separately well dispersed PEO and Laponite solutions in deionized water at a continuous stirring for 24 hours. Compatibilization of particles is crucial to obtaining exfoliation. Lyophilized samples of uncompatibilized particles have showed marks of re-aggregation [32, 34].

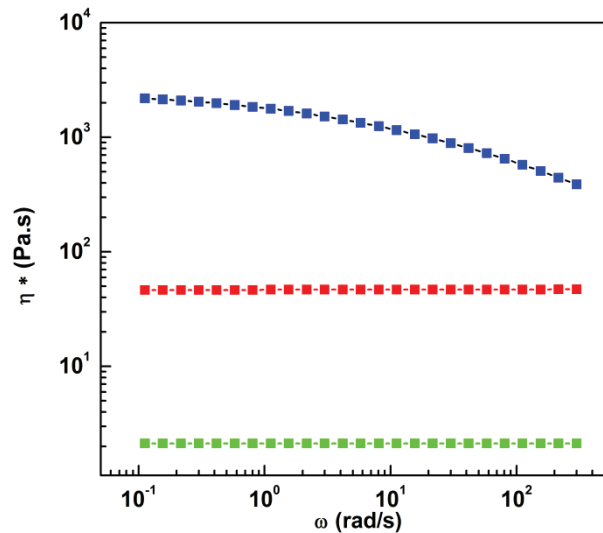


Figure1. Evolution of complex viscosity η^* vs frequency ω at 110 °C for pure PEO 10k (green), 35k (red) and PEO 130k (blue).

The nanocomposites were prepared by two methods. In the solution mixing method, a concentrated solution of PEO polymer was mixed with calculated volumes of stock solution of PEO protected Laponite particles and kept under stirring for 4-5 hours. In order to preserve as much as possible the homogeneous state of dispersion, this sterically stabilized suspension, in which the majority of particles are still non-aggregated, was frozen rapidly with liquid nitrogen and was freeze dried for 12 to 18 hours at -46 °C to remove the water. The freeze drying yields a fluffy powder that was finally compressed at 110 °C for 2 hours, to form 1 mm thick discs. To achieve a different dispersion state using mixing in the molten state of PEO, a master batch approach was adopted where a high concentrated (9.1 wt%) freeze dried sample was diluted by adding the matrix polymer PEO, in the molten state, using a Haake Minilab microcompounder under corotating twin-screws operating at 110 °C, at 50 rpm for 10 min. The processing conditions have been optimized for maximum rheological properties. The extrudates were finally compressed in the same way to give 1 mm discs.

PEO	N ^a	R _g [nm]	η _{PEO} ^a [Pa.s]	Z=M _w /M _e
PEO 10000	227	8.9	2.15	5.5
PEO 35000	796	16.8	46	19.4
PEO 130000	2955	32.3	2248	72

^aNumber of monomers. ^a Temperature of 110 °C

Table 1: Polymer properties

Characterization.

Rheology Measurements. Viscoelastic properties of PEO/Laponite nanocomposites were studied using a stress controlled Thermal Analysis ARG2 rheometer equipped with 25 mm diameter stainless steel parallel disks at 1 mm separation. Measurements were performed under oscillatory shear in the linear domain at a fixed temperature of 110 °C, which is well above the melting temperature of PEO. The viscoelastic properties of nanocomposites have been found to depend strongly on the flow history and they undergo a structural ripening with time [35-37]. Therefore, in order to allow for complete micro structural equilibration, the samples were first subjected to thermal annealing in the rheometer at a frequency of 0.1 rad/s for up to 6 hours. A comparison of the time sweep data collected at the end of equilibration showed slower ripening at high PEO molar mass (*refer supporting information*). Initially, nanoparticles are randomly dispersed in the polymer matrix. After annealing at high temperature, particles aggregate leading to a filler network which evolves towards thermodynamic equilibrium. Frequency dependency of storage and loss modulus of the equilibrated nanocomposite samples were measured by imposing very small deformations (0.5 %) in the frequency range from 100 to 5x10⁻³ rad/s.

Small Angle X- ray Scattering Studies (SAXS). X-ray scattering measurements were performed on solution and melt prepared samples with different PEO molar masses as well as varying Laponite contents at room temperature. A wide range of wave vectors ranging from 0.02 Å⁻¹ to 5 Å⁻¹ obtained by combining a 2D gas detector and a “flat image plate” for large angles using a RigakuTM copper rotating anode (λ ~ 1.54 Å) with high flux and resolution was made use of. All beam path and the 1 mm thick nanocomposite

pellets were under vacuum. A pair of OsmicTM confocal mirrors delivered a cylindrical beam of 2×10^7 photons/s over $350 \mu\text{m}$ in diameter with low angular divergence below 0.5 mrad . For reasons of clarity, the intensities are presented up to 1 \AA^{-1} (large angle peaks of crystallization of PEO chains are omitted), with absolute intensity scale units (cm^{-1} , i.e. cm^2 per cm^3 of sample).

2.3.3 Results

Identification of nanocomposite structures by SAXS-

The particle dispersion state in our samples was validated using SAXS. Figure 2 gives the scattering profiles for PEO 10k and 130k nanocomposites prepared by the solution route at varying Laponite contents. The pure PEO 10k polymer intensity (solid lines in figure) at lower angles falls along a characteristic slope in log-log scales corresponding to the Q^{-2} scattering law associated to the structuration of the polymer into crystalline lamellae.

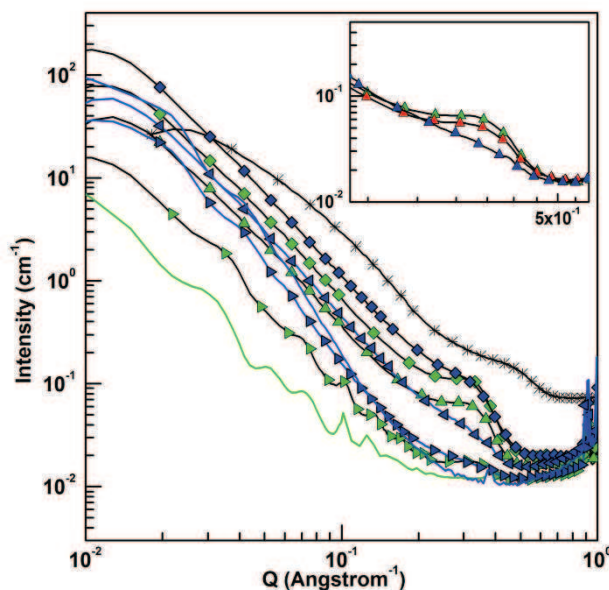


Figure 2. Small angle X-ray scattering profiles of PEO 10000 (green) and PEO 130000 (blue) containing various Laponite loadings (in weight percent); solid lines in green and blue are the scattering profiles for pure PEO 10000 and PEO 130000 respectively, 0.5 % (\triangleright), 3.3% (\triangle), 9.1 % (\square) and crude Laponite ($*$). The inset graph shows the profiles of PEO 10000 (green symbols), PEO 35000 (red symbols) and PEO 130000 (blue symbols) containing 3.3 percent by weight of Laponite prepared by solution route.

A slightly higher slope value in less crystalline pure PEO 130k is observed, and it shifts to a lower value of 2 in the nanocomposites because of prominent scattering from the Laponite discs. This strong scattering from the Laponite discs/PEO interfaces in PEO 10k

nanocomposites is also responsible for the diminished wiggles originating from pure PEO crystalline-amorphous periodicity.

A lower, constant Q value for the Laponite Bragg peak (peak at $Q = 0.35 \text{ \AA}^{-1}$) in the nanocomposites indicate PEO intercalated Laponite stacks. The peak intensities increased with clay loading and PEO molar mass. The Bragg peak intensities reflect the fraction of PEO intercalated Laponite stacks, either with a similar or varying number of clay stacks per aggregate. Considering the remaining fraction of clay particles to exist as particles, either well isolated and/or partially exfoliated, we performed a quantitative modeling of the SAXS profiles. Our results show that the shifted Laponite Bragg peak correspond to a fixed number of PEO intercalated stacks per aggregate (from 3 up to 5), independent of the Laponite content and PEO molar mass. Thus from figure 2, at a fixed Laponite content, the low Bragg peak intensities for PEO 130k samples would suggest better dispersion through clay exfoliation than the low molar mass counterpart. This is further clear from the inset graph in figure 2, which compares the scattering profiles for 3.3 wt % Laponite sample prepared using 10, 35 and 130k PEO by solution route. An almost complete exfoliation is attained with PEO 130k matrix.

In order to further investigate the polymer effect on exfoliation we analyzed the filler dispersions in the same polymer matrices, but prepared by melt route. Figure 3 compares the scattering profile for highly entangled PEO 130k polymer matrix nanocomposites prepared by solution and melt procedure.

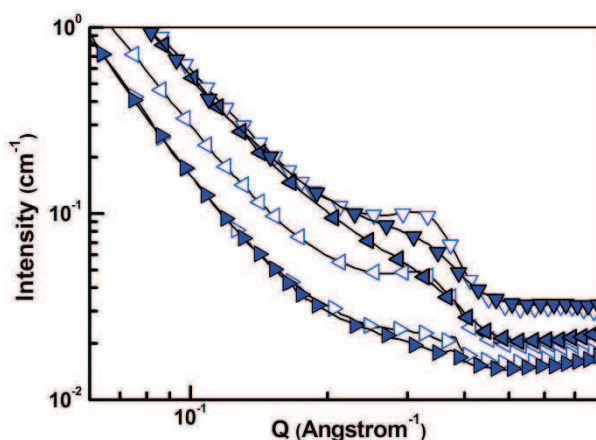


Figure 3. Small angle X-ray scattering profiles of PEO 130000 compared for nanocomposites prepared by solution route (closed symbols) and melt route (open symbols) containing various Laponite loadings (in weight percent); 0.5 % (\triangleright), 3.3% (\triangle), 9.1 % (∇).

As seen from the figure 3, for a given particle concentration, the dispersion via solution route provided samples with a lower fraction of Laponite aggregates, and thus a better particle dispersion. Remarkably, from our earlier studies, with PEO 10k matrix samples, the processing methods failed to make any difference in the degree of dispersion. Dispersions of Laponite in high molecular weight PEO in solution are capable of bridging and thus giving highly interconnected structures [38-40]. Previous studies on PEO using unprotected Laponite have shown a possible re-aggregation of Laponite stacks up on expulsion of water during freeze drying process [34]. The observed higher exfoliation with 130k therefore could be attributed to less aggregated, more stable, well dispersed final structures for high molar mass PEO130k/Laponite samples. In same Q window, figure 4 shows the Bragg peaks 10k and 130k nanocomposites obtained via melt route, i.e. by diluting a 9.1 % solution prepared master batch of 10k and 130k with the respective pure polymers by extrusion.

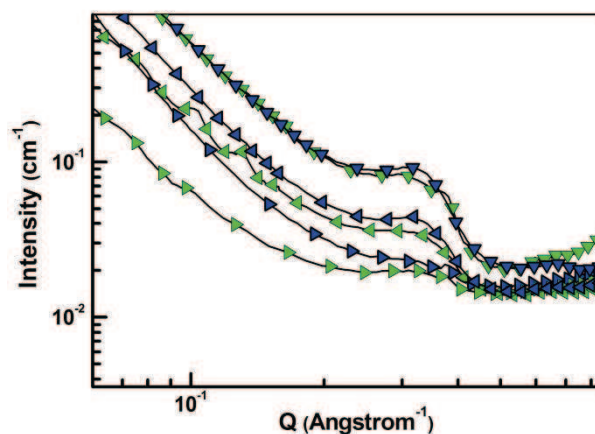


Figure 4. Small angle X-ray scattering profiles of nanocomposites prepared via melt route using PEO 10000 (green symbols) and PEO 130000 (blue symbols) containing various Laponite loadings (in weight percent); 0.5 % (\triangleright), 3.3% (\triangle), 9.1 % (∇).

The comparable peak intensity values between 10k and 130k nanocomposites indicate an identical fraction of Laponite aggregates, and thus similar dispersion states. Variable Laponite Bragg peak intensities with polymer molar mass clearly establish variances in the dispersion state. However, it is noteworthy that in SAXS, the subtle PEO connections between separated Laponite particles would be non addressable from such static scattering techniques and most of the X-ray contrast comes from the particles/PEO interface. Thus the above observed identical Bragg peak intensities for varying PEO molar masses in the melt prepared nanocomposites does not reflect in itself alone the nature of interaction between PEO chains and the partially/ fully exfoliated Laponite.

Rheology

Effect of PEO molecular weight: For the pure PEO 10k, or polymer containing no particles, the probed frequencies pertained to a terminal relaxation behavior having the linear viscoelastic moduli, $G''(\omega) \propto \omega^{-1}$ and $G'(\omega) \propto \omega^2$. A high entanglement density in the pure PEO 130k polymer gives $G''(\omega) \propto \omega^{-0.8}$ and $G'(\omega) \propto \omega^1$ reflecting only the beginning of the terminal regime. The linear viscoelastic response of nanocomposites with Laponite dispersed in varying PEO matrices was analyzed. We shall first discuss the solution prepared nanocomposites.

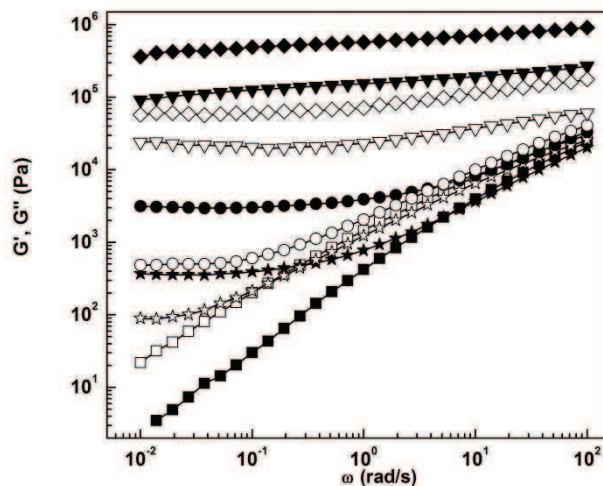


Figure 5. Storage modulus G' (closed symbols) & loss modulus G'' (open symbols) vs. frequency ω at 110 °C for several different Laponite particle loadings (weight percent). PEO 130000 neat (■□), 0.25 % (★☆), 1.0 % (●○), 3.3 % (▲△), 5.75 % (▼▽) and 9.1 % (◇◆). Solution prepared samples

Figure 5 shows the evolution of pseudo-solid like behavior for PEO 130000 matrix nanocomposites at various Laponite concentrations. Despite having low filler content a frequency independent plateau with a moderate storage modulus of 100 Pa was visible at lower frequencies for 0.25 wt % Laponite/ PEO 130k nanocomposite. The observed plateau suggests certain structural connectivity to account for the increased sample elasticity. It is now well established that a low frequency plateau is primarily caused by sample spanning percolating filler network, either with or without any added polymer effects [41-43]. The increase in G' is much more sensitive to Laponite content than that of G'' . This induces an additional crossover at lower frequencies which is visible for up to 1.0 wt % Laponite loading. At large frequencies i.e., above the additional G' , G''

crossover the relaxation behavior of the nanocomposites approaches that of the neat PEO 130k. The terminal plateau moduli increased with Laponite content. Above 1.0wt% the viscoelastic moduli were found independent of the measured frequency scale suggesting a highly elastic solid. Similar responses were also observed for 10k and 130k PEO/Laponite samples, but with varying degree of reinforcement. Figure6 compares the elastic moduli for PEO 10k, 35k and 130k nanocomposite samples. For the sake of simplicity we present only two filler loadings, at a lower (0.5) and one at a higher (2.0 wt %) Laponite content. As seen from the figure, at lower loading, i.e., for 0.5 wt% samples the additional G' , G'' crossover, both the modulus (G_c) as well as the cross over frequency (ω_c), are affected by the polymer viscoelasticity. The above observation is further used for building master curves and will be discussed later. In 2.0 wt % samples, irrespective of the PEO molar mass, the identical relaxation behavior observed for the viscous and elastic modulus suggests a three dimensional stable structure without any relaxations in the measured time scale. Thus no transient network structure exists as opposed to several other nanocomposite systems [44-47]. However some extent of relaxation is indeed observed for 130k nanocomposite suggesting certain energy dissipation.

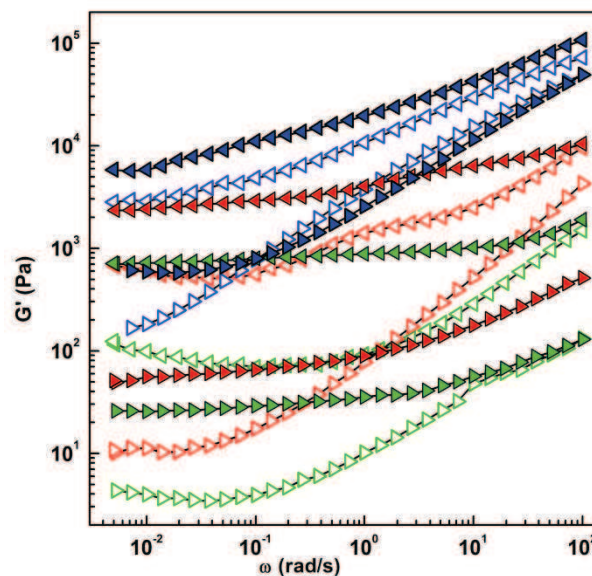


Figure 6: Evolution of storage modulus G' (closed symbols) & loss modulus G'' (open symbols) vs. frequency ω measured at 110 °C, for nanocomposites prepared by solution route using PEO 10k (green), PEO 35k (red) and PEO 130k (blue) with varying Laponite content (in weight percent); 0.5 % (\triangleright) and 2.0 % (\triangleleft).

The most important consequence from Figure 6 would be the matrix effect on the terminal plateau moduli (G'_0 & G''_0). Figure 7 and table 2 summarize the PEO molar mass

effect on the power law scaling behavior of terminal moduli versus the Laponite concentration for samples prepared by solution and melt routes.

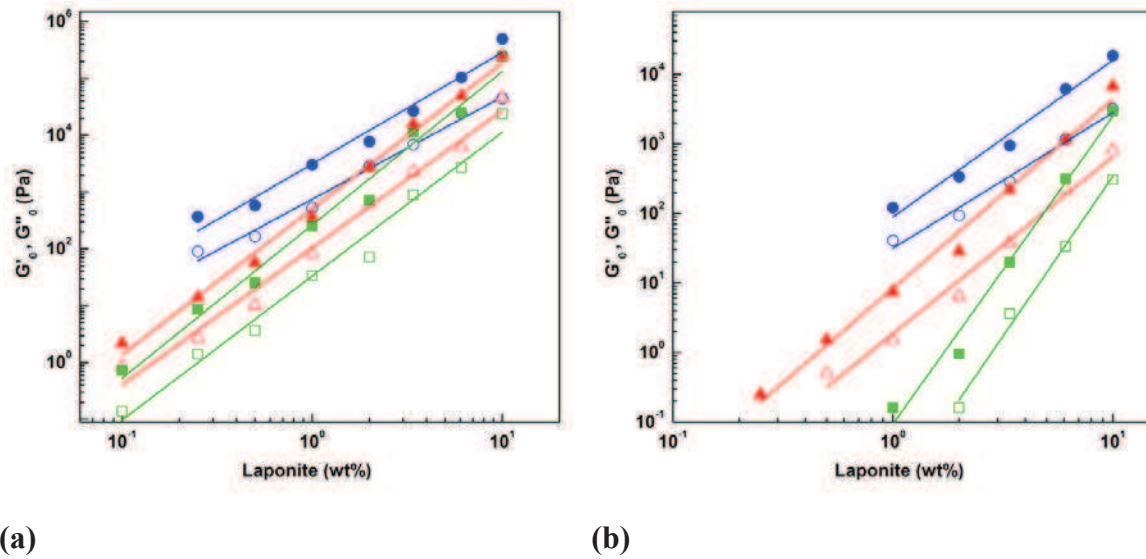


Figure 7: Scaling laws of G'_0 (closed symbols) and G''_0 (open symbols) vs. Laponite weight fraction for nanocomposites prepared by (a) solution procedure and (b) melt method using PEO 10000 (green), PEO 35000 (red) and PEO 130000 g/mol (blue) respectively. The solid lines are the respective power law fits.

PEO matrix	Power law exponent (α)			
	Solution route		Melt route	
	G'_0	G''_0	G'_0	G''_0
PEO 10000	2.7	2.5	4.1	4.3
PEO 35000	2.6	2.4	2.7	2.5
PEO 130000	2.0	1.8	2.3	1.9

Table 2: Power law exponents for nanocomposites prepared by solution procedure with varying PEO molar masses.

High molecular weight PEO offered better reinforcement, especially at lower Laponite concentrations. For example, in solution prepared nanocomposites, adding 0.25 wt% Laponite to PEO 130000 gave ten times more storage modulus than with a PEO 10000 matrix. With increasing clay content, the moduli reaches a limiting value irrespective of the PEO molar mass at the highest weight percent studied, i.e., at 9.1 wt%. Further, from table 2, the separate slope values for different PEO's indicated that the structures responsible for the observed solid behavior are not identical. In 35k and 130k, the identical power law values for solution and melt prepared samples suggest that the structures responsible for terminal moduli are identical. However, the fraction of Laponite contributing to the network varies to account for the differences in the absolute value of the moduli.

Master curve analyses of the viscoelastic moduli

The viscoelastic response of our samples with varying Laponite content could be categorized into those with and without an additional G' , G'' cross over and was studied separately using master curves.

In samples exhibiting additional cross over, i.e., at lower particle loadings, by considering a predominant filler network contribution to be responsible for solid behavior, the percolated particle clusters represents the building elements for elasticity. Interspersed throughout this structure is the polymer fluid, which has an intrinsic and filler-independent viscoelastic response that mixes with the network dynamics giving rise

to the complex frequency and volume fraction dependencies observed in figure 6. Because of the widely different temporal relaxation scales between the filler network (low frequencies) and the polymer melt (high frequency), the nanocomposite viscoelasticity could be approximately decomposed into the independent responses of the elastic particle network, primarily dependent on filler content and governing the long time scale response, and that of the suspending medium, dominating the high-frequency behavior. Figure 8 compares the pure polymer viscous modulus with that of the nanocomposites at the additional cross-over and the observed superimposition verifies the above view.

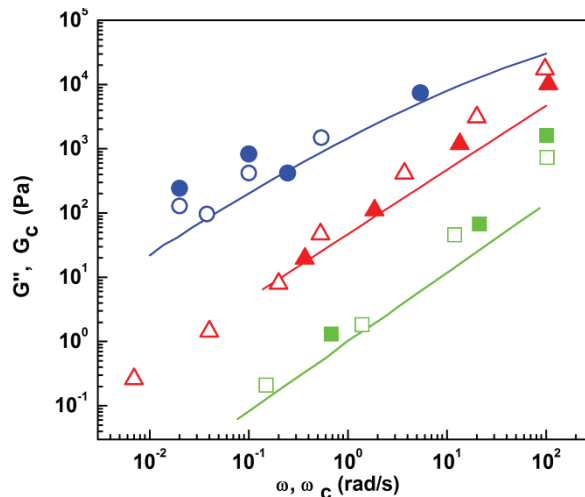


Figure 8: The pure polymer loss modulus (solid line) and the nanocomposite moduli at crossover (G_c) (symbols) plotted against frequency (ω) along with the crossover frequencies (ω_c) for PEO 10k (green), 35k (red) and 130k (blue) polymers and nanocomposites. Open symbols : melt route; closed symbols : solution route.

Thus the G' , G'' crossover sets the nanocomposite elasticity and corresponds to equally contributed network elasticity and polymer viscous modulus. Shifting the frequency and modulus independently across ω_c and G_c using frequency shift factor $a=1/\omega_c$ and the modulus shift factor $b=1/G_c$ for the various solution prepared PEO/Laponite nanocomposites successfully generated a master curve given by figure 9. PEO 10k nanocomposite sample prepared by solution method having a Laponite concentration of 2.0 wt % was used as the reference. Similar master curves for melt prepared samples were also generated using the same reference (figure not given).

The observed analogy with the dynamics of hard sphere suspensions has been applied extensively for nano filler dispersions to establish dominant filler-filler interactions [48][49][50]. Our interest is focused on understanding the matrix effect, if

any, towards the network elasticity, which is least explored. Theories predict that the diffusivity of particles decreases with an increase in viscosity of the fluid, and that the addition of particles increases the overall viscosity of the suspension. As shown in the insert graph in Fig. 9, and by considering figure 8, the nanocomposite elasticity at the crossover for a given PEO matrix (G_c) scales along the crossover frequency.

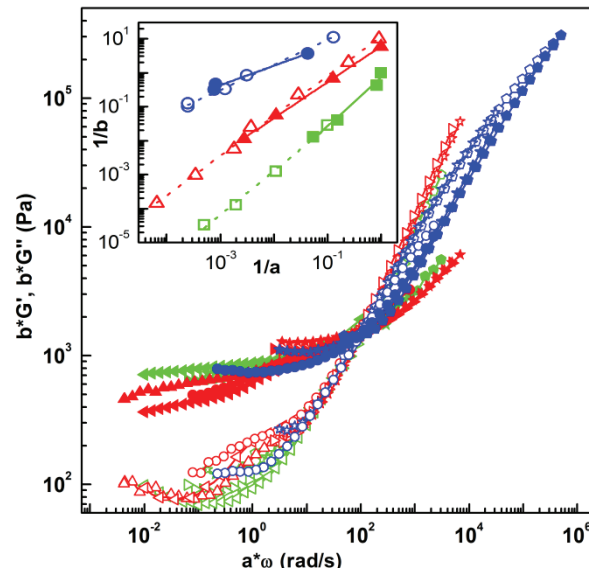


Figure 9: Master curve showing the scaled moduli for nanocomposites having varying particle concentrations (those with G' , G'' cross-over) with PEO molecular weights- 10,000 (black color), 35,000 (red color) & 130,000 g/mol (blue color) respectively. Inset graph shows the variation of moduli shift factor (b) with frequency shift factor (a) for nanocomposites prepared via solution (closed symbols) and melt (open symbols) routes using PEO 10000 (■□), PEO 35000(▲△) and PEO 130000 g/mol(●○) respectively. The solid and broken lines give the linear fit for the solution and melt prepared nanocomposites respectively.

Of particular interest is the variable scaling for polymer molar masses summarized by Table 3. With increasing polymer matrix molar mass the elasticity due to filler network varies less with the polymer viscosity

PEO matrix	Scaling factor	
	Solution route	Melt route
PEO 10000	1.3	1.4
PEO 35000	1.1	1.2
PEO 130000	0.6	0.7

Table 3: Scaling exponents from the master curve analysis for nanocomposites prepared by solution and melt procedure with varying PEO molar masses.

A second kind of master curve was constructed by the superposition of modulus curves corrected for the pure polymer relaxation times (i.e. plotted versus the reduced frequency $\omega\tau$) and is given by figure 10. The longest relaxation times for pure PEO 10000, 35000 and 130000 g/mol at 110°C are respectively 5.5×10^{-7} , 5.1×10^{-5} and 9.56×10^{-3} seconds.

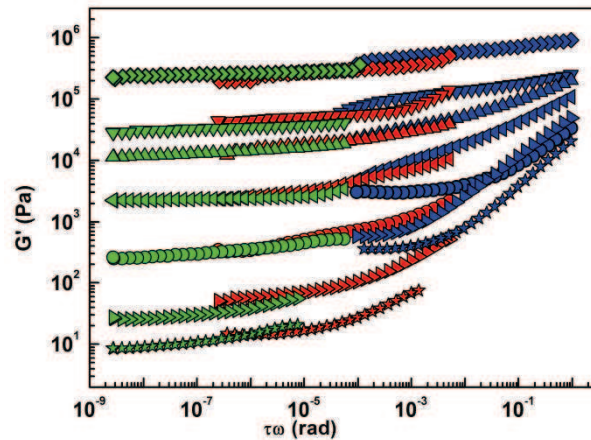


Figure 10 : Master curve showing storage modulus versus reduced frequency for solution prepared samples with varying PEO molecular weights-10,000 (green color), 35,000 (red color) & 130,000 g/mol (blue color) respectively. Concentrations above 2wt%.

The x- axis $\omega\tau$ is a chain length independent quantity and for $\omega\tau < 1$ indicates a predominant viscous region for the respective pure polymers. As seen from figure 10, at higher Laponite loadings, above 3.3 wt% the modulus curves superimpose well and the modulus is unaffected by polymer chain dynamics. To an excellent approximation, at the

highest loadings the polymer relaxations collapses onto a particle loading dependent constant value, which is close to the rubbery plateau modulus of pure PEO. However at lower loadings they do affect the plateau values. The superposition fails or is not as good in melt prepared samples as given by figure 11. It is possible that these samples are further from thermodynamic equilibrium than solution ones.

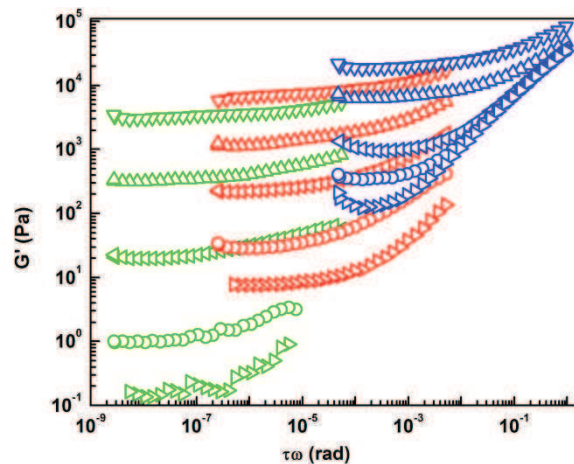


Figure 11: Master curve showing storage modulus vs reduced frequency for melt prepared samples with varying PEO molecular weights-10,000 (green color), 35,000 (red color) & 130,000 g/mol (blue color) respectively.

Role of adsorbed polymer chain dynamics

The existence of an additional crossover would indicate a region with predominant viscous behavior followed by a relaxation due to the impact caused by the particles. This pertains to heterogeneous dynamics, wherein the relaxation reflects the dynamics of distinctly relaxing elements, each of which relaxes at widely separated and/or with different rates. Such a situation could occur if only some of the polymers form a network, when their dynamics is effectively frozen on the time scale the free polymers are themselves relaxing. Moreover at high particle loadings an altered chain dynamics by confinement and bridging could correspond to the suppression of chain relaxations [33][51, 52]. It has been shown that in strongly adsorbing polymers the adsorbed chain thickness scales increases with molecular weight[53]. However, a rather flat conformation of adsorbed PEO chains has been observed on Laponite[54]. Hence we investigated the influence of polymer adsorbed chains on the solid behavior for our strongly interacting PEO-Laponite systems. We studied the plateau behavior for samples by fixing the particle dispersion as well as the PEO matrix chain dynamics for varying the molecular weight of PEO compatibilizer. Figure 12 compares the modulus values for

nanocomposites with intermediate molar mass 35k matrix, prepared by solution method using PEO10k and PEO 130k for Laponite adsorption.

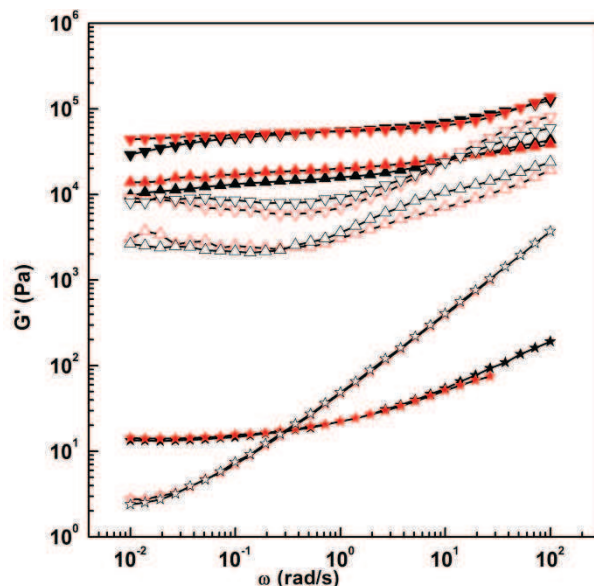


Figure 12. Evolution of storage modulus G' (closed symbols) and loss modulus G'' (open symbols) with frequency ω for PEO 35000/ Laponite nanocomposites containing Laponite adsorbed with PEO 10000 (red) and PEO 130000 (black) prepared by solution route; 0.25 % ($\star \star$), 3.3 % ($\blacktriangle \triangle$) and 5.75 % ($\blacktriangledown \triangledown$).

When PEO 35k solution is added to Laponite containing 10k adsorbed chains, the short chains can be replaced by 35k chains due to entropy gain. No kind of such replacement would occur with 130k adsorbed chains. A particle with adsorbed 130k has more adsorbed chain density due to larger number of possible trains and loops. We studied the sample viscoelastic responses at both low and high Laponite contents. The identical relaxation behavior between short chain PEO10k and long chain 130k adsorbed Laponite dispersed in an intermediate molar mass PEO 35k indicates negligible influence of adsorbed polymer molar mass. Similar result was also observed for melt processed samples. The results very well superimpose on the earlier master curves discussed for PEO 35 k (Figure 9 & 10). Also from our earlier studies it was established that the amount of polymer used for compatibilizing the particles does not appear to induce changes in the formation of elastic network, except through the fraction of particles included in the network [34].

For a uniform particle dispersion the interparticle distance (d) calculated for varying filler amount is given by Table 4.

Laponite (wt %)	Inter particle distance (nm)
9.1	27.9
5.75	32.6
3.3	39.3
2.0	46.9
1.0	58.7
0.5	73.7
0.25	92.6
0.1	125.6

Table 4: Inter-particle distance calculated for varying Laponite loadings in PEO nanocomposites.

Confinement of polymer chains arises for $d < R_g$. The degree of confinement at higher loadings is expected to vary with adsorbed PEO molecular weight[24]. In 5.75 wt % sample, from figure 12, any confinement of the adsorbed chains (primary confinement) or those between adsorbed chains (secondary) would have contributed differently towards the viscoelastic properties with 10k and 130k adsorbed chains. The above behavior establishes absence of the chain confinement to account for the viscoelasticity or even if exists it does not contribute predominantly to the observed viscoelastic behavior. This is further supported by the small effect of the molecular weight of the matrix chains as the concentration increases, i.e. when confinement effects of long polymer chains should be dominant.

2.3.4 Discussion and concluding remarks

In this discussion, we focus essentially on the results plotted in Figure 9, 10 and 11.

The viscoelastic behavior of filled polymers is governed by the spatial organization of the fillers in the matrix [55]. The elasticity coming from the self-assembly of the Laponite particles is controlled by degree of dispersion and is dependent on PEO molar mass as well as processing route. For processing via solution route PEO 130k gives better dispersion and higher moduli. The influence of the molecular weight is best seen at low concentrations of particles. It is possible that during mixing of the 10k adsorbed particles with PEO 130k some small chains desorb from the particles to allow for the adsorption of

longer ones. Bridging of the particles by long polymer chains is able to occur, whereas it is less probable with low molecular weights. This can produce high moduli even at low concentrations. At higher concentrations, long and shorter PEO chains are able to bridge the particles, which can explain the weaker influence of the chain length in these conditions.

In this study, we have been able to construct, at least within a first degree of approximation, master curves representing the viscoelastic response of Laponite-PEO nanocomposites. We have shown that for solution prepared samples (Figure 10), at high enough concentration, the level of the storage modulus at low frequency is essentially determined by the filler concentration, rather than the molecular weight of the matrix. This is no more true at low concentration, where we attributed the non-expected high level of elasticity within PEO 130k matrix to the bridging of the Laponite particles (or at least of part of them) by the polymer chains. This induces a complementary contribution to the modulus which prevails with respect to the structuration of the Laponite particles. The master curves also explain why, in some cases, the frequency dependence of the storage modulus is flat, and why this is not always the case. Indeed, independence of G' with frequency is obtained when the dynamics of the melt is rapid with respect to the investigated frequency range. It is likely that some polymer chains are moving (might be reptating) but thanks to a structuration of the particles inside the polymer a network is formed which prevents flowing.

When we increase the molecular weight of the chains, slower polymer dynamics occurs. The polymer chains bring an additional contribution to the modulus of the nanocomposite which is still a soft solid. This is very clear from the master curve of both moduli, obtained for various molecular weights at low concentration of particles (Figure 9). These master curves are simply obtained by shifting data horizontally and vertically in logarithmic scales, by rescaling on a crossover between G' and G'' , so the reciprocal of a relaxation time.

For the melt route, we need to consider what is occurring during the melt blending process. The viscosity scales with molecular weight with a power of 3.4. The high viscosity of the PEO 130k causes reduced diffusivity of the Laponite particles, thereby restricting formation of open percolating structures². The dilution of 9.1 wt % solution

² Note that to some extent an increase of the moduli is observed with high molecular weights at low concentration. This might come from structures that are not at equilibrium during the measurement time, which is rather long since low frequencies are considered

prepared master batch for 10, 35, 130k (all having polymer independent structures, as judged from the small influence of the molecular weight at high concentration) by pure polymers breaks some structural connectivity and thereby reduces the fraction of interconnected clusters contributing towards viscoelasticity. Considering the analogy with polymer blends, comparable viscosities between master batch and diluting polymer favors better dispersion. The effect of shear varies with polymer molecular weight. The high molecular weight PEO chains are capable of breaking the master batch structure since higher stresses are generated during mixing. This improves the mixing with respect to lower molecular weights and should generate fewer aggregates. However, SAXS data do not bring evidence for this behavior. It is thus possible that the structures responsible for the viscoelastic response in samples prepared by the melt route are not a network of isolated particles but rather clusters of particles that originate from the master batch. If the master batch can be separated in smaller dimensions a better dispersion of these clusters will be obtained. This will in some sense increase the effective volume fraction of the particles and will increase the moduli. A higher sensitivity is expected at low concentrations, leading to stronger effects in this range.

Looking at the exponents of the scaling laws, it is likely that the structure of melt dispersed nanocomposites is quite different from solution, especially with low molecular weight matrices. In this case, the large difference in viscosity between the master batch and the matrix renders even more difficult the rupture of the clusters.

2.3.5 References

1. Krishnamoorti, R. and E.P. Giannelis, *Rheology of end-tethered polymer layered silicate nanocomposites*. *Macromolecules*, 1997. **30**(14): p. 4097-4102.
2. Hyun, Y.H., et al., *Rheology of poly(ethylene oxide)/organoclay nanocomposites*. *Macromolecules*, 2001. **34**(23): p. 8084-8093.
3. Krishnamoorti, R. and K. Yurekli, *Rheology of polymer layered silicate nanocomposites*. *Current Opinion in Colloid & Interface Science*, 2001. **6**(5-6): p. 464-470.
4. Zhang, Q. and L.A. Archer, *Poly(ethylene oxide)/silica nanocomposites: Structure and rheology*. *Langmuir*, 2002. **18**(26): p. 10435-10442.
5. Lee, K.M. and C.D. Han, *Rheology of organoclay nanocomposites: Effects of polymer matrix/organoclay compatibility and the gallery distance of organoclay*. *Macromolecules*, 2003. **36**(19): p. 7165-7178.
6. Lee, K.M. and C.D. Han, *Effect of hydrogen bonding on the rheology of polycarbonate/organoclay nanocomposites*. *Polymer*, 2003. **44**(16): p. 4573-4588.
7. Li, J., et al., *Study on rheological behavior of polypropylene/clay nanocomposites*. *Journal of Applied Polymer Science*, 2003. **89**(13): p. 3609-3617.
8. Lim, S.T., et al., *Solidlike transition of melt-intercalated biodegradable polymer/clay nanocomposites*. *Journal of Polymer Science Part B-Polymer Physics*, 2003. **41**(17): p. 2052-2061.
9. Meincke, O., et al., *Viscoelastic properties of polystyrene nanocomposites based on layered silicates*. *Macromolecular Chemistry and Physics*, 2003. **204**(5-6): p. 823-830.
10. Ray, S.S., K. Okamoto, and M. Okamoto, *Structure-property relationship in biodegradable poly(butylene succinate)/layered silicate nanocomposites*. *Macromolecules*, 2003. **36**(7): p. 2355-2367.
11. Du, F.M., et al., *Nanotube networks in polymer nanocomposites: Rheology and electrical conductivity*. *Macromolecules*, 2004. **37**(24): p. 9048-9055.
12. Gu, S.Y., J. Ren, and Q.F. Wang, *Rheology of poly(propylene)/clay nanocomposites*. *Journal of Applied Polymer Science*, 2004. **91**(4): p. 2427-2434.
13. Zhao, J., A.B. Morgan, and J.D. Harris, *Rheological characterization of poly styrene-clay nanocomposites to compare the degree of exfoliation and dispersion*. *Polymer*, 2005. **46**(20): p. 8641-8660.
14. Goel, V., et al., *Viscoelastic properties of silica-grafted poly(styrene-acrylonitrile) nanocomposites*. *Journal of Polymer Science Part B-Polymer Physics*, 2006. **44**(14): p. 2014-2023.
15. Eslami, H., M. Grmela, and M. Bousmina, *Linear and nonlinear rheology of polymer/layered silicate nanocomposites*. *Journal of Rheology*, 2010. **54**(3): p. 539-562.
16. Akcora, P., et al., *"Gel-like" Mechanical Reinforcement in Polymer Nanocomposite Melts*. *Macromolecules*, 2010. **43**(2): p. 1003-1010.
17. Taghizadeh, E., G. Naderi, and C. Dubois, *Rheological and morphological properties of PA6/ECO nanocomposites*. *Rheologica Acta*, 2010. **49**(10): p. 1015-1027.

18. Du, F., et al., *Nanotube Networks in Polymer Nanocomposites Rheology and Electrical Conductivity*. *Macromolecules*, 2004. **37**(24): p. 9048-9055.
19. Dorigato, A., A. Pegoretti, and A. Penati, *Linear low-density polyethylene/silica micro- and nanocomposites: dynamic rheological measurements and modelling*. *Express Polymer Letters*, 2010. **4**(2): p. 115-129.
20. Dionne, P.J., R. Ozisik, and C.R. Picu, *Structure and dynamics of polyethylene nanocomposites*. *Macromolecules*, 2005. **38**(22): p. 9351-9358.
21. Kellarakis, A., et al., *Rheological study of carbon nanofiber induced physical gelation in polyolefin nanocomposite melt*. *Polymer*, 2005. **46**(25): p. 11591-11599.
22. Jouault, N., et al., *Well-Dispersed Fractal Aggregates as Filler in Polymer/Silica Nanocomposites: Long-Range Effects in Rheology*. *Macromolecules*, 2009. **42**(6): p. 2031-2040.
23. Sarvestani, A.S., *Modeling the solid-like behavior of entangled polymer nanocomposites at low frequency regimes*. *European Polymer Journal*, 2008. **44**(2): p. 263-269.
24. Kabanemi, K.K. and J.F. Hetu, *A reptation-based model to the dynamics and rheology of linear entangled polymers reinforced with nanoscale rigid particles*. *Journal of Non-Newtonian Fluid Mechanics*, 2010. **165**(15-16): p. 866-878.
25. Eslami, H., M. Grmela, and M. Bousmina, *A mesoscopic tube model of polymer/layered silicate nanocomposites*. *Rheologica Acta*, 2009. **48**(3): p. 317-331.
26. Fornes, T.D., et al., *Nylon 6 nanocomposites: the effect of matrix molecular weight*. *Polymer*, 2001. **42**(25): p. 09929-09940.
27. Ha, H., S.C. Kim, and K. Ha, *Effect of Molecular Weight of Polymer Matrix on the Dispersion of MWNTs in HDPE/MWNT and PC/MWNT Composites*. *Macromolecular Research*, 2010. **18**(5): p. 512-518.
28. Loyens, W., P. Jannasch, and F.H.J. Maurer, *Effect of clay modifier and matrix molar mass on the structure and properties of poly(ethylene oxide)/Cloisite nanocomposites via melt-compounding*. *Polymer*, 2005. **46**(3): p. 903-914.
29. Xu, L., et al., *Structure and melt rheology of polystyrene-based layered silicate nanocomposites*. *Nanotechnology*, 2005. **16**(7): p. S514-S521.
30. Zhu, Z., et al., *Investigating Linear and Nonlinear Viscoelastic Behavior Using Model Silica-Particle-Filled Polybutadiene*. *Macromolecules*, 2005. **38**(21): p. 8816-8824.
31. Goel, V., et al., *Linear Viscoelasticity of Spherical SiO₂ Nanoparticle-Tethered Poly(butyl acrylate) Hybrids*. *Industrial & Engineering Chemistry Research*, 2010. **49**(23): p. 11985-11990.
32. Loiseau, A. and J.F. Tassin, *Model nanocomposites based on laponite and poly(ethylene oxide): Preparation and rheology*. *Macromolecules*, 2006. **39**(26): p. 9185-9191.
33. Anderson, B.J. and C.F. Zukoski, *Rheology and Microstructure of Entangled Polymer Nanocomposite Melts*. *Macromolecules*, 2009. **42**(21): p. 8370-8384.
34. Loiseau, A., *Elaboration et caractérisation de Nanocomposites modèles Laponite/Polyoxyde d'éthylène*. 2006, Université du Maine Le Mans, France.
35. Vermant, J., et al., *Quantifying dispersion of layered nanocomposites via melt rheology*. *Journal of Rheology*, 2007. **51**(3): p. 429-450.

36. Mobuchon, C., P.J. Carreau, and M.C. Heuzey, *Structural analysis of non-aqueous layered silicate suspensions subjected to shear flow*. Journal of Rheology, 2009. **53**(5): p. 1025-1048.
37. Wang, X.L., et al., *Late-State Ripening Dynamics of a Polymer/Clay Nanocomposite*. Macromolecules, 2010. **43**(4): p. 1901-1906.
38. Mongondry, P., T. Nicolai, and J.F. Tassin, *Influence of pyrophosphate or polyethylene oxide on the aggregation and gelation of aqueous laponite dispersions*. Journal of Colloid and Interface Science, 2004. **275**(1): p. 191-196.
39. Baghdadi, H.A., H. Sardinha, and S.R. Bhatia, *Rheology and gelation kinetics in laponite dispersions containing poly(ethylene oxide)*. Journal of Polymer Science Part B-Polymer Physics, 2005. **43**(2): p. 233-240.
40. Can, V. and O. Okay, *Shake gels based on Laponite-PEO mixtures: effect of polymer molecular weight*. Designed Monomers and Polymers, 2005. **8**(5): p. 453-462.
41. Durmus, A., A. Kasgoz, and C.W. Macosko, *Linear low density polyethylene (LLDPE)/clay nanocomposites. Part I: Structural characterization and quantifying clay dispersion by melt rheology*. Polymer, 2007. **48**(15): p. 4492-4502.
42. Carastan, D.J., et al., *Linear viscoelasticity of styrenic block copolymers-clay nanocomposites*. Rheologica Acta, 2008. **47**(5-6): p. 521-536.
43. Manitiu, M., et al., *Role of polymer-clay interactions and nano-clay dispersion on the viscoelastic response of supercritical CO₂ dispersed polyvinylmethylether (PVME)-Clay nanocomposites*. Polymer, 2009. **50**(15): p. 3786-3796.
44. Sarvestani, A.S. and C.R. Picu, *Network model for the viscoelastic behavior of polymer nanocomposites*. Polymer, 2004. **45**(22): p. 7779-7790.
45. Sarvestani, A.S. and C.R. Picu, *A frictional molecular model for the viscoelasticity of entangled polymer nanocomposites*. Rheologica Acta, 2005. **45**(2): p. 132-141.
46. Abranyi, A., et al., *Formation and detection of clay network structure in poly(propylene)/layered silicate nanocomposites*. Macromolecular Rapid Communications, 2006. **27**(2): p. 132-135.
47. Romeo, G., et al., *Elasticity and dynamics of particle gels in non-Newtonian melts*. Rheologica Acta, 2008. **47**(9): p. 989-997.
48. Song, Y.H. and Q.A. Zheng, *Linear viscoelasticity of polymer melts filled with nano-sized fillers*. Polymer, 2010. **51**(14): p. 3262-3268.
49. Romeo, G., et al., *Effects of particle dimension and matrix viscosity on the colloidal aggregation in weakly interacting polymer-nanoparticle composites: a linear viscoelastic analysis*. Polymer Bulletin, 2009. **63**(6): p. 883-895.
50. Filippone, G., G. Romeo, and D. Acierno, *Viscoelasticity and Structure of Polystyrene/Fumed Silica Nanocomposites: Filler Network and Hydrodynamic Contributions*. Langmuir, 2010. **26**(4): p. 2714-2720.
51. Smith, K.A., M. Vladkov, and J.-L. Barrat, *Polymer Melt near a Solid Surface: A Molecular Dynamics Study of Chain Conformations and Desorption Dynamics*. Macromolecules, 2004. **38**(2): p. 571-580.
52. Pelletier, E., et al., *Dynamics of Compressed Polymer Layers Adsorbed on Solid Surfaces*. Macromolecules, 1995. **28**(6): p. 1990-1998.

53. Chen, B., et al., *A critical appraisal of polymer-clay nanocomposites*. Chemical Society Reviews, 2008. **37**(3): p. 568-594.
54. Nelson, A. and T. Cosgrove, *Dynamic Light Scattering Studies of Poly(ethylene oxide) Adsorbed on Laponite Layer Conformation and Its Effect on Particle Stability*. Langmuir, 2004. **20**(24): p. 10382-10388.
55. Inoubli, R., et al., *Nanostructure and Mechanical Properties of Polybutylacrylate Filled with Grafted Silica Particles*. Langmuir, 2006. **22**(15): p. 6683-6689.

2.4 Influence of the route of protecting the particles

2.4.1 Introduction

In recent years, studies have shown that, the addition of layered-silicate nanoparticles into polymer matrices is an effective strategy for achieving improved, thermal, electrical, optical, mechanical properties and morphology in the case of polymer blends of polymer materials. This strategy appeared in the 90ths in Toyota Central Research and Development¹, where it was demonstrated that at low loadings of clay particles, the modulus doubled, the strength increased by more than 50%, and the heat distortion temperature increased by 80°C compared to the pristine polyamide polymer. So far, it has been reported that, the degree of property enhancement achieved in the polymer nanocomposites depends on the state of nanoparticles dispersion and the ability of the particles surface to alter polymer segment dynamics. However, the state of dispersion is sensitive to the interaction forces between particles, between the polymer chains and the particles dispersed in the polymer and how these forces drive particles organization²⁻⁵. For a given pair of particles and polymer, molecular weight of the polymer matrix and preparation methods show a great effect on the final dispersion state of the particles⁶⁻¹⁰. Consequently, depending on the nature of the fillers distribution within the matrix, the morphology of nanocomposites can evolve from the intercalated structure with the regular alternation of layer silicates and polymer monolayer to the exfoliated (delaminated) structure with layered silicate randomly and homogeneously distributed inside the polymer matrix⁵. It is very important to mention that, creating specific interactions between particles and polymer matrix by surface treatment of the particles is considered as the best way to reach the exfoliation state, where the high specific surface of the particles becomes fully accessible to polymer chains.

Generally, surface treatment of the clay mineral with polymers is achieved by two different approaches. One is physical adsorption, and the second is chemical grafting of functional polymers or molecules onto the surfaces of the clay minerals². Mongondry et al¹¹ have reported on steric stabilization of Laponite particles against the aggregation by using chemical grafting polymers on the surface of clay particles. Loiseau et al¹² have achieved better dispersion of Laponite particles inside a poly(ethylene oxide) matrix with end grafting of polymer chains as compared to adsorbed ones. In a previous work, Loiseau¹³ has studied the influence of the molecular weight of the adsorbed chains on the viscoelastic properties of nanocomposites based on PEO/Laponite. He pointed out that, storage modulus increases with increase of adsorbed molecular weight up to 20kg/mole. This was attributed to the increase of entanglement of the adsorbed chains with the polymer matrix (PEO10k), whereas, for high molecular weight (35kg/mole and 130kg/mole) modulus found to decrease because of bridging of long polymer chains onto several Laponite particles which acts against dispersion of the particles, since they are partially stuck together. Up to now we are not aware with any study concerning the influence of the molecular weight of grafted chains on the properties of polymer nanocomposites.

In this present study, the aim was to investigate the influence of the length of the grafted chain (molecular weight) on the linear viscoelastic properties of model nanocomposites based on poly (ethylene oxide) and Laponite. For this purpose two procedures has been considered to prepare nanocomposites; solution mixing and melt dispersion¹⁴⁻¹⁵. Three different chain lengths of modified poly (ethylene glycol) have been investigated. In section II materials as well as samples preparation procedures will be described. Section III will show the linear viscoelastic results of the various controlled dispersions using dynamic linear rheology. Discussion and conclusion will be displayed in section IV.

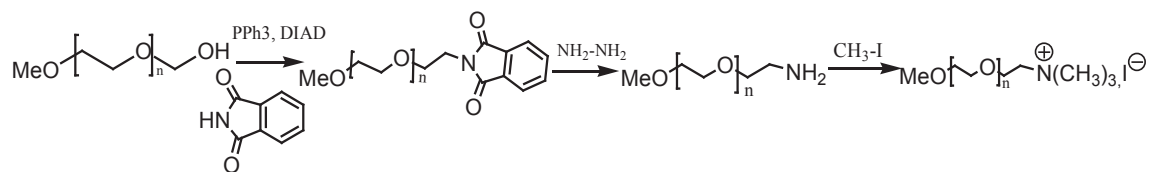
2.4.2 Experimental Section

Materials:

Poly (ethylene oxide) of molecular weight $M_w = 10000$ g/mol was purchased from Sigma Aldrich and was used as received. The melting temperature as measured by DSC is 67.5°C , while size exclusion chromatography (SEC) in THF gave $M_w = 9850$ g/mol and $M_w/M_n = 1.08$. Poly (ethylene glycol) methyl ethers with molecular weights: 1.000, 2.000, and 5.000 g/mole have also been purchased from Sigma Aldrich, and their hydroxyl (OH) end group has been modified to trimethylammonium salt. Laponite RD, supplied by Rockwood additives Ltd. (U.K), with density 2570 Kg/ m^3 was used. The cation exchange capacity is 0.95 mequiv/g , and the specific surface is $750 \text{ m}^2/\text{g}$.

Conversion of Hydroxyl-PEGs to Trimethylammonium-PEGs

The hydroxyl group at the chain end of poly (ethylene glycol) methy ether (MPEG) was converted to trimethylammonium-MPEGs in three steps, shown in scheme 1, according to the procedure introduced by Mongondry et al¹¹. In the first step Hydroxyl-PEGs is converted to Phthalimido-PEGs by using the Mitsunobu reaction described for the preparation of 2-Octylamine¹⁶. ^1H NMR confirmed 96% of this conversion, and the yield was found to be 94%. The second step, known as hydrazinolysis, was used to transform the phthalimido end group into an amino one. In this step, phthalimido-PEGs were treated with an aqueous solution of hydrazine hydrate under reflux for 3-4 hours using ethanol as solvent. The pH of the cold solution was adjusted in the range 2-3 by adding concentrated hydrochloric acid, and the precipitate was removed by filtration. After evaporation of ethanol and addition of basic water solution, the polymers were extracted with methylene chloride. The phthalimido-PEGs were further purified. Conversion and yield were 85 and 67% respectively. The third step is a quaternization of the amino group. A mixture of amino-PEGs, sodium bicarbonate methyl iodide and methanol was heated with stirring for 75h and methyle iodide was further added after 30h. The solid was removed by filtration, the reaction mixture was evaporated, the residual product was dissolved in water. After washing twice with diethyl ether, the aqueous solution was evaporated and the quaternary ammonium salts were recovered with conversion of 81.1% and yield of 76.9%.



Scheme 1

This synthetic scheme was carried out for poly (ethylene glycol) methyl ether of molecular weights 1000, 2000 and 5000 g/mol. The corresponding trimethylammonium salts polymers are noted as NPE1k, NPE2k, and NPE5k.

Nanocomposites preparation:

Model nanocomposites were prepared by two methods: melt dispersion and solution mixing. Melt dispersion¹⁴ method consists in two steps. The particles were first protected by adsorbed or grafted chains by dispersing separately the Laponite powder at a concentration of 2wt% and polymer chains (at a concentration of 0.6wt% for NPE1k, 0.84wt% for NPE2k, 1.04wt% for NPE5k and 2wt%) in milliQ water under gentle stirring for 24h. Equal volumes of two solutions were mixed for 24h leading to a suspension of protected particles, either with grafted chains or adsorbed chains. The polymer quantities with regard to Laponite were calculated from the adsorption isotherm. With NPE1k a very strong interaction with the particles is observed and the maximum surface coverage is 0.32 g of polymer/g of Laponite. The isotherm is less sharp for NPE2k and saturation is obtained of 0.46 g of polymer/g of Laponite. Finally, the NPE5k adsorption is even less sharp than with 2k, and the isotherm suggests that adsorption may come together with end-grafting. The saturation is 0.52 g of polymer /g of Laponite.

For solution mixing, a convenient quantity of these solutions was mixed with a PEO 10k solution at 10wt% in MilliQ water for additional 24h in order to get the targeted concentration of particles. The final suspension was further freeze dried to remove water, leading to fluffy powder, which was either hot pressed to provide samples for rheological characterization or further used as a master-batch for the melt preparation method.

For melt dispersion, a master-batch prepared as described above (solution mixing) containing 10 wt % of Laponite was further blended with the PEO matrix in the molten state, at the targeted concentrations, using a Haake minilab microcompounder under corotating twin-screws operating at 80°C 60 rpm for 10mn.

Rheological characterization

Samples for rheological characterization were disks of 25 mm diameter and 1 mm thickness that were prepared by molding at 90°C followed by cooling at room temperature. The linear viscoelastic properties of the samples were studied, with the aim of determining the parameters that act on the low frequency modulus of the samples by

using ARG2 rheometer from TA instruments. Measurements were performed under oscillatory shear in the linear domain at a fixed temperature of 80°C, which is well above the melting temperature of PEO. In order to allow for complete micro structural equilibration or mechanical equilibration of the samples, time sweep measurements have been carried out. The samples were first subjected to thermal annealing in the rheometer at a frequency of 0.1 rad/s until the independency of loss modulus and storage modulus with time is observed. Strain sweep was carried out to determine the linear domain. Frequency dependence of storage and loss modulus of the equilibrated nanocomposites samples was measured by imposing very small deformations (0.5%) in the frequency range from 100 to 5×10^{-3} rad/s

2.4.3 Results

The linear viscoelastic response of nanocomposites with Laponite protected by either adsorbed PEO10k or one of the three types of grafted trimethylammonium-PEG (1k, 2k, and 5k) dispersed in PEO 10k as matrix was analyzed. We first present the results for samples prepared by melt route procedure and, secondly with samples prepared by solution dispersion route. Our previous work had demonstrated that, the increase of storage modulus (G') is much more sensitive to Laponite concentration as well as the matrix molecular weight than the loss modulus (G''). In this study for sake of simplicity and clarity just storage modulus will be presented in all the results.

Results for samples prepared by melt dispersion

Figure 1 shows the frequency dependence of the storage modulus (G') measured at 80°C for sample prepared by melt dispersion containing Laponite particles protected by either adsorbed PEO10k (crossed Symbol) or grafted trimethylammonium-PEG (NPE1k, NPE2k, and NPE5k) with various Laponite namely 2wt%, 3.5wt%, and 6.5wt%. Figure 1, clearly shows that, as the concentration of Laponite particles increases, storage modulus increases over all the frequency range. This is also the case of the loss modulus G'' (not showed in figure). A low frequency plateau is apparent for all the samples, reflecting the solid like character of these polymer nanocomposites. This behaviour shows that all the samples are well above the percolation threshold which appears to be very low in the Laponite-PEO system. It is however highly dependent on the type of protection of the particles. Loiseau et al¹² reported that, the percolation threshold for Laponite-PEO system shown to be decreased from 1 wt% when the surfaces of particles are not fully covered down to 0.5wt% with saturated particles.

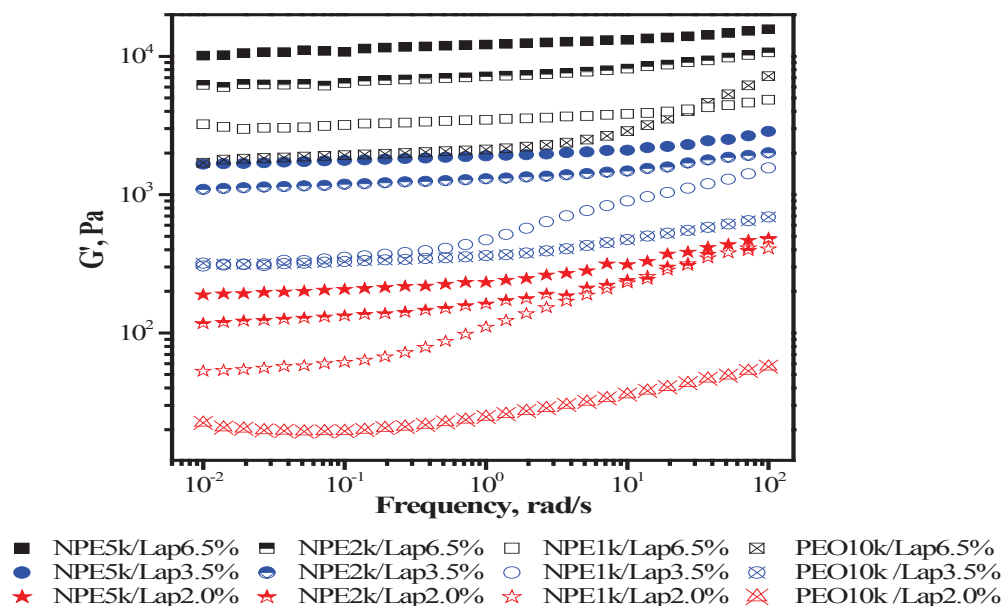


Figure 1. Storage modulus G' versus frequencies at 80°C for samples prepared by melt dispersion route with different Laponite loadings (2, 3.5, and 6.5wt% referred to Black, Blue and Red, respectively). Laponite particles are protected by adsorbed PEO10k and grafted modified-PEG (NPE) 1k, 2k, and 5k.

Whatever the Laponite concentration, samples with Laponite particles protected by grafted chains achieve higher modulus as compared to that with adsorbed chains. This observation is in agreement with our previous work¹²⁻¹³. Among the three different lengths of grafted chains, the modulus increases significantly with increasing the grafted chains molecular weight.

Figure 2 presents the influence of the type of protection of the particles on the scaling behavior of the low frequency modulus versus the Laponite concentration for samples prepared by melt procedure. It is worth to mention that, samples with grafted NPE5k Laponite at 1wt% shows higher modulus than those with adsorbed PEO10k at 2wt%. Qualitatively, samples with adsorbed PEO10k need twice more Laponite loadings to reach the same modulus of samples NPE5k grafted Laponite. Figure 2 also shows that, at low loadings of Laponite particles, influence of the type of protection of the particles on the modulus is higher than at high concentration. If we draw a fictive horizontal line in figure 2, we can deduce that the same level of modulus can be obtained either by choosing the particle concentration or the type of surface protection. Figure 2 shows that scaling laws relating the modulus to the concentration of particles are obtained with different values of the exponent, linked to the nature of the modified PEO particles. The different scaling exponent values ($G'_0 \propto \phi^x$) for different types of particle's protection the

particles ($x= 4\pm 0.2$, 3.2 ± 0.2 , 3.2 ± 0.2 , and 3.1 ± 0.1 for PEO10k, NPE1k, NPE2k, and NPE5k respectively) might indicate that, the structures responsible for the observed solid behavior are not identical.

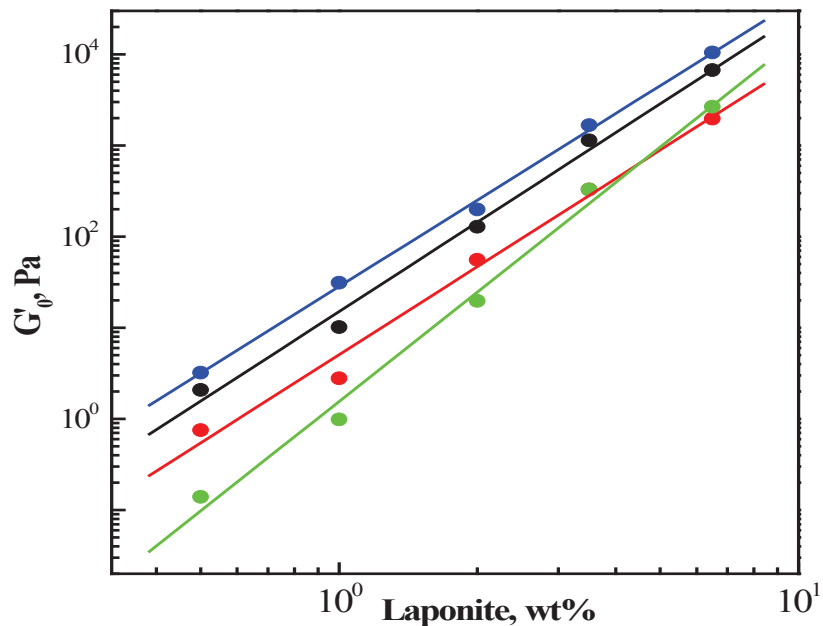


Figure 2. Scaling exponent of G'_0 vs. Laponite weight fraction for samples prepared by melt dispersion using different types of protected Laponite particles: adsorbed PEO10k (green), grafted NPE1k (red), NPE2k (black), and NPE5k (blue).

Results for samples prepared by solution mixing

Figure 3 shows the frequency dependence of the storage modulus (G') measured at 80°C for samples prepared by solution mixing containing Laponite particles protected by either adsorbed PEO10k or grafted trimethylammonium-PEG (NPE1k, and NPE5k) with various Laponite loadings 2wt%, 3.5wt%, and 6.5wt%. Comparison between Figure 1 and Figure 3 shows that, for a given type of protection and a given concentration of particles, the modulus of samples prepared by solution mixing is higher than the modulus of samples prepared by melt dispersion (figure 3). This agrees with what has been established in our previous study concerning the influence of the preparation methods on the properties of nanocomposites.

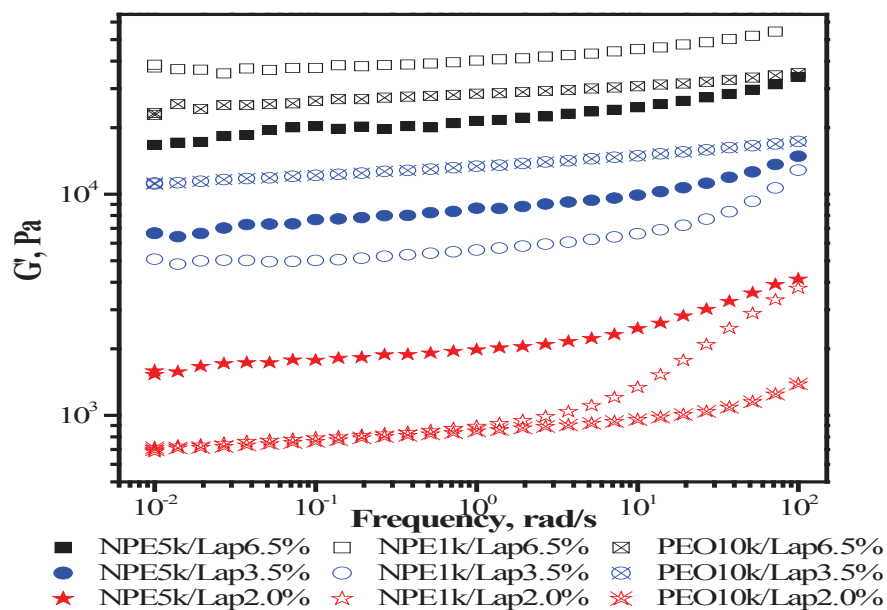


Figure 3. Storage modulus G' Vs. frequency at 80°C for samples prepared by solution mixing with different concentration of Laponite loading (2, 3.5, and 6.5wt% referred to red, blue, and black respectively). Laponite particles have been protected by adsorbed PEO10k (crossed symbols) and (NPE1k (open symbols)) and NPE5k (filled symbols).

To analyze these data, we plotted in Figure 4 the zero frequency modulus versus the Laponite concentration for the different types of Laponite. Figure 4 does not allow us to point for any influence of the type of protection of the particles when the samples are solution prepared, although a wide range of Laponite loadings has been covered. The values of the scaling exponents ($G'_{0\neq\phi^x}$) are $x=2.7\pm 0.2$, 2.5 ± 0.2 , and 2.6 ± 0.2 for PEO10k, NPE1k, and NPE5k respectively. These values are very similar and Figure 4 shows that the points are essentially randomly scattered along the average line (exponent 2.6 ± 0.1). We must admit that the reproducibility of the experiments does not bring better than a factor on the order of 2-3 for the modulus. We are inclined to conclude that for solution prepared samples, the structures responsible for the zero frequency modulus are indistinguishable, in contrast with what has observed with melt prepared samples.

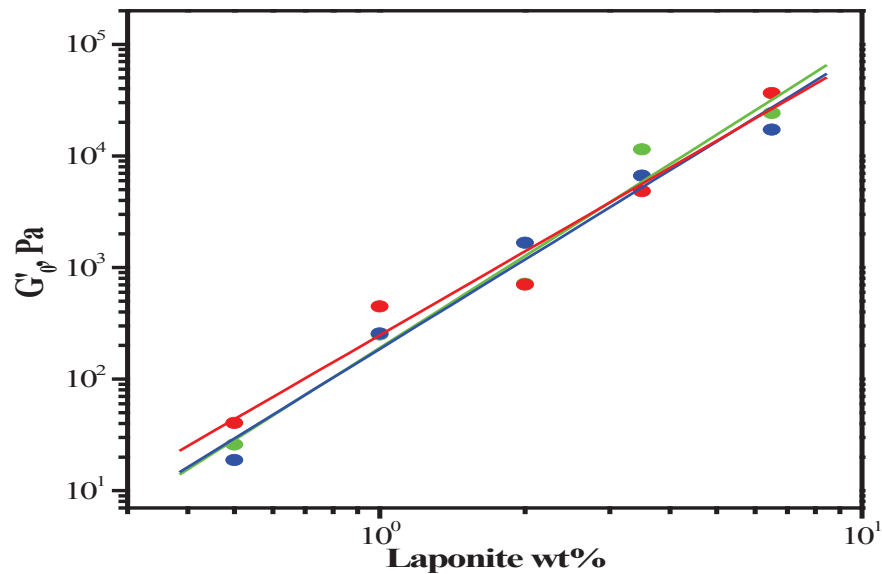


Figure 4: Scaling exponent of G'_0 vs. Laponite weight fraction for samples prepared by solution mixing. With different route of protecting Laponite particles: adsorbed PEO10k (green), grafted NPE1k (red), and NPE5k (blue).

2.4.4 Discussion

In this discussion, we would like to emphasize the main tendencies observed with viscoelastic properties when the protection of Laponite particles varies from adsorbed to grafted chains.

Three main effects have been observed. Two are linked to the protection of the particles.

- Particles bearing grafted chains lead to higher values of the modulus than particles with adsorbed chains.
- Grafted chains onto the Laponite particles lead to an higher modulus when the length of the chain increases,

The third effect is rather linked to the method of preparation of the nanocomposite. Whatever the type of protection, preparation of the suspension by freeze drying of a polymer solution containing particles leads to nanocomposites with similar properties, for the range of molecular weights that have been investigated.

This latter observation can be understood if we admit that the solution route leads to melt suspensions that reflect at best the optimum dispersion of the particles that can occur in solution. From our previous studies^{11, 17}, it has been established that PEO adsorbs onto Laponite particles and that adsorbed PEO chains create a steric barrier acting against the aggregation of particles in water, which leads to the formation of gels which can be destroyed by application of shear¹⁸⁻²⁰. The structure of these gels, which has been studied by light scattering, shows a fractal dimension on the order of 2, whatever the type of

protection. However, it was shown that flocculation occurred when long enough polymer chains were used to protect the particles¹⁷, leading eventually to so call shake-gels i.e. shear thickening systems²¹. This case was not studied here.

We can thus postulate that under the conditions of molecular weight considered here, the suspensions before freeze drying are all in the same state. It is likely that sublimation of water followed by hot pressing of the resulting fluffy powder leads to the same type of materials. We attribute the large scatter of the data, depending on the molecular weight to differences in the kinetics of aggregation in water due to the molecular weight of the chains and small variations of the duration of the mixing in solution.

The higher moduli observed when the nanocomposites are obtained from solution mixing rather than melt blending has been already explained in a previous paper and is simply attributed to the optimum state of dispersion that is reached using this procedure.

In the case of the melt dispersion route, a 10 wt% Laponite suspension is diluted, in the molten state, with neat PEO to adjust the concentration in the range 0.5 – 6.5 wt%, i.e. dilution by factors between 1.5 and 20. From previous results we can assume that initial state of dispersion of the particles in the 10wt% Laponite master batch does not depend on the type of protection of the nanoparticles, since the master batch has been prepared by solution mixing. All the blends have been obtained under identical conditions in the micro-compounder, so that the shear forces are mainly related to the viscosity of the matrix (which is low). It is however likely that for small dilutions (i.e. rather concentrated nanocomposites), interactions between the concentrated zones in Laponite arising from the master-batch contribute to an increase of viscosity. We can assume, as a first approximation, commonly used in the rheology of suspensions, that the volume fraction of the dispersed phase governs the viscosity. It should thus not be much influenced by the surface treatment of the particles.

We have thus to consider the mixing of a concentrated phase of surface treated platelets into a polymer matrix. We assume that, aside from shearing forces during the mixing, this problem bears some analogy with surface anchored polymer brushes and polymer melts of the same chemical nature. The problem is slightly different from grafted particles in polymer solutions²²⁻²³ where flocculation can be observed due to the depletion effect when the grafting density increases. Hasegawa et al²⁴ reported the existence of a minimum of the storage modulus in the low frequency plateau in ABS polymers when the grafting density of the polybutadiene particles by poly-(acrylonitrile-co-styrene) increases. The lowest plateau was attributed to the less aggregated particles (thus the best dispersed state). This optimum grafting density does not depend on the particle size, neither on the particle volume fraction, and was therefore attributed to the minimal attraction between particles. These authors demonstrate theoretically that this is due to the interaction energy between polymer brushes which becomes attractive in the polymer matrix. The origin of the attractive energy relies on the fact that in polymer melts, the brush and the matrix do not mix with each other (although there might be partial penetration, which has been the purpose of theoretical considerations²⁵⁻²⁶), and there is a

positive interfacial energy at the interface. If the dense brushes touch each other, the interface between brush and matrix disappear and the free energy of the system decreases, accounting for aggregation of the particles. On the other hand, if the brushes are not dense enough (mushroom regime), compression of the polymer layer leads to repulsion.

Figure 5 reproduces²⁷ the phase diagram of different regimes of interaction between matrix chains of polymerization degree P , grafted chains of length N and grafting density.

When applied to our case, P is constant and N increases from NPE1k to NPE5k. However, the graft density decreases as N increases. Thus, wetting appears easier for NPE5k. In other words, matrix chains will be more easily incorporated into the brushes with NPE5k, rather than NPE1k. However, from the amount of adsorbed chains, we can estimate that the grafting density σ decreases by 1/3 when going from NPE1k to NPE5k.

The length, h , of the swollen brush is given by²⁵ :

$$h \approx N\sigma^{1/3}P^{-1/3}$$

so that h for NPE5K is 3.4 times larger than with NPE1k. We thus deduce that chain length effects are dominant with respect to grafting density.

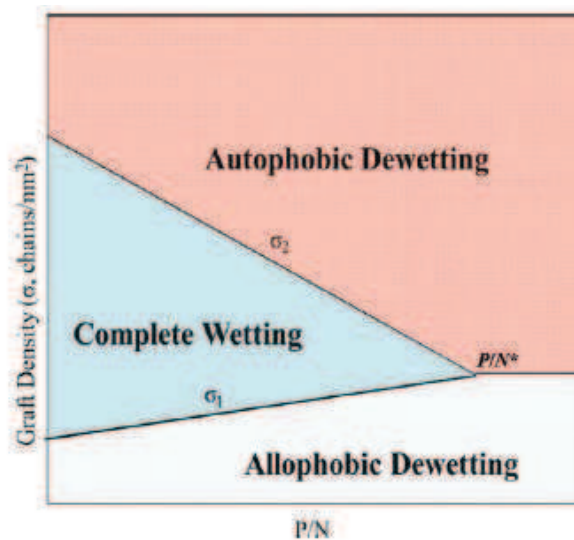


Figure 5 : Phase diagram for nanoparticle stability as function of graft density and ratio P/N of matrix versus grafted chains length. Stability (i.e. best dispersion) is observed in the complete wetting region.

We assume that having longer brushes with the same number of particles is by some way equivalent to increase the volume fraction of the particles. This accounts qualitatively for the chain length effect, since about the same modulus is obtained for

NPE1k suspensions than NPE5k suspension if the weight fraction is increased by a factor on the order of 2. Furthermore, the external part of grafted NPE5k chains might entangled with the PEO10k matrix which is able to swell the brush. Because of the chain length difference, entanglements are more probable than with short chains of NPE2k and NPE1k, since the molecular weight between entanglements for PEO is on the order of 2000 g/mol.

In the case of adsorbed chains, in the molten state, it has been shown that the thickness of the adsorbed layer is independent of L and simply proportional to the adsorbed quantity²⁸. We thus deduce that a rather flat layer is obtained and that the effective volume fraction of covered particles is even lower than with NPE1k. This argument reinforced by the small entanglement of the adsorbed chains with the surrounding chains accounts for the smaller moduli with this type of protection.

2.4.5 Conclusion

The influence of the type of protection of the particles is often considered as an important parameter to control the dispersion state of the particles in a polymer matrix^{25, 27}. As compared to most of the studies reported on layered silicates, the singularity in our Laponite/PEO system is to cover the particles with polymer chains rather than with surfactants (small molecules). In this present study, the aim was to study the influence of the type of protection of the particles on the rheological properties of the model nanocomposites. Thanks to the ability to obtain PEO chains containing a quaternary ammonium salt at one end, we were able to graft polymer chains instead of simply adsorbing them.

The nanocomposites obtained by the so called solution mixing procedure showed rheological properties that were, within the scattering of the data, independent of the protection of the Laponite particles. On the opposite, when starting from a master batch of grafted or adsorbed particles that were further dispersed in the molten state inside the polymer matrix, noticeable differences in the rheological properties were noted. It was shown that increasing the length of the grafted chain increases the storage modulus at zero frequency. In addition, grafted chains even of low molecular weight were more efficient than adsorbed ones to obtain higher moduli.

This observation recovered the results of a previous work. In this case, we were able to access X-Ray data to show that grafted chains were providing better dispersion of the Laponite particles, leading in other words to an higher effective volume fraction of particles involved in the structuration of the particles.

With grafted chains we proposed an interpretation based on the degree of wetting of the grafted chains by the chains of the matrix to explain the molecular weight differences. It would be tempting to use even longer chains but unfortunately only chains with two hydroxyls groups at the chain ends are commercially available with higher molecular weights.

2.4.6 References

1. Usuki, A. K., Yoshitsugu; Kawasumi, Masaya; Okada, Akane; Fukushima, Yoshiaki; Kurauchi, Toshio; Kamigaito, Osami, *Synthesis of nylon 6-clay hybrid. Journal of Materials Research* **1993**, 8, (5), pp.1179-1184.
2. Peng, L., *Polymer modified clay minerals: A review. Applied Clay Science* **2007**, 38, (1-2), 64-76.
3. Anderson, B. J.; Zukoski, C. F., *Rheology and Microstructure of an Unentangled Polymer Nanocomposite Melt. Macromolecules* **2008**, 41, (23), 9326-9334.
4. Anderson, B. J.; Zukoski, C. F., *Rheology and Microstructure of Entangled Polymer Nanocomposite Melts. Macromolecules* **2009**, 42, (21), 8370-8384.
5. Morgan, A. B.; Wilkie, C. A., *Flame retardant polymer nanocomposites*. Wiley-Interscience: 2007.
6. Loyens, W.; Jannasch, P.; Maurer, F. H. J., *Effect of clay modifier and matrix molar mass on the structure and properties of poly(ethylene oxide)/Cloisite nanocomposites via melt-compounding. Polymer* **2004**, 46, 903-914.
7. Ko, M. B.; Jho, J. Y.; Jo, W. H.; Lee, M. S., *Effect of matrix viscosity on clay dispersion in preparation of polymer/organoclay nanocomposites. Fiber. Polym.* **2002**, 3, (3), 103-108.
8. Fornes, T. D.; Yoon, P. J.; Keskkula, H.; Paul, D. R., *Nylon 6 nanocomposites: the effect of matrix molecular weight. Polymer* **2001**, 42, (25), 09929-09940.
9. Fornes, T. D.; Yoon, P. J.; Keskkula, H.; Paul, D. R., *Nylon 6 nanocomposites: the effect of matrix molecular weight* (vol 42, pg 9929, 2001). *polymer* **2002**, 43, (7), 2121-2122.
10. Tanoue, S.; Utracki, L. A.; Garcia-Rejon, A.; Sammut, P.; Ton-That, M. T.; Pesneau, I.; Kamal, M. R.; Lyngaae-Jorgensen, J., *Melt compounding of different grades of polystyrene with organoclay. Part 2: Rheological properties. Polym. Eng. Sci.* **2004**, 44, (6), 1061-1076.
11. Mongondry, P.; Bonnans-Plaisance, C.; Jean, M.; Tassin, J. F., *Mild Synthesis of Amino-Poly(ethylene glycol)s. Application to Steric Stabilization of Clays. Macromol. Rapid Commun.* **2003**, 24, (11), 681-685.
12. Loiseau, A.; Tassin, J. F., *Model Nanocomposites Based on Laponite and Poly(ethylene oxide): Preparation and Rheology Macromolecules* **2006**, 39, 9185-9191.
13. Loiseau, A. *Elaboration et caractérisation de Nanocomposites modèles Laponite/Polyoxyde d'ethylene*. Ph.D, du maine, Le mans, 2006.
14. Alexandre, M.; Dubois, P., *Materials Science and Engineering* **2000**, (28), 1-63.
15. Lepoittevin, B.; Pantoustier, N.; Devalckenaere, M.; Alexander, M.; Kubbies, D.; Calberg, C.; R. Jérôme; Dubois, P., *Polymer/layered silicate nanocomposites by combined intercalative polymerization and melt intercalation: a masterbatch process. Polymer* **2003**, 44, 2033-2040.
16. Mitsuhashi, T.; Jones, W. M., *Carbene-carbene rearrangements. Importance of bond order. Journal of the American Chemical Society* **1972**, 94, (2), 677-679.

17. Mongondry, P.; Nicolai, T.; Tassin, J. F., *Influence of pyrophosphate or polyethylene oxide on the aggregation and gelation of aqueous laponite dispersions. Colloid and Interface Science* **2004**, 275, 191–196.
18. Nicolai, T.; Cocard, S., *Light scattering study of the dispersion of laponite. Langmuir* **2000**, 16, (21), 8189-8193.
19. Nicolai, T.; Cocard, S., *Dynamic light-scattering study of aggregating and gelling colloidal disks. Journal of Colloid and Interface Science* **2001**, 244, (1), 51-57.
20. Nicolai, T.; Cocard, S., *Structure of gels and aggregates of disk-like colloids. European Physical Journal E* **2001**, 5, (2), 221-227.
21. Can, V.; Okay, O., *Shake gels based on Laponite-PEO mixtures: effect of polymer molecular weight. Des Monomers Polym* **2005**, 8, (5), 453-462.
22. Gast, A. P.; Leibler, L., *effect of polymer-solutions on sterically stabilized suspensions. Journal of Physical Chemistry* **1985**, 89, (19), 3947-3949.
23. Gast, A. P.; Leibler, L., *interactions of sterically stabilized particles suspended in a polymer-solution. Macromolecules* **1986**, 19, (3), 686-691.
24. Hasegawa, R.; Aoki, Y.; Doi, M., *Optimum graft density for dispersing particles in polymer melts. Macromolecules* **1996**, 29, (20), 6656-6662.
25. Ferreira, P. G.; Ajdari, A.; Leibler, L., *Scaling law for entropic effects at interfaces between grafted layers and polymer melts. Macromolecules* **1998**, 31, (12), 3994-4003.
26. Gay, C., *Wetting of a polymer brush by a chemically identical polymer melt. Macromolecules* **1997**, 30, (19), 5939-5943.
27. Sunday, D.; Ilavsky, J.; Green, D. L., *A Phase Diagram for Polymer-Grafted Nanoparticles in Homopolymer Matrices. Macromolecules* **2012**, 45, (9), 4007-4011.
28. Aubouy, M.; Guiselin, O.; Raphael, E., *Scaling description of polymer interfaces: Flat layers. Macromolecules* **1996**, 29, (22), 7261-7268.

2.5 General conclusion

Strong interactions between dispersed clay particles and polymer matrix can fairly change the rheological behavior of composites in the molten state. Dispersion state of the particles is considered as the key to get maximum of properties. When clay particles are largely exfoliated the melt rheology of a composite can change from a melt-like to a gel-like state, which essentially suggests that the dispersed clay platelets either behave as physical cross links or undergo structuration in the melt, leading to gelation. The structures responsible for the viscoelastic behavior of polymer nanocomposites at low frequency are found to be governed by three parameters:

- Preparation procedures
- Matrix molecular weight
- Type of protection of the particles.

As it has been mentioned in the introduction of this chapter, the aim of the work was to study the influence of these parameters that have an effect on rheological properties of model nanocomposites based on Laponite and Poly (ethylene oxide).

In this conclusion we recall the main findings gathered in the three draft papers of chapter 2. We also add the results of other experiments, which were carried out using the same procedures, which show the coherence of the data.

First of all, to study the effect of the preparation method on rheological properties of composites, two preparation methods have been considered in this work: solution mixing and melt dispersion. Laponite particles were protected by adsorbed PEO10k. Linear viscoelastic response of nanocomposites showed that, samples prepared by solution mixing achieved higher modulus compared to that prepared by melt dispersion. Solution mixing was chosen to reach the best state of dispersion we were thinking of. Nevertheless SAXS data pointed that some stacks of a few Laponite particles remain. The lower moduli obtain after dilution of the master-batch suggests a reduction in the network structures modulus during melt processing, which, however fails to alter the clay spatial distribution in the nanoscale.

A nice proof of this idea was obtained by preparing a 1% nanocomposite from the dilution of master batches at different concentration, where it was shown that higher moduli are observed when starting from more diluted master batches. This behavior was qualitatively explained using the analogy with the polymer blends. It was argued that the higher the viscosity differences between the polymer matrix and the master batch, the lower the dispersion of the structures in the matrix.

The coherence of these findings is supported by the same kind of experiments carried out with grafted NPE1k chains rather than adsorbed ones. The results are shown in figure IV.1 and agree with those obtained with adsorbed PEO10k. The scalings are also presented in Figure IV.2. The exponent of 2.5 obtained for solution mixing is in total agreement with the one (2.7) obtained for adsorbed 10k. This also confirms the conclusions of the third paper, in the sense that the values of moduli are coherent with those of solution prepared samples with adsorbed 10k chains.

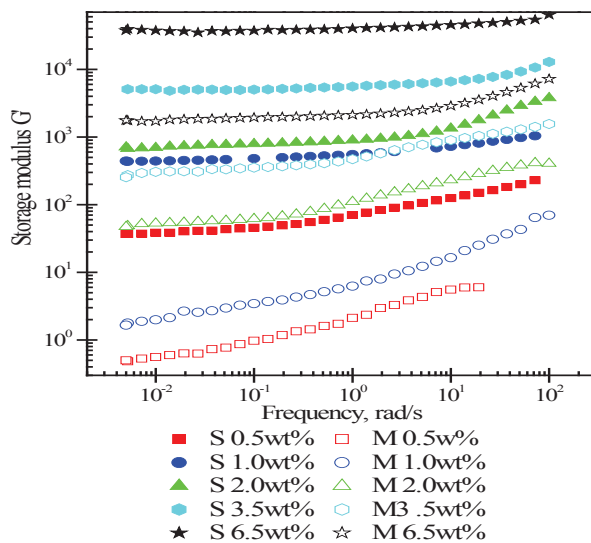


Figure. IV.1: Storage modulus G' Vs frequency at 80°C for different concentrations (by weight) of Laponite particles protected with grafted chains (NPE1k) dispersed into PEO 10k matrix for samples prepared by solution mixing(closed symbols), and melt dispersion (open symbols)

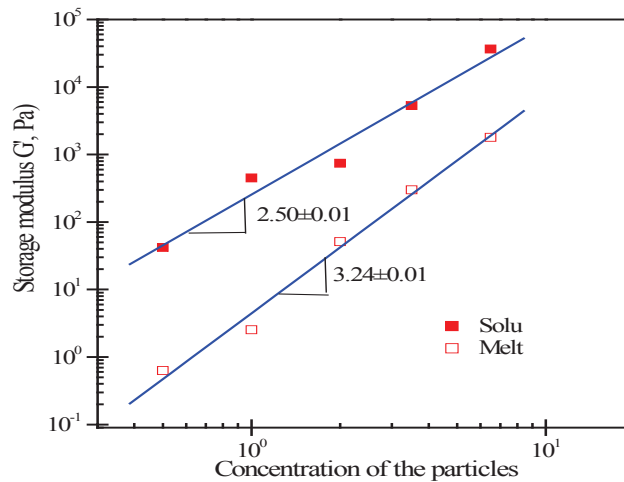


Figure IV.2 Scaling laws of storage modulus G' Vs Laponite weight fraction for nanocomposites prepared by two procedures : melt dispersion (open symbols), and solution mixing (closed symbols). Protection of the particles using grafted chains NPE1k.

Effect of matrix molecular weight on properties of nanocomposites was studied. Linear viscoelastic modulus was found to be increased significantly with the increase of matrix molecular weight. This increase was more pronounced at low loadings of Laponite particles rather than high loading of Laponite particles. This might indicate that the particles stability at high loading is largely controlled on the polymer segmental level rather than on the polymer molecule level. The high molecular weight PEO chains are capable of breaking the master batch structures into small clusters. These clusters can be well mixed into the matrix and generate structuration of the nanocomposite. The second paper of this chapter deals with molecular weights above 10k. The conclusions are still valid if lower molecular weight matrices are consider, as indicated in Figure IV.3 where the viscoelastic response of nanocomposites containing 3.5wt% of Laponite particles protected by grafted NPE1k is plotted for PEO matrices ranging from 2k to 35k. We recall that solution mixing shows pronounced differences for rather low concentrations of particles, which is the case here.

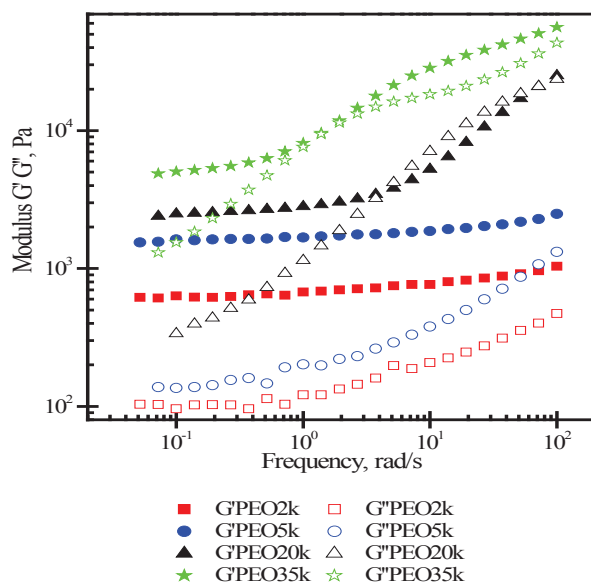


Figure 3. Modulus Vs frequency (rad/s) for samples prepared by solution route with 3.5wt% of Laponite loading protected by grafted NPE1k.

Influence of the type of protection of the particles has also been considered. A change in properties has been observed when the particles bear grafted chains rather than adsorbed ones in the case of melt prepared samples. The type of protection was essentially negligible following a preparation in solution. Lacking of SAXS data for this part of the work, we assumed that equivalent interpretations as previously were still valid. However, here the same matrix is considered, and it is likely that the properties of the master batch do not depend strongly on the surface treatment of the particles. To interpret the data, we point an analogy with the dispersion of grafted particles in melts which has been the subject of various investigations and also of theoretical considerations. Based on them, we discussed the wetting of the polymer brush on the particles by the matrix chains as a function of the length of the grafted chains and of the grafting density. We came up with the conclusion that conditions for partial wetting of the brush were gathered (rather than dewetting and aggregation) and that we could explain partly the observation by the change of volume fraction of the particles when covered with long or shorter grafted chains.

More experiments were carried out to confirm the independence of modulus for samples prepared by solution procedure regardless of the amount of adsorbed or grafted chains on Laponite. Figure IV.4 shows the behavior of nanocomposites prepared by solution mixing containing 2wt% of Laponite bearing grafted chains NPE1k, NPE2K or NPE5k or adsorbed 10k. The ratio between Laponite and grafted or adsorbed chains has been set at (1:1). We recover expected results, i.e. independency for moduli on the surface treatment of the particles. In the same idea, the ratio of NPE2k with respect to the amount of Laponite has been varied (see Figure IV.5), but no influence on the moduli has been detected.

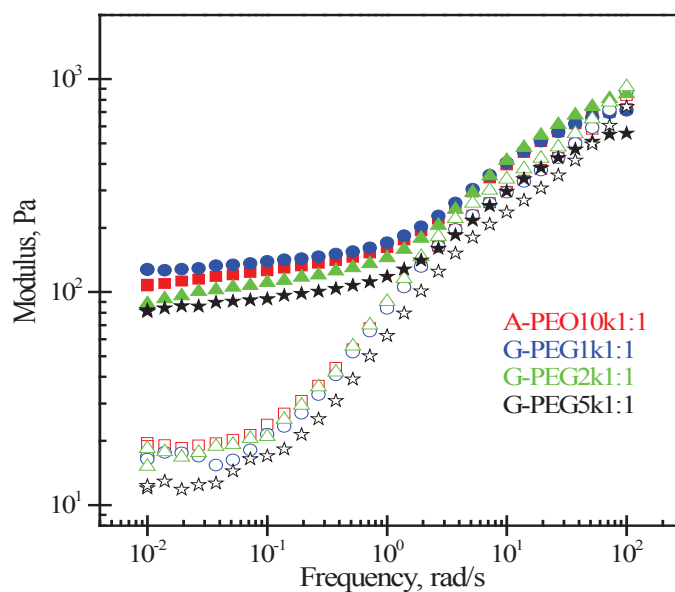


Figure IV. 4. Moduli Vs frequency (rad/s) for samples prepared by solution route at 2wt% of Laponite loading protected by different methods. Molecular weight of the matrix is PEO10k

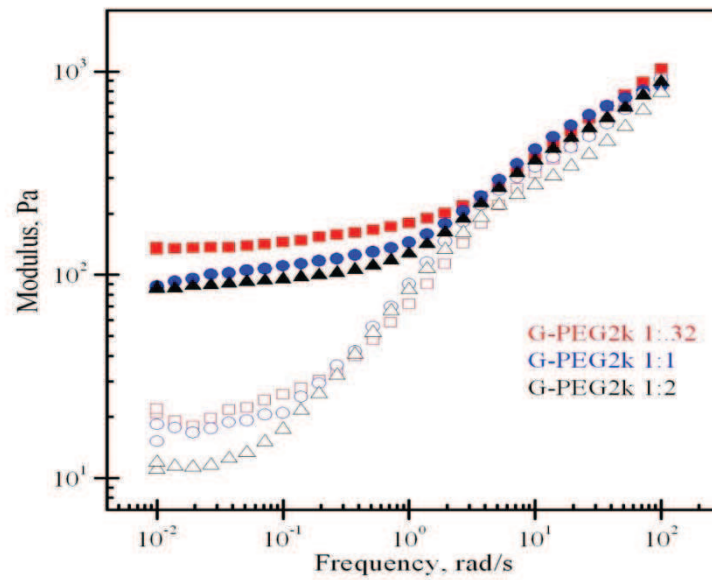


Figure IV.5: Moduli Vs frequency (rad/s) for samples prepared by solution route at 2wt% of Laponite loading protected with varying quantities of grafted NPE2k chains. Molecular weight of the matrix is PEO10k.

Chapter 3: Polymer blends nanocomposites based on PMMA-PEO blends/Laponite

3.1 Introduction

Polymer nanocomposites are materials in which a filler phase, made of particles where at least one dimension is less than 100nm, is dispersed in a polymer matrix. When dispersion is obtained at the scale of the individual particles, an improvement of the mechanical properties of the polymer is observed as well as an increase in solvent resistance, ionic conductance, heat resistance, and gas permeability and flammability¹⁻⁵.

Blending polymers is a useful technique for creating new materials⁶ which has been applied for several polymeric system of commercial importance. Polymer blends are most often incompatible, so that a macroscopic phase separation occurs between the two phases, leading in the general case to poor mechanical properties which can be improved using compatibilization techniques. Some systems⁶, such as polystyrene – polydimethylphenyleneoxyde, polystyrene – polyvinylmethylether, show miscibility at the molecular scale over all the composition range. Taking into account our previous studies on the dispersion of Laponite particles in PEO, it was tempting to extend these studies to compatible polymer blends containing PEO and more precisely to PMMA/PEO blends.

PMMA/PEO blends have been early recognized to be miscible in the liquid state⁷⁻⁹, i.e. above the melting temperature of PEO. The analysis of melting point depression as well as Small Angle Light Scatterings (SALS), and Small Angle Neutron Scattering (SANS) experiments confirmed PMMA/PEO miscibility with negative (and small) values of interaction parameter (χ'_{12})¹⁰. Since they consist of an amorphous and a crystallizable component, crystallization of PEO is expected under given conditions. For PEO concentrations less than roughly 20%, an amorphous blend is observed, with a single Tg which decreases when the PEO content increases. Quenching experiments have been used to inhibit PEO crystallization and characterize Tg versus composition¹⁰. For higher concentrations of PEO, crystallization appears, but the degree of crystallinity of the PEO is reduced as compared to the neat polymer. The content of PEO in the amorphous phase has been determined using NMR investigations¹¹⁻¹². About 10wt% PEO is included in the PMMA rich phase for PMMA contents ranging from 40 to 60%. Poly (ethylene oxide) (PEO)/poly (methyl methacrylate) (PMMA) blends have been the subject of numerous investigations in the past, but also more recently where attention has been paid due to extreme difference in mobility between PEO and PMMA since about 12 orders of magnitude separate the fast PEO dynamics and the slow PMMA one¹³.

PMMA/PEO blends nanocomposites have received significant interest in recent years due to their superior properties as compared to the polymer itself. It has been observed by many authors¹⁴⁻¹⁷ that PMMA/PEO blends shows high affinity to layer-silicates, as

organically modified montmorillonite¹⁶, Laponite¹⁷, and N⁺-rich montmorillonite (MMT)¹⁴. So far, nanocomposites based on PMMA/PEO blends and low contents of montmorillonite achieved an exfoliated morphology, with the enhancement of ionic conductivity as well as segmental dynamics^{13, 18}. Moreover, referring to the literature ideas^{16, 19}, PMMA/PEO blends nanocomposites achieved higher tensile modulus, elasticity (at low frequency) and elongation at break than pristine polymer blends. According to Kim et al¹⁶ the increase of elasticity at low frequency region is originating from the nanoscopic interaction between polymers and nanoparticles.

Relatively few papers have been published to date on PMMA/PEO blends containing layered silicates such as Laponite or Montmorillonite. Some of them are related to the beneficial enhancement of ionic conductivity (of Li⁺ or Na⁺ species) within the solid state batteries field of application. In this case, the content of nanoparticles is quite high (on the order of 70wt% or more). Intercalation is sought in this case. Organically modified montmorillonite (OMMT) has been dispersed in PEO and PMMA using dichloromethane as cosolvent^{16, 19}. Intercalation of the blend inside the clay galleries was proven by X-Ray diffraction and enhancement of the Young modulus in the solid state was observed with respect to pristine blends. Thermodynamical analysis of the melting point depression was used to measure the interaction parameter, from which it was suggested that PMMA had a greater affinity towards the OMMT than PEO. Rheological properties of the blends were checked in the molten state for equivalent ratio of PMMA and PEO. A slight increase in G' and G'' was reported, but no real evidence of a physical network of particles and polymers was obtained¹⁶. Melt intercalation was studied by Shen *et al.*^{14, 20}, who used both non modified sodium Montmorillonite (MMT) and OMMT. It was shown that PEO could intercalate between both MMT and OMMT, whereas PMMA was only able to intercalate in OMMT. In these studies intercalation was the goal of the work so that long annealing times were studied. It was shown that the OMMT was able to host a higher concentration of polymer chains from a miscible blend rather than from either polymer alone. PEO/PMMA blends with 20wt% PEO containing Na⁺ MMT were prepared using solution methods and their melt rheological properties were investigated²¹. Influence of 2wt% particles was seen (as an increase of complex viscosity and a shift in relaxation times) when the MMT particles already mixed in PEO were further dissolved in PMMA using a co-solvent, whereas essentially no modification was observed when the particles were dispersed in the two polymers in a single step. TEM pictures clearly showed that compact aggregates of MMT are formed in the latter case, whereas some dispersion is observed with the former one.

The aim of this chapter is to study the internal structure, thermal properties and rheological properties in molten state for polymer blends nanocomposites based on PMMA-PEO blends and Laponite. The direct visualization of internal structure was conducted using Transmission Electronic Microscopy (TEM) and Scanning Electronic Microscopy (SEM). Thermal and rheological properties give complementary information and all techniques have been combined to get the most detailed inside into the structure of the nanocomposites.

3.2 Experimental part

Materials

PEO and PMMA were considered as the base materials for the polymer blends in this study. PEO, of molecular weight 10 000 g/mol was obtained from Fluka AG. PMMA was provided by Arkema. Its molecular weight, as analyzed by Size Exclusion Chromatography in THF, was determined as $M_n = 50.178$, $M_w = 110.140$ g/mol. Laponite RD, supplied from Rockwood additives Ltd. (U.K), with density 2570 Kg/ m³ was used. The cation exchange capacity is 0.95 mequiv/g, and the specific surface is 750 m²/g.

Samples preparation

A master batch containing PEO and Laponite was prepared according to the solution method following our previous studies. MilliQ water was used as solvent for PEO and dispersing media for Laponite particles. Nanocomposites based on PMMA-PEO blends and Laponite were prepared by a combination of solution mixing and melt dispersion procedures³⁻⁴. Initially, Laponite powder and poly (ethylene oxide) with molecular weight 10.000g/mole were dispersed separately under gentle stirring in deionized water (milli Q) for 24 hours at a concentration of 1% (w/w). The solutions of PEO 10k g/mole and Laponite were mixed in equal proportions, leading to a 50% wt of Laponite with respect to PEO. Adsorption of PEO onto the Laponite particles was allowed for 24 hours and the particles were further diluted with PEO solutions to obtain targeted concentration of Laponite particles of either 10wt% or 20wt%. The mixtures were frozen rapidly with liquid nitrogen and were freeze dried for 12 to 18 hours at -46 °C to remove the water; finally a fluffy powder was obtained and is considered hereafter as a master batch.

The master batch were mixed with PMMA in molten state in different ratios , thanks to a Haake Minilab microcompounder under corotating twin-screws operating at 160 °C, at 60 rpm for 10 min. The 10wt% and the 20wt% master batch were used depend on the targeted concentration of Laponite.

PMMA/PEO blends with PEO content ranging from 10 to 60 wt% were thus obtained.

Measurements

Samples for rheological characterization were disks of 25 mm diameter and 1 mm thickness that were prepared by moulding at 190°C followed by cooling at room temperature. The linear viscoelastic properties of the samples were studied, with the aim of determining the parameters that act on the low frequency modulus of the samples by using a strain controlled Rheometer RDAII.

Calorimetric measurements were performed on 2920 modulated DSC from TA instruments using sealed aluminum pans. Instrument was calibrated for the melting endotherm using Indium standard. About 8-10 mg of the sample was used. The sample was first heated up to 160°C at 10°C/mn, than annealed at 160°C during 10 mn and further cooled at 10°C/mn down to -60°C. The DSC traces were recorded during the next heating at a rate of 10°C/mn.

Samples for SEM were prepared by cutting with microtome (glass knife) to obtain very smooth surface, then poured into miliQ water to dissolve and remove as much possible of the PEO phase, and dried under vacuum at 50°C. The measurements were carried out with SEM HITASHI S3200N.

For TEM characterizations, samples with ultrathin sections were cut using an ultramicrotome (Leica UC7) at room temperature and under dry condition and then transferred onto a 300 mesh Cu grids coated with a Lacey carbon film. The microstructures were studied by Transmission Electron Microscopy (TEM) using a HF2000 Hitachi (Field Emission Gun 100kV, point to point resolution = 0.23 nm).

3.3 Results and discussions

Miscibility of PMMA/PEO blends.

The miscibility of PMMA/PEO blends and their nanocomposites has been studied using visual observation, X-ray diffraction, DSC, TEM and SEM.

The transparency of the samples is an easy way to detect immiscibility, since scattering of light will appear as soon as a difference in the refractive indices of the two phases exist and the size of the phase is not small as compared to the wavelength of light. Figure 1 illustrates qualitatively the transparency of PMMA/PEO disks of 2 mm thickness containing from 10 to 50wt% PEO. The concentration of Laponite increases from 0.9 with 10wt% of Laponite to 4.8wt% with 50%. Up to 30wt% of PEO a rather good transparency is observed, whereas immiscibility is quite obvious for higher PEO contents.

As Laponite is added, a slight decrease of transparency is observed. It is more marked in PEO rich blends, since to concentration of particles is higher.

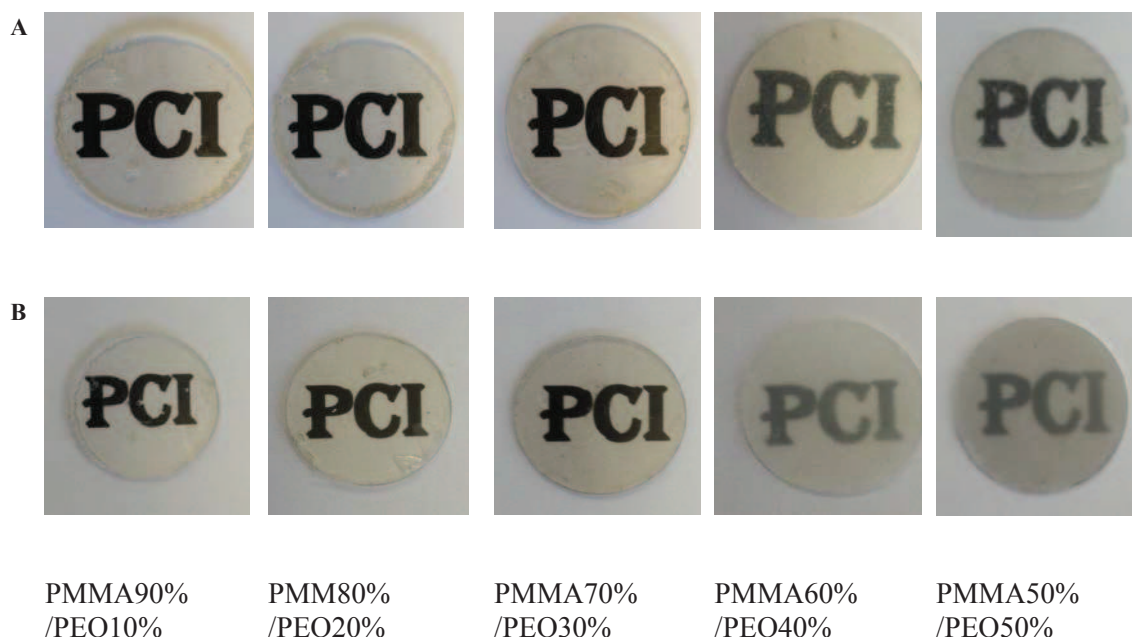


Figure 1. Apparent transparency of PMMA/PEO disks of 2 mm thickness in different ratios without Laponite (A) and with Laponite (B). (Laponite concentration from left to right 0.9, 1.9, 2.9, 3.8, and 4.8wt% respectively)

Miscibility of the components implies that the PEO is mixed at the molecular level with PMMA, so that amorphous blends must be obtained.

X-Ray diffraction spectra shown in figure 2 demonstrate that samples with PMMA concentration higher than 70% are completely amorphous. The spectra show three broad peaks which essentially coincide with those of pure PMMA. A more careful examination shows that, small crystallization peaks of PEO can be detected for 30wt % of PEO. These weak signs disappear when Laponite is added.

For 40 and 50 wt% of PEO crystallization of PEO is clearly seen. The introduction of Laponite decreases the apparent crystallinity of the samples, as seen from the decrease of intensity of the peaks and the increase of width at half height which denotes that smaller or more imperfect crystals are obtained.

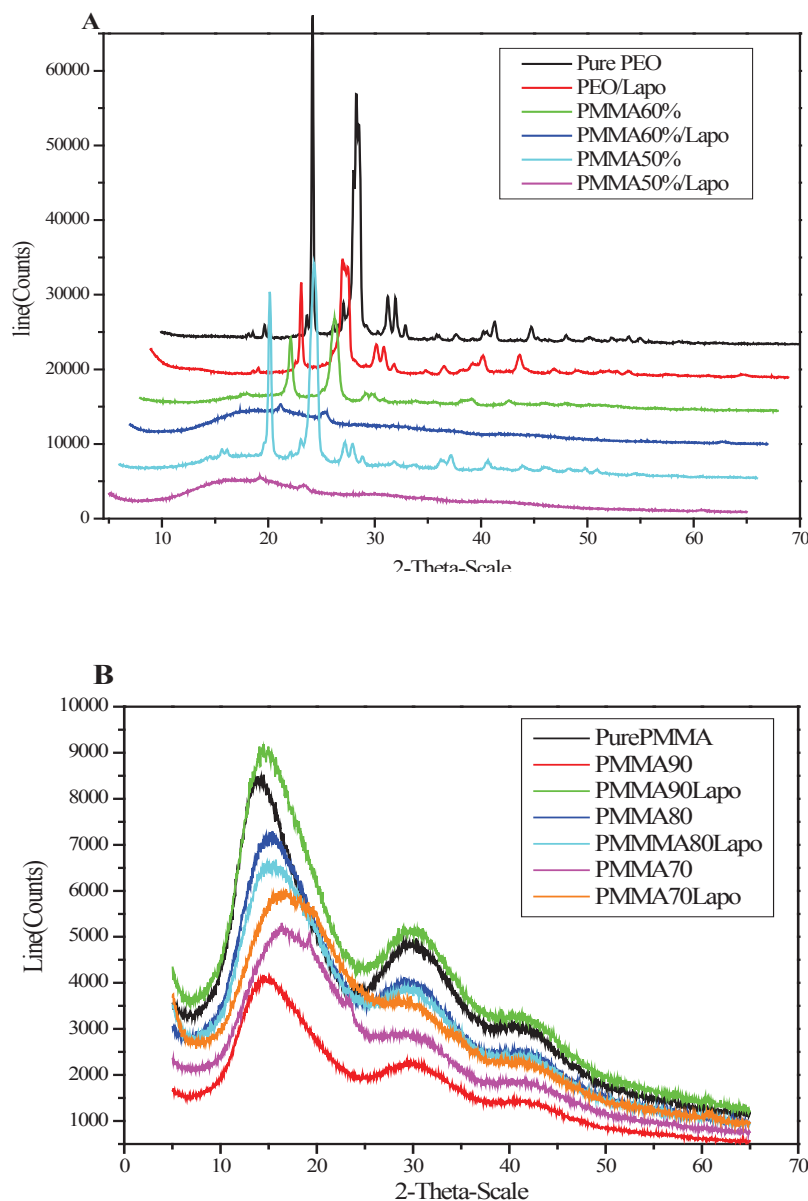


Figure 2. X-ray diffraction for PMMA/PEO blends and their nanocomposites for crystalline and amorphous. A: samples with PEO concentration higher than 50%, B: samples with PEO contents less than 30%. Data have been shifted along the Y axes for clarity.

The thermal properties (T_g , T_m and crystallinity) have been characterized using DSC. DSC traces for samples with an increased content of PEO are presented in figure 3, The T_g s of individual components after passing through the extrusion were found to be 109°C and -50°C for PMMA and PEO respectively. For PEO contents lower than 30 wt% the DSC traces are typical of compatible amorphous polymers, since a single T_g is observed. The glass transition temperature decreases when the PEO content increases and does not seem affected by the presence of Laponite particles. At a PEO content of 30% and above

melting of PEO is observed and the glass transition of PMMA appears difficult to detect on the DSC traces.

By comparing 30wt% PEO blends with or without Laponite, it appears that the melting endotherm is of lower intensity with Laponite. Melting of PEO appears at a slightly lower temperature than pure PEO (55°C instead of 60°C). This is coherent with the X-Ray diffraction data which showed a slight crystallinity and rather broad peaks, sign of small or un-perfect crystals. The onset of the glass transition temperature appears at 25 – 30°C for this blend without Laponite. With Laponite, T_g of PMMA rich phase cannot be observed. For higher PEO contents, the DSC trace reveals essentially crystallization (broad exothermic peaks in the range from -25°C to 400C) followed by a clear melting peak at 60°C. Obviously, the presence of Laponite particles decreases the crystallinity of the PEO phase.

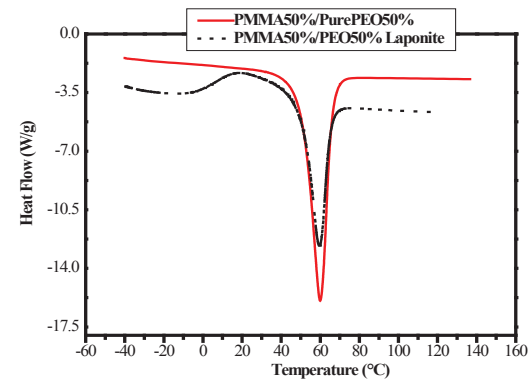
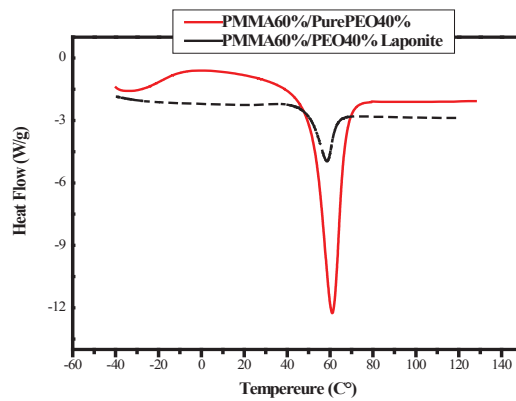
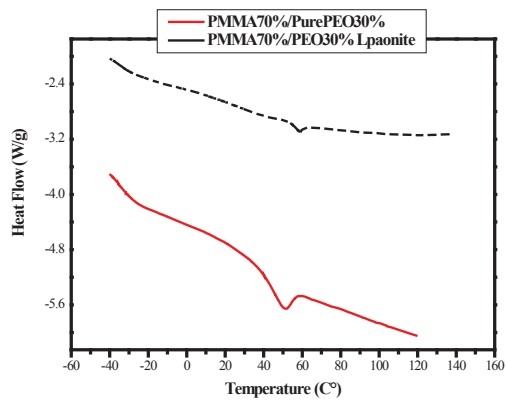
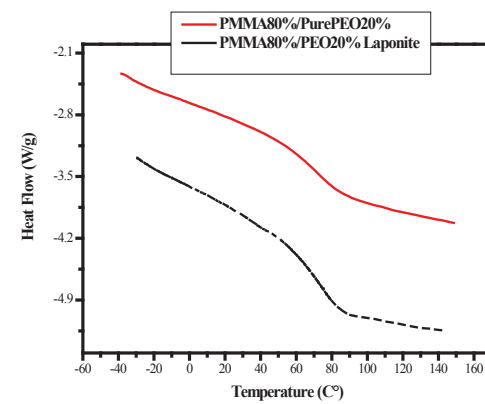
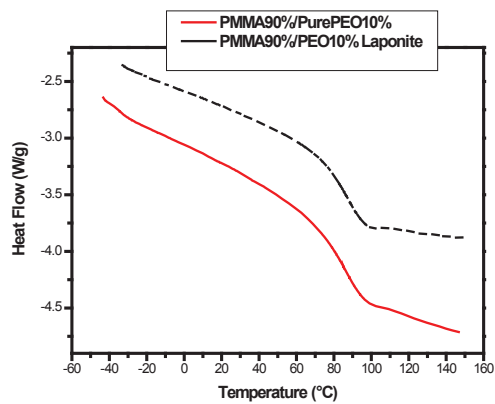
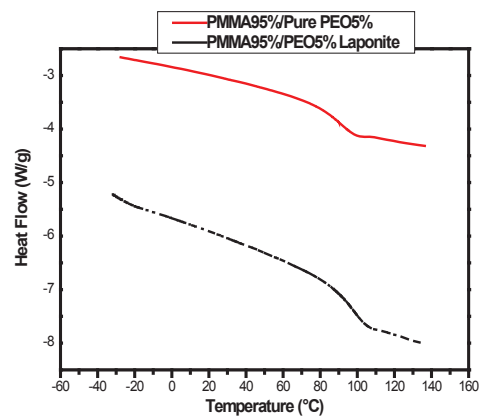


Figure 3 DSC traces for PMMA/PEO blends, with (dashed blue line) and without (red line) Laponite particles.

observed by scanning electronic microscopy (SEM). The results are displayed in figure 4, where we aim at comparing different PEO contents and the influence of Laponite.

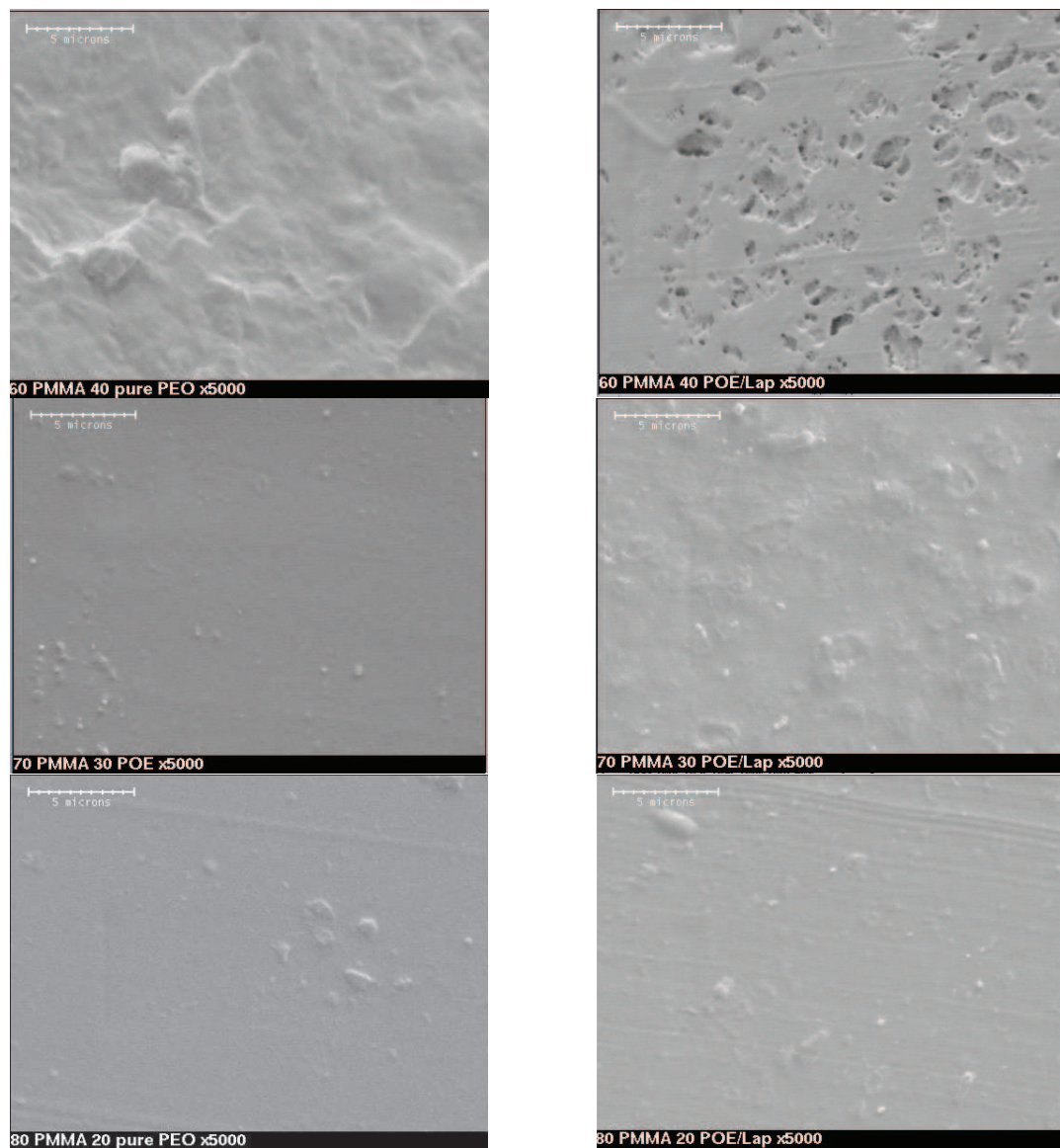


Figure 4. SEM micrographs of PMMA/PEO blends in different ratios with (right column) and without (left column) Laponite.

From figure 4, PMMA/PEO blends up to 30wt% PEO appear quite homogeneous, although some deposits of about 1 up to 2 microns size are observed. With 40% PEO, the surface of the sample is no more smooth, but droplets of PEO are not observed. When Laponite is added, the heterogeneity of the surface is increased. Some micron size craters are apparent at 30% PEO, which is not the case without Laponite. With 40% PEO these

craters transform into holes whose sizes vary from about a fraction of micron to 3 microns. There is here a clear sign of the introduction of Laponite particles which seem to act against the dispersion of the PEO phase inside the material.

TEM micrographs of the samples, given in Figure 5, confirm the previous observations. With up to 30% PEO and absence of Laponite, the samples are quite homogeneous. At higher concentrations, crystallization of the PEO phase is obvious. When adding Laponite, the existence of domains with a size ranging from a fraction of micron to a few microns is observed. These domains show a strong electron density due to the high concentration of Laponite particles. Apparently inside these domains Laponite particles have various degrees of dispersion. Some domains are very dark, indicating existence of aggregates of Laponite. Others contain rather well dispersed particles, although their concentration is quite high (3.8wt%). There is apparently no sharp interface between the Laponite rich domains and the matrix. In some cases, it seems that some light grey zones between darker domains contain essentially individual particles.

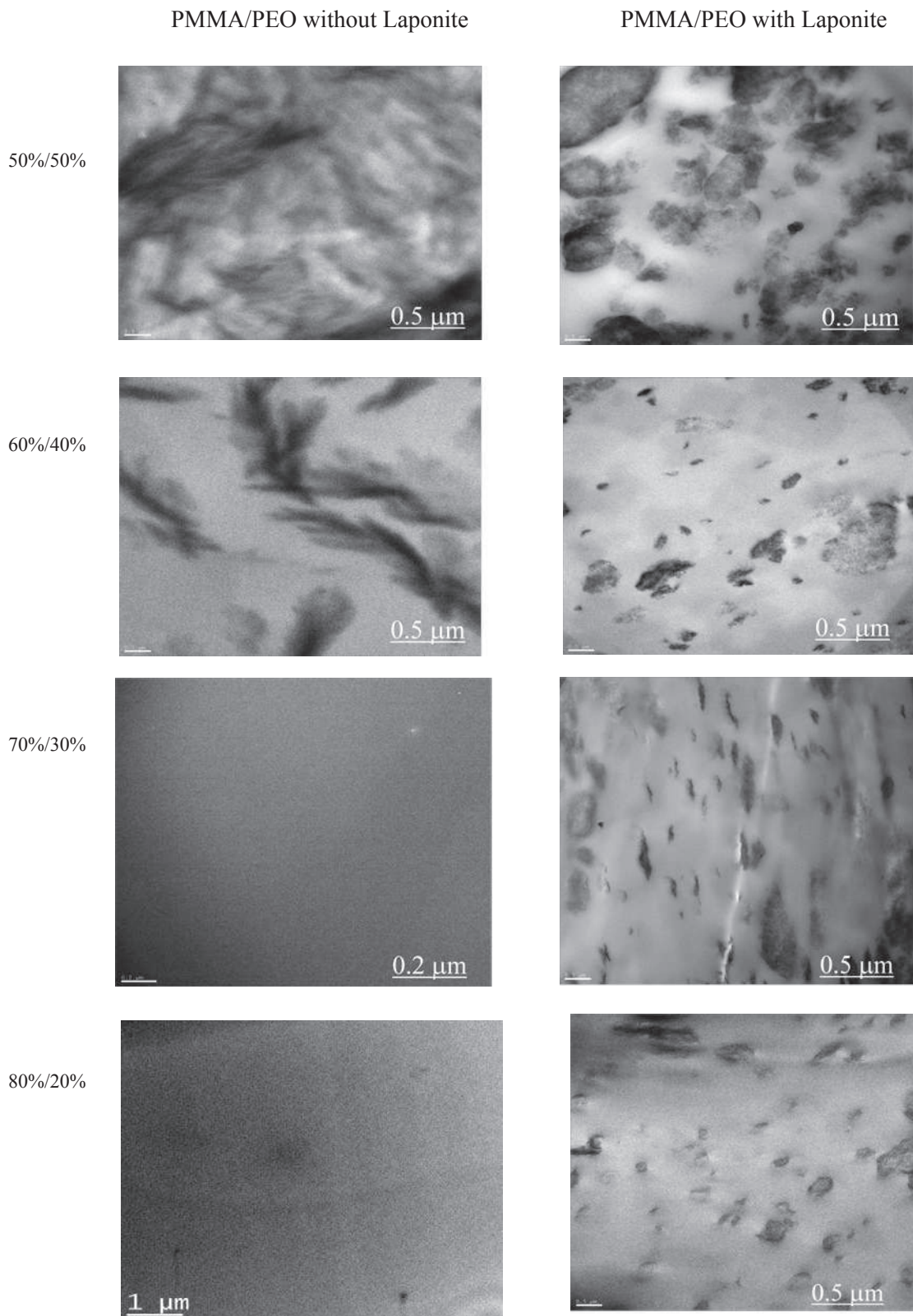


Figure 5. TEM micrographs of PMMA/PEO blends in different ratios without (left column) and with (right column) Laponite particles

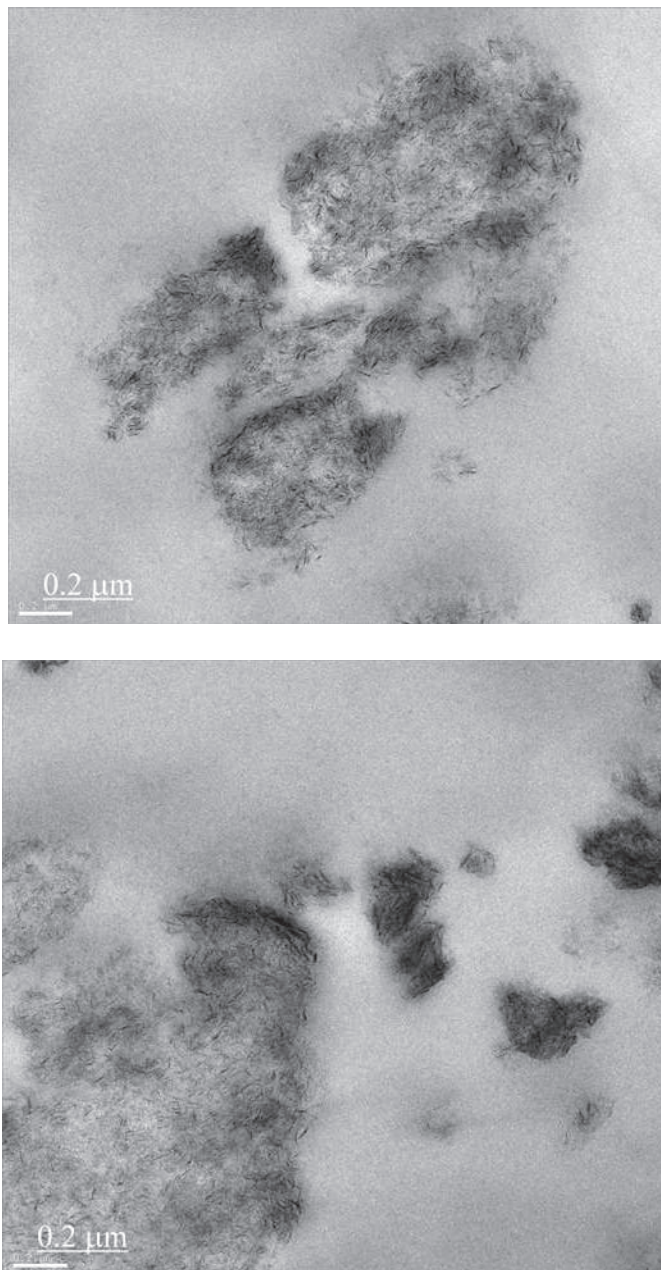


Figure 6. TEM micrographs of PMMA 60%/PEO 40% blends containing Laponite.

The continuity of one phase is often checked in polymer blends by the measurement of the weight loss of the sample after dissolution of one phase in a selective solvent. The continuity of the PEO phase has been checked using dissolution in water and the results are plotted in Figure 6. The weight loss is expressed as the percentage with respect to the mass of PEO of the sample, rather than the total mass.

It can be seen that without Laponite about 100% of the PEO is dissolved for compositions above 40wt% of PEO in the blend. Surprisingly, already at 30% of PEO, about 80% of the total content of PEO is dissolved, which means that a high degree of continuity is observed. This is not contradictory with the fact that a high degree of compatibility is

observed for this concentration. In compatible blends, PEO is extracted above 10 wt%. However, the extracted mass is only 30% of the maximum.

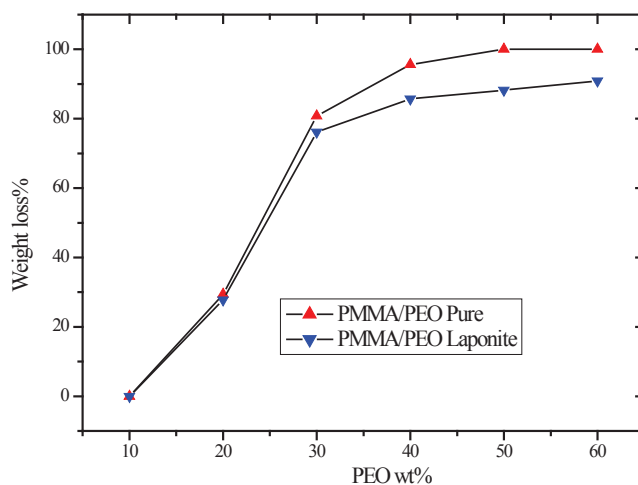


Figure 7. Weight loss vs. Laponite concentration in PMMA/PEO blends with and without Laponite Blue and Red respectively

When Laponite is added and for PEO concentrations higher than 30wt%, a slight decrease of the extracted amount of PEO is observed. One possible interpretation originates from the fact that if strong interactions between PEO protected Laponite particles and PMMA chains exist, the extraction of PEO will be more difficult. The strong interactions can develop either at the interface between the PEO/Laponite rich domains and the PMMA matrix or eventually inside the matrix because of the tiny dispersion of particles in the matrix, as can be seen from the TEM pictures.

From the above characterization we can conclude that our studies confirm the compatibility between PEO and PMMA for concentrations of PEO up to slightly less than 30 wt%. For higher concentrations, although the blends are reputed miscible in the molten state crystallization of the PEO phase occurs on cooling. When Laponite particles are added, it is likely that, even in the molten state, the master batch of PEO containing Laponite does not disperse in the PMMA phase. Indeed, small domains containing high concentrations of particles are visible on the TEM pictures. However, some degree of mixing seems to exist, since regions with more dilute concentrations of particles can be observed.

In immiscible polymer blends, nanoparticles often act as compatibilizer²²⁻²⁶, leading to a reduction of the size of the dispersed phase. Hydrophilic particles like Laponite are unlikely to disperse in PMMA. It was thus tempting to protect them by a compatible polymer to help their dispersion in the PMMA matrix. This apparently only works very partially since only a very small fraction of Laponite particles is dispersed.

Rheological properties

The rheological properties of PMMA/PEO blends have been characterized at 110°C, fig 8 compare blends with or without Laponite but with the same PMMA/PEO composition.

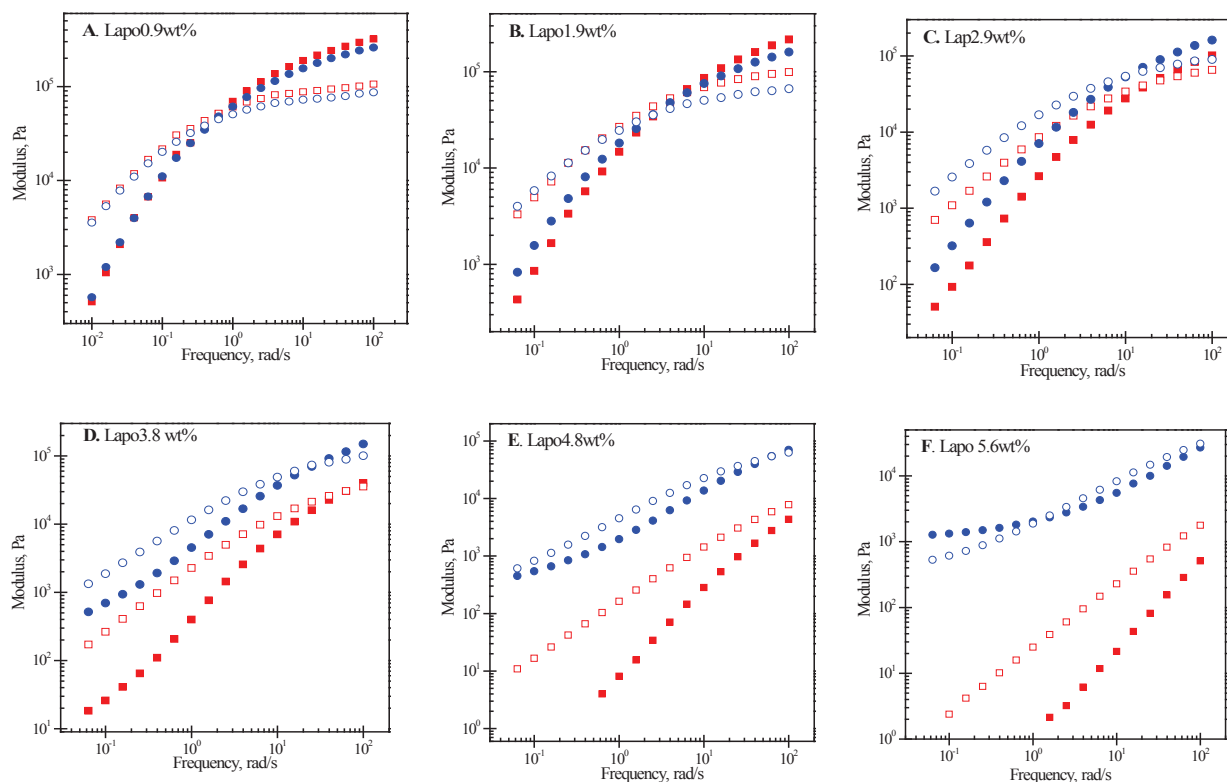


Figure 8. Frequency-dependence of the storage (filled symbols) and loss modulus (open symbols) of PMMA/PEO blends in different ratios (90%/10%, 80%/20%, 70%/30%, 60%/40%, 50%/50% and 40%/60%, labeled as A, B, C, D, E, and F respectively) without and with Laponite red and blue respectively. Measurements were performed at 160°C.

In compatible blends (10 and 20% PEO), no large change of the viscoelastic behavior is observed when particles are added. At 10 wt% the terminal behavior is essentially unchanged, whereas in the "plateau zone" a slight decrease of the plateau modulus is observed. The moduli at high frequency are also depressed when Laponite is added with 20wt% PEO, but now a kind of reinforcing effect is observed at low frequency. The viscosity increases by a factor 1.3 and some additional contribution to G' can be noticed.

For concentrations of 30% PEO and above, the moduli with Laponite are systematically higher than those of the pristine blends. In addition, a large change in the frequency dependence is observed with the nanoparticles. Progressively, G' increases towards low frequency and a low frequency plateau appears in the frequency window for 60 wt% PEO.

Figure 9 allows us to better appreciate the variations of moduli (G' & G'') with the composition of the blends for pristine polymer blends as well as polymer blends

nanocomposites. At a given temperature, the moduli (G' & G'') of pristine polymer blends as well as nanocomposites increase with PMMA concentration in the blends. This is very clear in the high frequency region. In the low frequency side, this observation is still true for pristine blends, but no more in nanocomposites where the shape of G' is strongly affected by the PEO content and a plateau observed G' at high PEO contents.

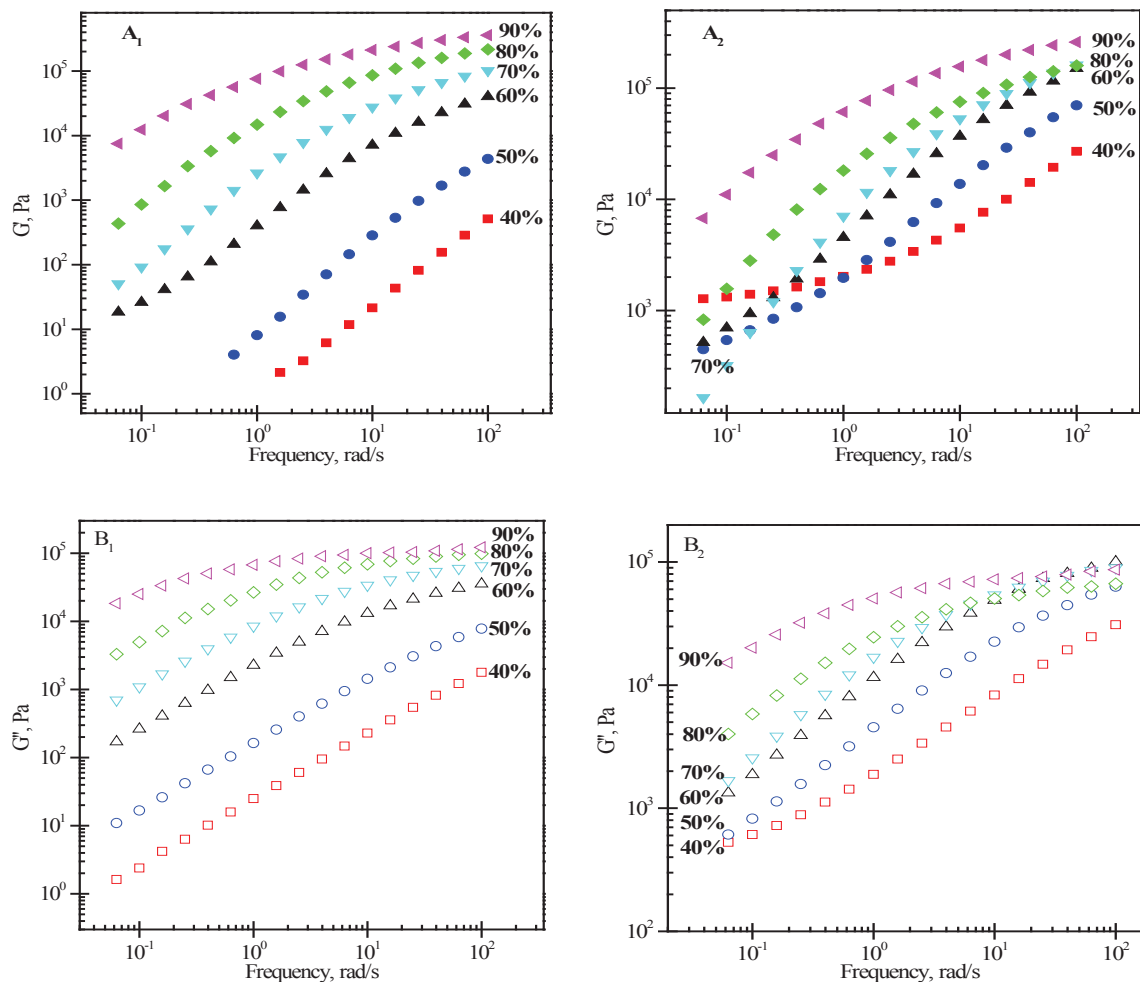


Figure 9. Frequency-dependent storage and loss modulus of PMMA/PEO blends in different ratios, A₁&A₂ referred to G' for pristine and blends nanocomposites respectively and B₁&B₂ referred to G'' for pristine and blends nanocomposites respectively.

With pristine blends, since the two components are miscible in the molten state, the decrease of the moduli can be simply attributed to the decrease of the glass transition temperature with the PEO content, and thus to an increase of the dynamics of both polymers at a given temperature. When Laponite particles are added, even if only the high frequency region is considered this effect is strongly reduced. This is an obvious sign of the fact that PEO chains do not totally mix with PMMA. Whereas G'' was dropping by almost two decades from 10 to 60% PEO for pristine blends, the decrease is only a factor of 5 with Laponite. If we assume a direct relation between the change in high frequency loss modulus and the PEO content of the blend, we can try to estimate the concentration

of PEO inside the PMMA phase in the presence of nanoparticles. With the PMMA/PEO 40/60 blend a concentration on the order of 40% can be estimated.

Above 30wt% of PEO, the large change of G' and to a lesser extent of G'' especially at low frequency suggests a typical behavior of a two phases system, when a filler is progressively added and percolates. One might note that the level of the plateau modulus for 60% PEO is very close to the one obtained with pure PEO containing Laponite at the same concentration (5.6 wt%). It is likely that a percolation of the PEO rich phase which contains the Laponite particles occurs in the molten state and leads to this rheological behavior. This is further substantiated by the almost full extraction of the PEO phase in water.

It is noteworthy to mention that Laponite concentrations are not same in all the blends but increase with PEO content. To study the influence of Laponite concentration, we focus on two blends, one (PMMA80%/PEO20%) is miscible; the other (PMMA60%/PEO40%) is immiscible.

Effect of Laponite concentration

The influence of Laponite concentration has been studied from the miscibility and the viscoelasticity points of view.

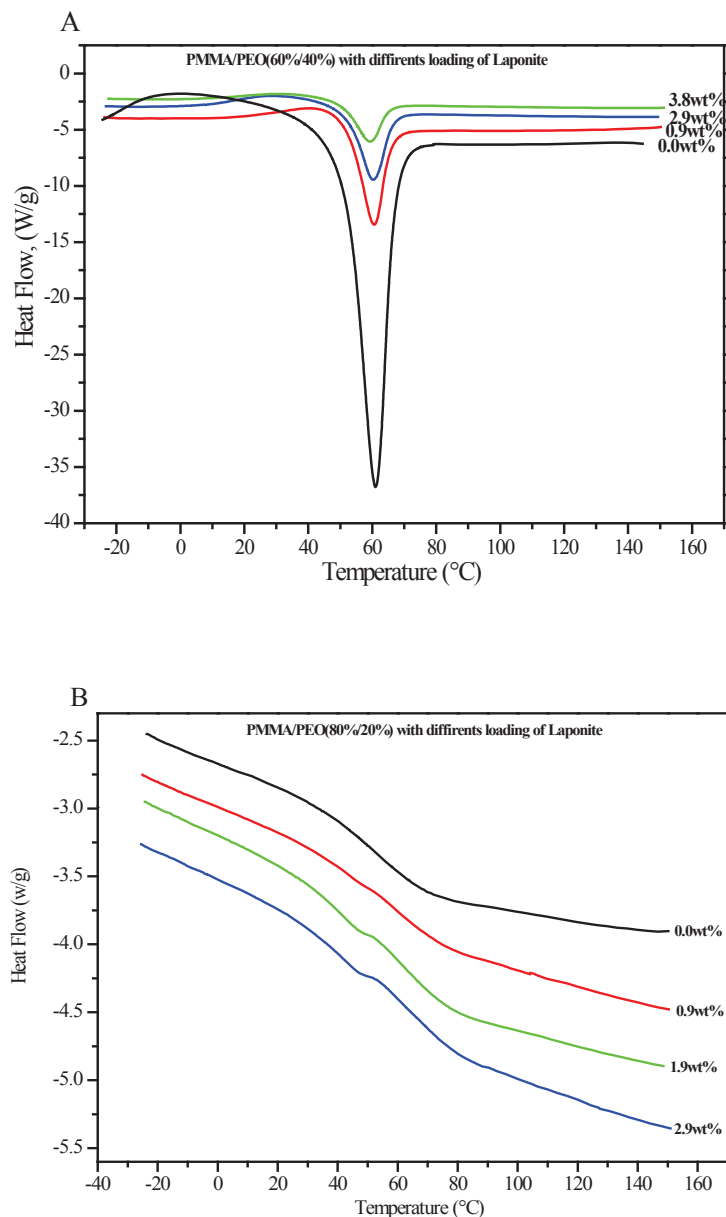


Figure 10. Effect of Laponite concentration on crystallinity of immiscible blends (A) and T_g 's of miscible blends (B).

DSC measurements show that the crystallinity of PMMA/PEO blends nanocomposites decreases sharply with the increase of Laponite concentration for immiscible blends (PMMA60%/PEO40%). For miscible blends (PMMA80%/PEO20%) the T_g 's do not

seem much affected by the introduction of Laponite, as displayed in the figure 10 (B) above. The decrease of crystallinity with increase of Laponite content agrees with what has been observed with melt prepared PEO/Laponite nanocomposites²⁷, but the strength of the decrease is much higher in the blends. The decrease in the crystallinity gives a hint that Laponite particles are preferentially located in a PEO environment rather than in the PMMA phase.

A shift of the Tg of the blends would be indicative of a change in the local composition of the blends. If we assume that the PEO phase is concentrated around Laponite particles that does not mix with PMMA, and that this tendency is increased with the concentration of Laponite, one should expect an increase of the Tg of the blend with the Laponite content. This is not clearly seen experimentally. However, the breadth of the transition zone seems to increase, pointing for an increased local heterogeneity inside the blend.

In order to investigate the influence of Laponite concentration, we performed linear viscoelastic measurement on composites with various particles composition (0, 1.9, 2.9, 3.8 wt %).

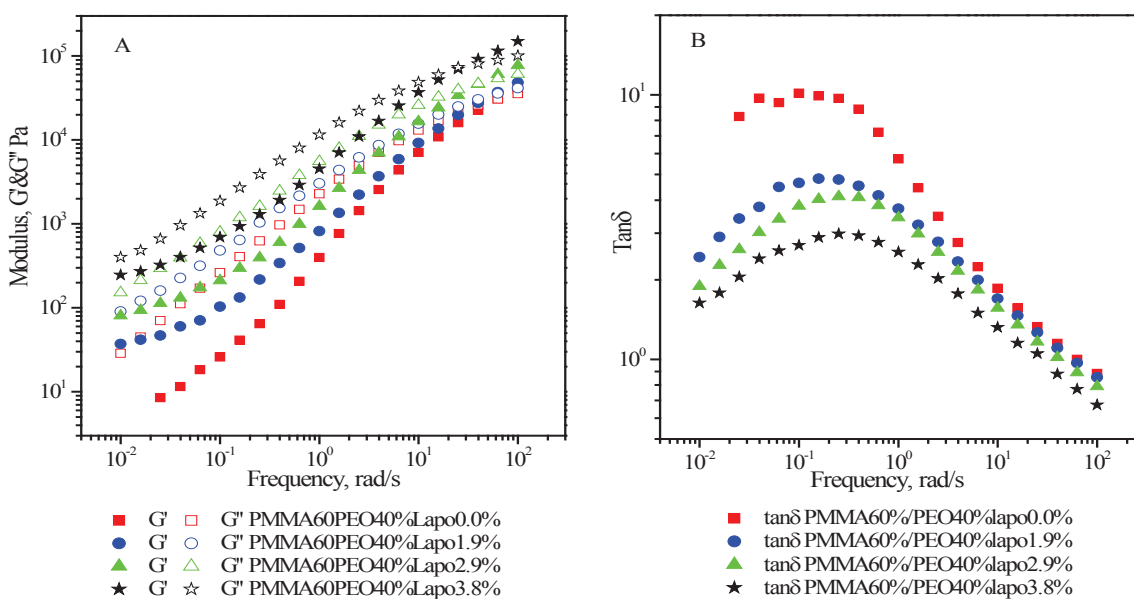


Figure11. (A) Influence of Laponite concentration on the viscoelastic properties of immiscible PMMA60%/PEO40% blends nanocomposites and (B) relaxation phenomena of polymers blends

We focus first on the (immiscible) composite which shows two phases at room temperature as revealed by SEM and TEM (figures 4 and 5 respectively). The linear viscoelastic measurements (figure 11 A) show the progressive appearance of a low-frequency plateau in the storage modulus when increasing the concentration of Laponite particles. Furthermore, both storage and loss moduli increase with Laponite concentration. The change is more pronounced at low frequencies rather than at high

ones. This is in agreement with our previous work with simple PEO/Laponite nanocomposites²⁸⁻²⁹. From our studies, the increase of modulus and appearance of plateau at low frequency region originates from nanoscopic interactions between polymers and nanoparticles¹⁶. In this immiscible system, where most of the particles are located in the PEO phase, the pseudo solid-like mechanical behavior even at low particles loadings is due to a continuous PEO/Laponite phase, even at high temperature. A physical network is built from the interactions between particles and PEO chains.

The high frequency increase of both moduli might be connected to a slight decrease of the PEO content in the PMMA phase, which induces a slight increase of T_g when the Laponite concentration is increased.

Figure 11 B gives evidence that the relaxation of polymer chains decreases with the increase of Laponite concentration. The relaxation time associated to the maximum of $\tan\delta$ is not affected by the Laponite concentration. Only the amplitude of the process decreases.

In contrast to these findings, the linear viscoelastic measurements on the “miscible” blends (figure 12 A) showed that, the solid-like rheological character does not appear even with Laponite concentrations up to 3.87wt%. The influence of Laponite concentration on the values of storage and loss modulus is very limited, as compared to the immiscible blends in the same range of concentration of Laponite. However, an increase of the moduli is noted when Laponite particles are added and there is no marked change in the polymer dynamics, except a general slowing down upon introduction of Laponite. One possible interpretation could be that the quantity of PEO mixed at a molecular level with PMMA is slightly less than in the pristine blend. This leads, at the same temperature, to an almost frequency independent slowing down of the dynamics. Furthermore, it does not vary strongly by adding more Laponite.

The Laponite particles are not homogeneously dispersed in the blend as it appeared clearly on the TEM measurements. The concentration of Laponite in the remaining PEO rich domains that originate from the master batch is thus very high since a large amount of PEO has diffused inside the matrix.

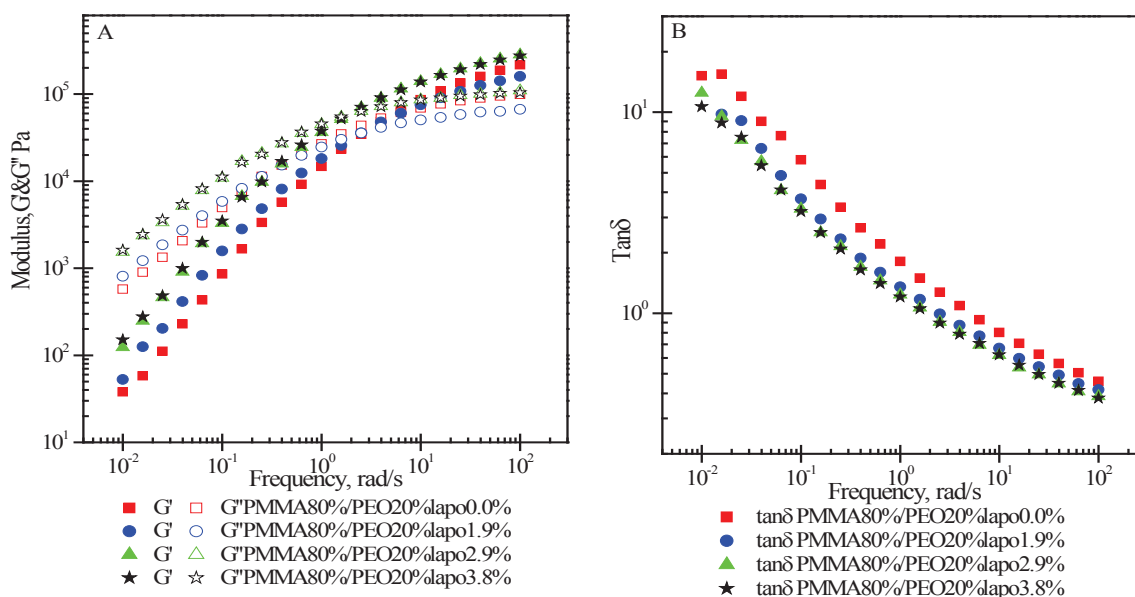


Figure 12. Influence of Laponite concentration on the viscoelastic properties of miscible PMMA80%/PEO20% blends nanocomposites (A) and relaxation phenomena of polymers blends (B)

Consequently, the influence of Laponite concentration appears to be more pronounced with immiscible blends rather than miscible blends. For concentration on the order of 40wt% PEO, a continuous structure of a PEO phase containing the large majority of Laponite particles is obtained. As in the case of simple PEO melts containing Laponite, a gel like structure is formed. The zero frequency modulus of this gel increases strongly with the Laponite concentration.

When blended with PMMA, the value of G' at low frequency increases by about one decade when the Laponite concentration has doubled. This is slightly less than expected from PEO melts. This might indicate that a given part of the Laponite particles is incorporated in the PMMA phase.

In filled polymers, the reinforcement due to particles is often expressed as the ratio between the storage modulus of the filled polymer and that of the neat one. This quantity is plotted in Figure 13 at low and high frequency, for immiscible and miscible blends. The SEM pictures are also displayed. This figure gathers the interpretations proposed to explain the difference in the influence of Laponite between these two blends. The existence of cavities containing PEO and Laponite that can be extracted by water is obvious in the "immiscible" blend, whereas it is not the case in the miscible one. The TEM pictures shown above indicate that Laponite is concentrated in small domains.

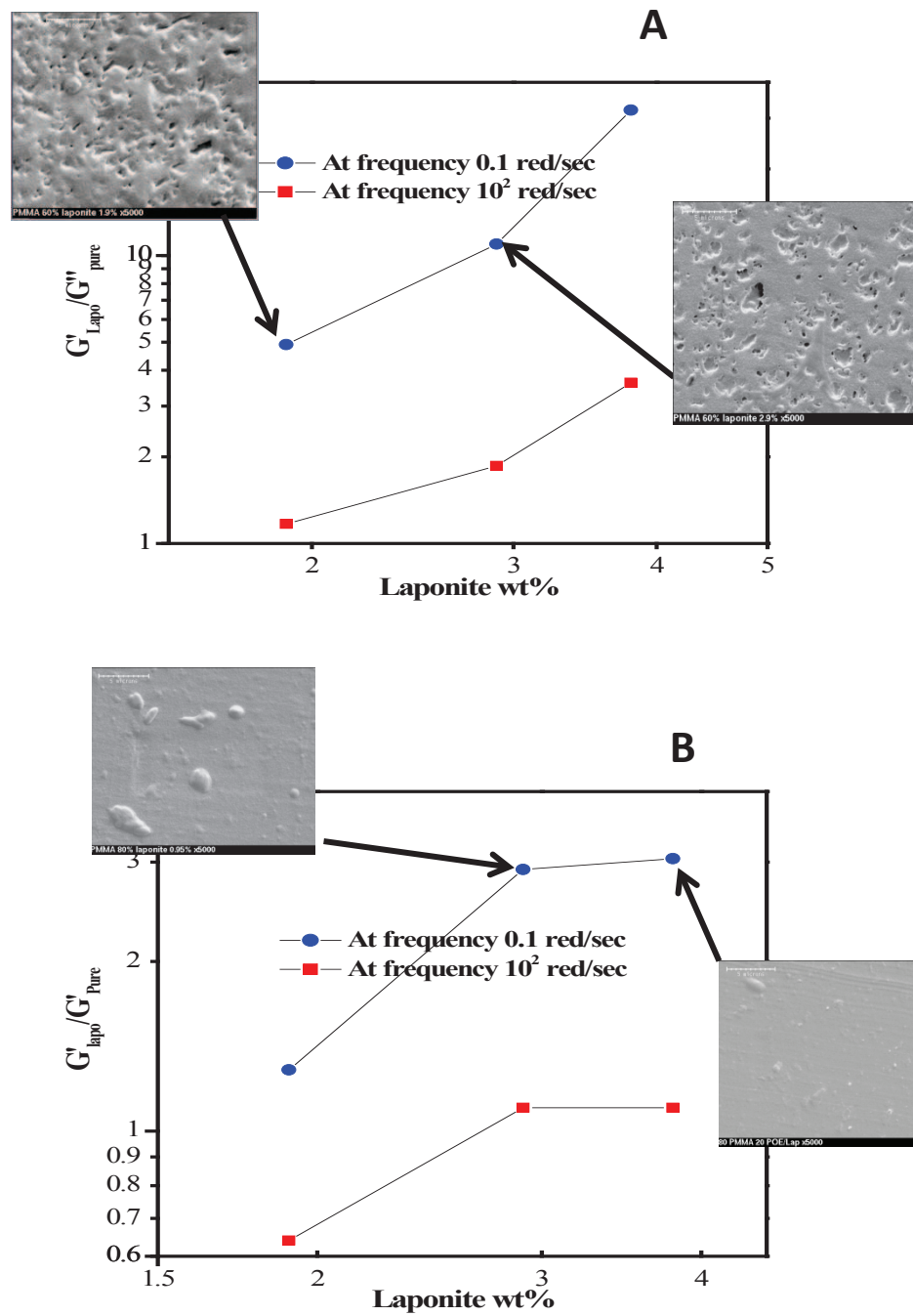


Figure 13. Reinforcement of Laponite concentration related to the structure for immiscible blends (A) and miscible blends (B).

3.4 Conclusions

PMMA/PEO blends and their nanocomposites were prepared by a combination of solution mixing to generate PEO protected Laponite particles and melt dispersion to blend the PEO/Laponite master batch with PMMA. Morphology, thermal properties, and rheological properties of these composites were investigated by using various techniques namely; Rheology, DSC, TEM, SEM, and X-Ray diffraction with aim of correlate their morphology and properties.

PMMA/PEO blends appear to be miscible at room temperature only for PEO concentration less than 30wt%, in agreement with data reported in the literature. However, in the molten state, rheological data indicate miscibility between PMMA and PEO. The introduction of Laponite particles which are, in the master batch, located inside the PEO phase does not lead to their dispersion in the blend. On the contrary, a large majority of them remain in PEO domains. However, diffusion of PEO inside the PMMA phase is observed in the molten state since glass transition temperature and rheological properties of the blends with 20wt% PEO are almost identical to those of the pristine melt with the same composition. The slight differences are explained by a smaller concentration of PEO blended with PMMA. Most of the Laponite particles are concentrated in droplets. They act as simple fillers, without interactions between them, which only provides a weak reinforcing effect.

On the contrary, at high concentrations of PEO, it has been demonstrated that a continuity of the PEO phase is observed where most of Laponite particles are located. Some particles, but their fraction cannot be estimated, seem to be inside the matrix. These types of nanocomposite blends show a non vanishing zero frequency storage modulus. Its origin is attributed to the formation of a Laponite PEO network as in PEO melts filled with Laponite. These results show that Laponite particles, such as those used in this study, i.e. protected by PEO chains, do not act as compatibilizer in these blends in contrast to other layered silicate nanocomposites. On the opposite, TEM micrographs showed that Laponite particles partially hinder the diffusion of PEO in PMMA/PEO blends and thereby limit its miscibility.

3.5 References

1. Gupta, R. K.; Kennel, E.; Kim, K. J., *Polymer nanocomposites handbook*. CRC Press.
2. Galgali, G.; Ramesh, C.; Lele, A., A Rheological Study on the Kinetics of Hybrid Formation in Polypropylene Nanocomposites. *Macromolecules* **2001**, 34, (4), 852-858.
3. Lepoittevin, B.; Pantoustier, N.; Devalckenaere, M.; Alexander, M.; Kubbies, D.; Calberg, C.; R. Jérôme; Dubois, P., Polymer/layered silicate nanocomposites by combined intercalative polymerization and melt intercalation: a masterbatch process. *Polymer* **2003**, 44, 2033-2040.
4. Alexandre, M.; Dubois, P., *Materials Science and Engineering* **2000**, (28), 1-63.
5. Sun, L.; Boo, W. J.; Clearfield, A.; Sue, H. J.; Pham, H. Q., Barrier properties of model epoxy nanocomposites. *J. Membr. Sci.* **2008**, 318, (1-2), 129-136.
6. Robeson, L. M., *Polymer Blends: A Comprehensive Review*. Hanser: 2007.
7. Zhao, Y.; Jasse, B.; Monnerie, L., Orientation and relaxation in uniaxially stretched poly(methyl methacrylate)-poly(ethylene oxide) blends. *polymer* **1989**, 30, (9), 1643-1650.
8. Martuscelli, E.; Pracella, M.; Wang, P. Y., Influence of composition and molecular mass on the morphology, crystallization and melting behaviour of poly(ethylene oxide)/poly(methyl methacrylate) blends. *Polymer* **1984**, 25, (8), 1097-1106.
9. Silvestre, C.; Cimmino, S.; Martuscelli, E.; Karasz, F. E.; MacKnight, W. J., Poly(ethylene oxide)/poly(methyl methacrylate) blends: Influence of tacticity of poly(methyl methacrylate) on blend structure and miscibility. *Polymer* **1987**, 28, (7), 1190-1199.
10. Zawada, J. A.; Ylitalo, C. M.; Fuller, G. G.; Colby, R. H.; Long, T. E., Component relaxation dynamics in a miscible polymer blend: poly(ethylene oxide)/poly(methyl methacrylate). *Macromolecules* **1992**, 25, (11), 2896-2902.
11. Parizel, N.; Lauprêtre, F.; Monnerie, L., N.m.r. and d.s.c. investigations of the miscibility of poly(methyl methacrylate)/poly(ethylene oxide) blends. *Polymer* **1997**, 38, (15), 3719-3725.
12. Jin, X.; Zhang, S.; Runt, J., Broadband Dielectric Investigation of Amorphous Poly(methyl methacrylate)/Poly(ethylene oxide) Blends. *Macromolecules* **2004**, 37, (21), 8110-8115.
13. Jeedi, K.; Qazvini, N. T.; Jafari, S. H.; Khonakdar, H. A.; Seyfi, J.; Reuter, U., Investigating the Effect of Nanolayered Silicates on Blend Segmental Dynamics and Minor Component Relaxation Behavior in Poly(ethylene oxide)/Poly(methyl methacrylate) Miscible Blends. *J. Polym. Sci. Pt. B-Polym. Phys.* **2011**, 49, (4), 318-326.
14. Chang, C. C.; Hou, S. S., Intercalation of poly(methyl methacrylate) into tyramine-modified layered silicates through hydrogen-bonding interaction. *Eur. Polym. J.* **2008**, 44, (5), 1337-1345.
15. Fang, F. F.; Kim, J. H.; Choi, H. J.; Kim, C. A., Synthesis and electrorheological response of nano-sized laponite stabilized poly(methyl methacrylate) spheres. *Colloid Polym. Sci.* **2009**, 287, (6), 745-749.
16. Kim, H. B.; Choi, J. S.; Lee, C. H.; Lim, S. T.; Jhon, M. S.; Choi, H. J., Polymer blend/organoclay nanocomposite with poly(ethylene oxide) and poly(methyl methacrylate). *Eur. Polym. J.* **2005**, 41, (4), 679-685.
17. Wheeler, P. A.; Wang, J. Z.; Mathias, L. J., Poly(methyl methacrylate)/laponite nanocomposites: Exploring covalent and ionic clay modifications. *Chemistry of materials* **2006**, 18, (17), 3937-3945.

18. Jeddi, K.; Qazvini, N. T.; Jafari, S. H.; Khonakdar, H. A., Enhanced ionic conductivity in PEO/PMMA glassy miscible blends: Role of nano-confinement of minority component chains. *Journal of Polymer Science Part B: Polymer Physics* **2010**, 48, (19), 2065-2071.
19. Lim, S. K.; Kim, J. W.; Chin, I.; Kwon, Y. K.; Choi, H. J., Preparation and Interaction Characteristics of Organically Modified Montmorillonite Nanocomposite with Miscible Polymer Blend of Poly(Ethylene Oxide) and Poly(Methyl Methacrylate). *Chemistry of materials* **2002**, 14, (5), 1989-1994.
20. Shen, Z.; Cheng, Y.-B.; Simon, G. P., Sequential and Simultaneous Melt Intercalation of Poly(ethylene oxide) and Poly(methyl methacrylate) into Layered Silicates. *Macromolecules* **2005**, 38, (5), 1744-1751.
21. Ghelichi, M.; Taheri Qazvini, N.; Jafari, S. H.; Khonakdar, H. A.; Reuter, U., Nanoclay dispersion in a miscible blend: an assessment through rheological analysis. *Journal of Polymer Research* **2012**, 19, (3), 1-9.
22. Gelfer, M. Y.; Song, H. H.; Liu, L.; Hsiao, B. S.; Chu, B.; Rafailovich, M.; Si, M.; Zaitsev, V., Effects of organoclays on morphology and thermal and rheological properties of polystyrene and poly(methyl methacrylate) blends. *Journal of Polymer Science Part B: Polymer Physics* **2003**, 41, (1), 44-54.
23. Wang, Y.; Zhang, Q.; Fu, Q., Compatibilization of Immiscible Poly(propylene)/Polystyrene Blends Using Clay. *Macromol. Rapid Commun.* **2003**, 24, (3), 231-235.
24. Sinha Ray, S.; Pouliot, S.; Bousmina, M.; Utracki, L. A., Role of organically modified layered silicate as an active interfacial modifier in immiscible polystyrene/polypropylene blends. *polymer* **2004**, 45, (25), 8403-8413.
25. Sinha Ray, S.; Bousmina, M., Compatibilization Efficiency of Organoclay in an Immiscible Polycarbonate/Poly(methyl methacrylate) Blend. *Macromol. Rapid Commun.* **2005**, 26, (6), 450-455.
26. Sinha Ray, S.; Bandyopadhyay, J.; Bousmina, M., Effect of Organoclay on the Morphology and Properties of Poly(propylene)/Poly[(butylene succinate)-co-adipate] Blends. *Macromolecular Materials and Engineering* **2007**, 292, (6), 729-747.
27. Loyens, W.; Jannasch, P.; Maurer, F. H. J., Poly(ethylene oxide)/Laponite nanocomposites via melt-compounding: effect of clay modification and matrix molar mass. *Polymer* **2004**, 46, 915-928.
28. Loiseau, A.; Tassin, J. F., Model Nanocomposites Based on Laponite and Poly(ethylene oxide): Preparation and Rheology *Macromolecules* **2006**, 39, 9185-9191.
29. Loiseau, A. Elaboration et caractérisation de Nanocomposites modèles Laponite/Polyoxyde d'ethylene. Ph.D, du maine, Le mans, 2006.

General conclusion and Perspectives

In this study we focused on the rheological behavior in the molten state and on the structure of model nanocomposites based on Laponite and PEO. Many efforts have been done to prepare samples using well defined conditions of particle protection and incorporation of the protected particles in polymer matrices. The protection of the particles was varied using either adsorbed chains or end-grafted chains of various lengths. The trimethylammonium terminated chains were synthesized for this purpose. We used two routes of preparation of the suspensions. We tried to transfer in the solid state the disordered and dispersed state of the PEO/Laponite solutions by freeze drying these suspensions. This state is, to our knowledge, the best dispersion of the particles we could achieve. It is however of limited use if industrial considerations are taken into account. Rather, it is tempting to produce nanocomposites using the melt dilution in a twin screw extruder of a concentrated master batch of compatibilized particles. This way of preparation was studied and called the melt route.

In a first chapter, after a bibliographic review, we have carefully studied the influence of the preparation method using the combination of linear viscoelastic measurements, Small Angle X-Ray Scattering and melting properties of the samples. We have been able to show that the preparation method is of primary importance to control the state of dispersion of the particles and thus the properties. With a given kind of compatibilization (i.e. adsorption), we have shown that melt prepared samples show a lower modulus than solution prepared ones, especially at low concentrations. It is most probable that a completely different structure exists in these two kinds of materials since the exponents of the scaling law relating the zero frequency modulus to the concentration are different. By preparing samples from master batches at different concentrations, we have shown that the state of the samples was not determined by thermodynamic equilibrium but was rather dependent on the blending process. Since nanocomposites with a higher connectivity were obtained from a less concentrated master batch we made an analogy with the rheological behavior of polymer blends where one tries to mix a high viscosity liquid with a matrix of low viscosity. The effect is even worse here, since the master batch does not flow at rest but is rather a soft (breakable) solid.

The relatively good state of dispersion that can be produced using the solution route was supported by many other results, like influence of the molecular weight of the matrix chains, influence of the type of protection of the particles, since the properties of these samples do not depend much on these parameters.

Using master curves, we were able to understand the differences in the shape of the moduli versus frequency curves. Master curves could be constructed over a given concentration range by simple horizontal and vertical shifts in logarithmic scales. This shows that the samples mainly differ by the time scale of their dynamics.

The concept of breaking of the master batch structure during the blending process has been used again to explain the increase of the moduli when using matrices with large molecular weight chains.

Finally, by looking at the influence of the length of grafted chains, we connected the observed behavior with the idealized problem of wetting a polymer brush with a polymer melt of the same chemical nature. This problem was treated theoretically and we could deduce that our particles bearing grafted chains can be wetted by the polymer, which improves their dispersion. The longer the grafter chain, the more the wetting and the better the dispersion. This can be seen as increasing the volume fraction of the particles accounting qualitatively for the observed results.

In the last chapter of this work we opened the system to one polymer compatible with PEO, i.e. polymethylmethacrylate (PMMA). We have been able to produce such nanocomposites with a good level of transparency, which is not possible if the particles are not protected. Using this system, we could obtain TEM pictures of Laponite dispersed in one phase that is supposed to contain mainly PEO. To our knowledge, these are the first micrographs of Laponite inserted into a polymer matrix. In the case of pure PEO as matrix, the poor mechanical properties inhibit the preparation of ultrathin samples.

By analyzing the rheological data, we could argue on the diffusion of PEO into the PMMA phase for low contents of PEO (20wt% or less) and also retrieve the properties of a connected phase of Laponite particles when the PEO concentration is high enough to generate cocontinuous phases. Unfortunately we were not able to fully disperse particles even recovered with adsorbed chains inside the PMMA phase.

Nevertheless, we think that choosing optimum conditions with this type of blends could be used to improve the conductivity of solid state batteries electrolytes. Indeed, we have shown that above 30wt% of PEO, a continuous PEO rich phase is formed. The crystallinity of this phase can be kept low, leading to an increase in ionic conductivity. It is most likely that, increasing the Laponite content will even push the crystallization of PEO towards higher concentrations.

Abstract

Polymer nanocomposites appear in the beginning of the 90ths and consist usually in the dispersion of inorganic nanoparticles inside a polymer matrix. Nanocomposites can show improved mechanical properties with a very low inorganic content. Widely studied classes of inorganic particles are clays. However, most often, organophilic clays derived from Montmorillonite are used.

In this thesis model nanocomposites based on a geometrically well-defined nanoparticles (Laponite) and on a hydrophilic polymer (polyethylene oxide – PEO, alone or blended with polymethylmethacrylate – PMMA) were considered. This study focuses on the relationships between rheological properties in molten state and dispersion state of the particles, as characterized by X-Ray diffraction data using three experimental parameters, namely preparation method, PEO matrix molecular weight, and method of steric protection the particles.

Laponite particles were protected by adsorbing PEO (Mw=10k) or end grafting shorter chains (Alkyl-Ammonium terminated PEO Mw=5k, 2k and 1k) by using two methods of preparation : melt dispersion and solution mixing. Several grades of PEO were used as matrix to investigate the influence of PEO matrix molecular weight.

Samples prepared by solution mixing achieved higher modulus and the best state of dispersion as compared to those prepared by melt dispersion. A picture based on the blending of incompatible polymer melts of various viscosities was used to interpret the results.

The storage modulus (G') for samples prepared by solution mixing is independent on the route of protecting the particles, whereas, properties of melt dispersed samples strongly depend on the route of protecting the particles. The modulus are higher when longer chains are grafted onto the particles. Grafted chains appear more efficient than absorbed ones. This was attributed to the intercalation of the polymer matrix between particles either by diffusion or a mechanical peeling mechanism during melt dispersion.

Mixing in a higher molecular weight polymer matrix leads to higher moduli in the molten state, especially for low contents of Laponite. This is interpreted as the consequence of an higher viscosity of the melt during the mixing process, allowing an easier breakdown of domains containing a high concentration of particles.

Since protection by the same polymer as the matrix seems an effective way to prepare rather well dispersed nanocomposites, an extension of this concept was checked by using a polymer matrix which is compatible with PEO. The characterization of PEO/PMMA blends and their nanocomposites, so far, internal structure, thermal and rheological properties of these composites was investigated using several techniques such as Rheology, DSC, TEM, SEM, and X-ray diffraction with the aim of correlating morphologies and properties. PMMA/PEO blends are known to be miscible over all the concentration range in the molten state, whereas PEO undergoes crystallization above 30wt%. For low PEO contents, Laponite particles do not seem to decrease the compatibility with PMMA, since no crystallization of PEO neither domains of PEO are observed. However, the structuration of the melt through particle-particle interactions is lost. For higher PEO contents, phase separated blends are observed where the Laponite particles are clearly located in the PEO rich domains. This has allowed us to obtain TEM pictures of Laponite particles dispersed in PEO, which was not possible due to the difficult in preparing ultrathin samples of PEO.